NORTHWESTERN UNIVERSITY

Theta-Frequency Oscillatory Mechanisms for Human Hippocampal Function

A DISSERTATION

SUBMITTED TO THE GRADUATE SCHOOL
IN PARTIAL FULFILLMENT OF THE REQUIREMENTS

for the degree

DOCTOR OF PHILOSOPHY

Field of Neuroscience

By

Sarah Marissa Lurie

EVANSTON, ILLINOIS

March 2023

Abstract

Findings in both humans and animal models have associated the hippocampal theta oscillation with hippocampal memory function. In animal models, previous research supports that the theta oscillation contributes to memory via phase-dependent changes in hippocampal network connectivity, wherein memory encoding versus retrieval are optimized at different phases of the theta oscillation. However, it is unclear whether this phase-dependence exists in humans. In this dissertation, I describe two lines of research I carried out to investigate how theta phase impacts human hippocampal physiology and memory function. First, using network-targeted intracranial stimulation and invasive recordings of the human hippocampus, I assessed whether hippocampal connectivity with network afferents varies according to theta phase. I observed a continuous relationship between local theta phase at stimulation onset and the amplitude of the hippocampal evoked response, supporting phase-dependent changes in hippocampal connectivity with its network. Next, to investigate whether associative memory encoding and retrieval performance vary with the theta oscillation, I attempted to causally manipulate hippocampal theta phase using theta-patterned noninvasive transcranial magnetic stimulation targeted to a cortical location in the hippocampal network. Although I observed a significant effect of stimulated phase on memory encoding performance, it was unclear whether stimulation successfully impacted hippocampal theta. Collectively, these findings demonstrate that the human hippocampus undergoes phase-dependent changes in network connectivity, confirming a putative oscillatory mechanism for hippocampal function. These findings suggest that phase-dependent hippocampal connectivity changes occur locally according to long axis position, rather than globally throughout the hippocampus. Finally, I discuss potential future research directions to better

characterize this phase-dependence, including assessing the impact of long axis position on local connectivity and developing new approaches to experimentally manipulate theta phase during task performance.

Acknowledgments

Thanks to my advisor, Dr. Joel Voss; to my thesis committee, Drs. John Disterhoft, Christina Zelano, and Daniel Dombeck; to the past and present members of the Center for Neurocognitive Outcomes Improvement Research née the Laboratory for Human Neuroscience; and to the research participants, whose patience, trust, and generosity enabled this work.

List of Abbreviations

EP: evoked potential

FIR: finite impulse response

fMRI: functional magnetic resonance imaging

IIR: infinite impulse response

iTBS: intermittent theta burst stimulation

LME: linear mixed-effects

MS/DBB: medial septum and diagonal band of Broca

OFC: orbitofrontal cortex

rTMS: repetitive transcranial magnetic stimulation

SD: standard deviation

sEEG: stereotactic electroencephalography

SEM: standard error of the mean

Table of Contents

Abstract **2**

Acknowledgments **4**

List of Abbreviations **5**

List of Figures and Tables **8**

Chapter 1: Background **9**

1.1 The hippocampal theta oscillation 9

1.2 Causal evidence for theta's role in hippocampal-dependent memory 11

1.3 The phase-dependent connectivity model of hippocampal memory function 13

1.4 Theta phase varies across the hippocampus 15

Chapter 2: Introduction **17**

2.1 Problem Statement 17

2.2 Approach 17

2.3 Description of Data Chapters 18

Chapter 3: Identifying phase-dependent hippocampal responsivity via intracranial stimulation and recording **20**

3.1 Introduction 20

3.2 Materials and Methods 22

3.3 Results 30

3.4 Discussion 57

Chapter 4: Investigating memory performance as a function of stimulation-entrained theta **61**

4.1 Introduction 61

4.2 Materials and methods 64

4.3 Results 72

4.4 Discussion 83

Chapter 5: Discussion **86**

5.1 Conclusions 86

5.2 Future directions 87

References **92**

List of Figures and Tables

Figure 1.1, page 9. The theta oscillation appears prominently in local field potential recordings of hippocampus.
Figure 1.2, page 11. Prestimulus hippocampal theta power predicts successful memory encoding.
Figure 1.3, page 14. Hypothesized hippocampal connectivity states supporting encoding (left) versus retrieval (right).
Figure 1.4, page 16. Hippocampal theta phase varies with laminar depth.
Table 3.1, page 31. Participant characteristics.
Figure 3.1, page 32. Hippocampal recordings and evoked response.
Figure 3.2, page 36. Continuous theta phase predicted response amplitude during early and late EP components.
Figure 3.3, page 38. Hippocampal EPs and isolated responses binned according to theta phase at stimulation delivery.
Figure 3.4, page 40. Stimulation at theta peak versus trough produced differences in early-component amplitude.
Figure 3.5, page 43. Control regions showed less temporal specificity in their phase-amplitude relationships and no difference in peak versus trough or falling versus rising early response amplitudes.
Figure 3.6, page 46. Phase estimation method yielded consistent, low-magnitude offset to ground-truth phase in pseudotrial analysis.
Figure 3.7, page 49. Theta phase distribution of stimulation pulses did not change according to order in the experimental session.
Figure 3.8, page 50. Effect of peak versus trough stimulation on hippocampal isolated response amplitude is temporally specific to components.
Figure 3.9, page 55. Distributions of phase offsets between lateral temporal and hippocampal theta were uniform across electrodes.
Figure 4.1, page 68. Study and test trial format in Experiment 1.
Figure 4.2, page 69. Schematic of visual stimulus alignment to the theta-patterned rTMS train.
Figure 4.3, page 71. Study and test trial format in Experiment 2.
Figure 4.4, page 72. Setup for validation of visual stimulus timing relative to TMS.
Figure 4.5, page 73. Left parietal (in-network) stimulation locations across the participant cohort.
Figure 4.6, page 75. Visual stimuli were presented within 6° of desired phase on the entraining oscillation.
Figure 4.7, page 77. No effect of stimulation site on overall memory accuracy or proportion of recall hits.
Figure 4.8, page 79. Hippocampal network-targeted entraining stimulation produces phase-dependent memory effect during encoding.
Figure 4.9, page 81. No effect of position in the experimental session on memory performance.
Figure 4.10, page 83. Differences in the relationship between response time and performance across Experiments 1 and 2.

Chapter 1: Background

1.1 The hippocampal theta oscillation

The theta oscillation is a high-amplitude, relatively low-frequency (~3-8 Hz) signal which is prominent in local field potential recordings of the hippocampus. Hippocampal theta was first reported in rabbit and rodent models (Jung & Kornmüller, 1938), where it was initially associated with exploratory and orienting behaviors (e.g., Vanderwolf, 1969). Although its precise characteristics vary (including, for example, its typical frequency range [Jacobs, 2014; Watrous et al., 2013] and the consistency of its amplitude [Stewart & Fox, 1991; Goyal et al, 2020; Watrous et al., 2013]; **Figure 1.1**), hippocampal theta is present across many species including humans and non-human primates (e.g., Arnolds et al., 1980; Jutras et al., 2013; Kahana et al., 1999; Stewart & Fox, 1991; Zhang & Jacobs, 2015).

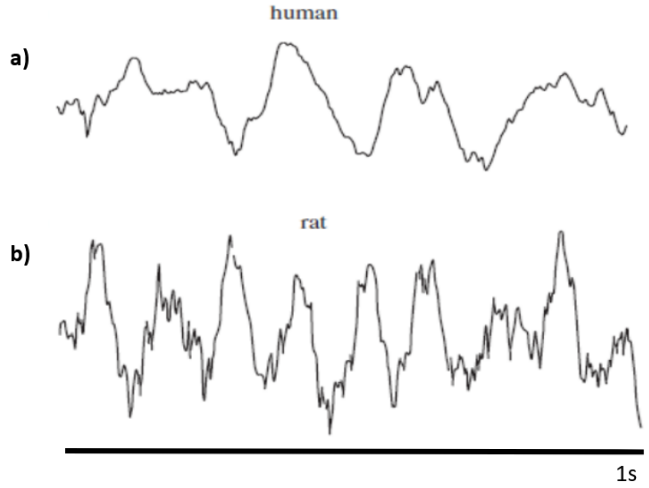

Figure 1.1. **The theta oscillation appears prominently in local field potential recordings of hippocampus.** Example local field potential recordings from A) human and B) rodent hippocampus. Adapted from Jacobs, 2014.

Owing to the known role of the hippocampus in learning and memory (Eichenbaum, 2000; Buzsáki & Moser, 2013), the theta oscillation has since been commonly studied for its relationship to memory function. In animal studies, hippocampal theta power has been widely

associated with successful nonspatial and spatial learning (Seager et al., 2002; Berry & Thompson, 1978; Winson, 1978; McNaughton et al., 2006; Markowska et al., 1995). In humans, findings relating invasively-recorded hippocampal theta power (i.e., recorded via surgically-implanted, intracranial electrodes) to memory are somewhat more variable. Studies variously report positive (e.g., Fell et al., 2011) and negative (e.g., Greenberg et al., 2015) relationships between human hippocampal theta power and memory performance (see Herweg et al., 2020). This difference is likely contributed to by differences in referencing and recording schemes across model species (for example, bipolar referencing is common in human invasive studies, but may fail to capture power enhancement spanning neighboring electrodes [Arnulfo et al., 2015; Herweg et al., 2020]). Under linked-mastoid referencing – wherein all intracranial channels share a common reference – hippocampal theta power during the prestimulus period has been positively associated with a greater likelihood of successful episodic memory encoding (Fell et al., 2011; **Figure 1.2**). Intracranial studies have also demonstrated enhancement of human hippocampal theta power during spatial exploration (Ekstrom et al., 2005; Vivekananda et al., 2021) as well as during non-spatial memory tasks (Raghavachari et al., 2001). In addition, studies of theta as measured noninvasively at the scalp have repeatedly demonstrated a positive association between memory performance and both pre- and post-stimulus (likely neocortical [Kahana et al., 2001; Long et al., 2014]) theta power (e.g., Addante et al., 2011; Hanslmayr et al., 2009; Jacobs et al., 2006; Klimesch et al., 1996; Summerfield & Mangels, 2005).

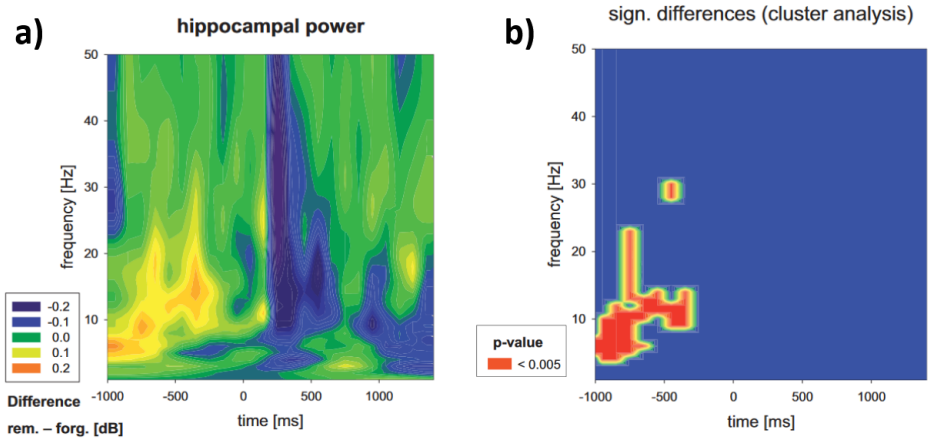

Figure 1.2. **Prestimulus hippocampal theta power predicts successful memory encoding.** Spectral analysis of human hippocampal activity around memorandum presentation. Difference plots for subsequently remembered versus forgotten words. A) Normalized power. B) *p* values resulting from a cluster-based analysis. Adapted from Fell et al., 2011.

1.2 Causal evidence for theta's role in hippocampal-dependent memory

Some of the strongest evidence for the theta oscillation's importance to hippocampal memory function comes from animal model studies in which the theta oscillation is experimentally manipulated. The medial septum and diagonal band of Broca (MS/DBB) are subcortical nuclei postulated as key theta rhythm pacemakers for the hippocampus as well as other theta-expressing structures including amygdala and entorhinal cortex (Huh et al., 2010). Cholinergic and GABAergic cell populations in the MS/DBB have reciprocal projections with the hippocampus (Baisden et al., 1984; Senut et al., 1989; Toth et al., 1993). Both cholinergic and GABAergic septal neurons fire in bursts which are phase-locked to hippocampal theta (Borhegyi et al., 2004; Stewart & Fox, 1989). In evidence of the MS/DBB's role as a hippocampal pacemaker, hippocampal theta power is diminished by lesions to the MS/DBB (Lee et al., 1994; Mitchell et al., 1982), but septal theta-frequency bursting does not depend on feedback from the hippocampus (Stewart & Fox, 1989).

Interventions targeting the MS/DBB modify hippocampal theta power as well as hippocampal-dependent behavior. Lesioning the MS/DBB reduces hippocampal theta power and impairs performance on memory and spatial navigation tasks (Knox & Keller, 2016; McNaughton et al., 2006; Mitchell et al., 1982). Conversely, administering an acetylcholine agonist to the MS/DBB enhances hippocampal theta power and concomitantly improves performance on memory tasks (Markowska et al., 1995). After lesioning the MS/DBB, restoring the hippocampal theta rhythm by electrical stimulation of the fornix also restores memory performance (McNaughton et al., 2006; Shirvalkar et al., 2010). This finding supports that the memory impairment associated with blocking MS/DBB input to the hippocampus is specifically related to the loss of the hippocampal theta rhythm.

In humans, sensory entrainment provides a noninvasive – albeit less anatomically-selective – method to experimentally manipulate theta. Simultaneously pulsing auditory and visual stimuli at a theta frequency increases scalp EEG theta power during subsequent memory tasks and enhances memory performance (Roberts et al., 2018; Wang et al., 2018). However, the power enhancements reported in these studies were recorded noninvasively at the scalp, and were likely neocortical rather than hippocampal in origin (Long et al., 2014). Findings from noninvasive brain stimulation also support a role of hippocampal theta power in human memory. When delivered at a rhythm which is endogenously expressed by a target stimulation site, repetitive transcranial magnetic stimulation (rTMS) can produce local entrainment, including power enhancement at the entrained frequency. rTMS entrainment of an endogenous rhythm has been demonstrated with alpha-frequency stimulation in parietal cortex (Thut et al., 2011; Klimesch et al., 2003), beta-frequency stimulation in motor cortex (Romei et al., 2016), and theta-frequency stimulation in prefrontal cortex (Chung et al., 2018). Recent work from our laboratory has shown

that theta-frequency stimulation targeting the hippocampal network can impact associative memory and hippocampal activity and network connectivity (Hebscher et al., 2021; Hermiller et al., 2019; Hermiller et al., 2020). However, these studies were methodologically unable to verify whether stimulation impacted hippocampal theta.

1.3 The phase-dependent connectivity model of hippocampal memory function

Why does theta relate to hippocampal-dependent memory? One proposed mechanism for this relationship is that theta orchestrates changes in hippocampal connectivity, optimizing the hippocampus for the oppositional processes of encoding versus retrieval at different phases of the theta rhythm. Episodic memory encoding and retrieval are thought to involve distinct hippocampal connectivity states. During memory formation, fragments of information which comprise an episode are bound into coherent memory traces by the hippocampus (Davachi, 2006; Shapiro & Eichenbaum, 1999; Wixted et al., 2014). This is thought to involve increased connectivity of input from entorhinal cortex to CA3 (Hasselmo et al., 2002; see Brankačk et al., 1993; Fernández et al., 1999; Kamondi et al., 1998; Maass et al., 2014) as well as reduced recurrent hippocampal connectivity (see Brankačk et al., 1993; **Figure 1.3**). This connectivity pattern enhances the sensory signal to be bound into memory and prevents interference from reactivation of previously bound traces. During memory retrieval, these hippocampal traces are reactivated, causing reinstatement of the activity pattern present during encoding (Eichenbaum, 2004; Gelbard-Sagiv et al., 2008; Tanaka et al., 2014; Tayler et al., 2013; Waldhauser et al., 2016). Retrieval involves reduced entorhinal input to the hippocampus (Hasselmo et al., 2002)

and increased recurrent hippocampal connectivity (Duncan et al., 2014; Montgomery & Buzsáki, 2007; **Figure 1.3**), maximizing reactivation of traces.

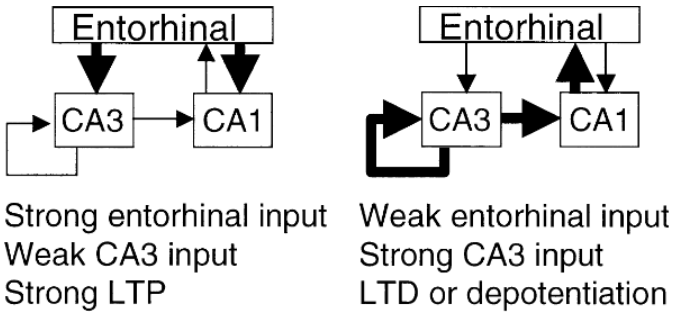

Figure 1.3. **Hypothesized hippocampal connectivity states supporting encoding (left) versus retrieval (right)**. Adapted from Hasselmo et. al, 2002.

It has been hypothesized that the phase of the hippocampal theta oscillation orchestrates the transition between these connectivity states. In rodents, theta synchrony is known to support both memory formation and retrieval (**Section 1.2**), but with potentially different theta phases for these two states. For instance, tetanic electrical stimulation of hippocampal CA1 results in long-term potentiation when delivered at local theta peak versus long-term depression when delivered at local theta trough (Hyman et al., 2003; Hölscher et al., 1997), supporting theta-phase dependence of memory encoding readiness. Further, disrupting the theta cycle appears to differentially impact encoding and retrieval according to local theta phase. In a 2014 study conducted by Siegle & Wilson, mice performed a spatial navigation task where the correct direction to turn for a reward was signaled by environmental cues visible only at the starting location. Using optogenetic stimulation, fast-spiking inhibitory interneurons in CA1 were driven during either the peak or trough of theta as measured at the stimulation site. When stimulation occurred during the encoding segment, memory performance was increased by peak-triggered but not trough-triggered inhibition. In contrast, stimulation during the retrieval segment improved memory when triggered at trough but not peak. These findings support a theta-phase dependence of memory formation versus retrieval in rodents.

1.4 Theta phase varies across the hippocampus

The previous section described a widely hypothesized model in which the phase of the hippocampal theta oscillation relates to hippocampal connectivity states. However, theta phase not unitary throughout the hippocampus; in other words, at a given timepoint, the phase of the theta oscillation varies by hippocampal layer and position on the long axis. How does this spatial phase shift relate to the hypothesized relationship between phase and connectivity?

In depth penetrations of the hippocampal CA1 subfield, theta phase is stable through the strata oriens and pyramidale then undergoes a gradual phase shift. This results in a 180° phase difference at the fissure compared to dorsal layers (Bragin et al., 1995; Brankačk et al., 1993; **Fig. 1.4)**. Studies of theta in rodent models frequently estimate phase at the stratum lacunosum-moleculare of CA1, near the hippocampal fissure. Besides the benefit of fissural theta's especially high amplitude (Brankačk et al., 1993), this approach provides a unitary measure of theta phase. Fissural theta trough versus peak are the phases commonly related to maximal versus minimal receptivity to external input. However, studies in rodents have reported maximal entorhinal input variously at the recorded hippocampal trough (from fissural recording, as in Brankačk et al., 1993), peak (from pyramidal layer recording, as in Douchamps et al., 2013), and falling phases (from recording in variable layers; as in Siegle & Wilson, 2014), depending on laminar depth of the recording.

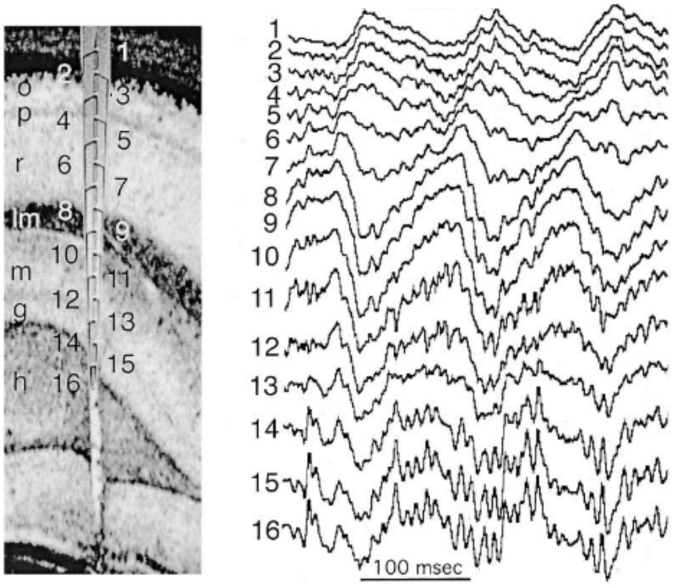

Figure 1.4. **Hippocampal theta phase varies with laminar depth**. Left: probe in the rat CA1-dentate gyrus axis. Right: Theta waves recorded during exploration. Adapted from Bragin et al., 1995 via Buzsáki, 2002.

Recent evidence suggests that theta phase also varies across the long axis of the hippocampus. In rodents, theta phase has been found to fully reverse between the longitudinal poles (Patel et al., 2012). Monotonic phase shift across the long axis has also been demonstrated to occur within individual CA subfields (Lubenov & Siapas, 2009). In a 2015 study, local field potentials were recorded along the human hippocampus via depth electrodes implanted along the long axis . Human hippocampal theta phase was found to shift monotonically across space (Zhang & Jacobs, 2015). The implications of this septotemporal phase shift for phase-dependent connectivity changes have yet to be addressed (see **Chapter 5**).

Chapter 2: Introduction

2.1 Problem Statement

Findings in rodent models have emphasized the relevance of the phase of hippocampal theta to memory function via hippocampal connectivity changes across the theta wave. However, the question of whether hippocampal theta phase is related to instantaneous ability to encode versus retrieve information has not been adequately addressed in humans. This is a critical gap in our current understanding of human memory mechanisms, as hippocampal theta differs in humans versus rodents across key characteristics including dominant frequency, prominence, and the functional significance of high-powered oscillatory bouts (Watrous et al., 2013; Goyal et al., 2020; Buzsáki et al., 1983; Kahana et al., 1999). As such, previous findings from rodent studies are not necessarily generalizable to humans. The question of whether hippocampal processing varies with the phase of the theta oscillation is significant both as a basic insight into human memory mechanisms as well as a potential motivator for new treatments for memory disorders.

2.2 Approach

In this dissertation, I describe two lines of experiments I performed to investigate the relationship between hippocampal theta phase and hippocampal function in humans. Studying human hippocampal theta phase is challenging because it cannot be measured with confidence using noninvasive methods. Each line of experiments presented in this dissertation takes a different approach to address this challenge.

In the first line of research, described in **Chapter 3**, I investigated the foundational hypothesis that human hippocampal connectivity varies according to theta phase. This research capitalized

on a rare opportunity to record directly from the human hippocampus via intracranial stereotactic depth electrodes in a group of patients undergoing invasive monitoring as part of their clinical care. Using direct electrical stimulation as a proxy for endogenous hippocampal network signaling, I stimulated network afferents to the hippocampus and observed the downstream hippocampal evoked potential (EP). I then investigated how the magnitude of the hippocampal response differed according to theta phase at stimulation onset.

In the second line of research, described in **Chapter 4**, I investigated whether episodic memory encoding and retrieval performance varied with the theta oscillation. Instead of observing the theta wave directly, I attempted to causally manipulate hippocampal theta phase using noninvasive transcranial magnetic stimulation (TMS) targeted to a cortical location in the hippocampal network. Using a novel associative memory task designed to align specific phase angles of the theta oscillation to encoding and retrieval events, I then investigated performance on the memory task as a function of stimulation-entrained phase.

2.3 Description of Data Chapters

Chapter 3 contains work which has been previously published as a manuscript. It has been edited from its original form to eliminate redundant background information (Introduction) and contextualize its place in the dissertation (Introduction, Methods, and Discussion). **Full citation:** Lurie, S. M., Kragel, J. E., Schuele, S. U., & Voss, J. L. (2022). Human hippocampal responses to network intracranial stimulation vary with theta phase. *ELife*, *11*, e78395. https://doi.org/10.7554/eLife.78395

Author contributions: Sarah Lurie designed and performed research, wrote data analyses, interpreted results, wrote the initial manuscript, and revised the manuscript. James Kragel performed research, interpreted results, and revised the manuscript. Stephan Schuele performed research and supervised participant eligibility and safety. Joel Voss designed and performed research, interpreted results, and revised the manuscript.

Chapter 4 contains work which has not been previously published as a manuscript. Portions of the Introduction and Materials and Methods sections have been adapted from conference abstracts (for which I was the first author). **Author contributions:** Sarah Lurie designed and performed research, wrote data analyses, and interpreted results. Joel Voss designed research and interpreted results. MRI sequence parameters, as well as the protocols and custom scripts related to selection of in-network stimulation targets based on functional connectivity, were designed and implemented by Jane Wang, Molly Hermiller, Todd Parrish, and Joel Voss.

Chapter 3: Identifying phase-dependent hippocampal responsivity via intracranial stimulation and recording

3.1 Introduction

Hippocampal-dependent memory is thought to be supported by distinct connectivity states, with strong input to the hippocampus benefitting encoding and weak input benefitting retrieval. Previous research in rodents suggests that the hippocampal theta oscillation orchestrates the transition between these connectivity states, with opposite phase angles predicting minimal versus maximal input (see **Chapter 1**). However, it is unclear whether the human hippocampus exhibits a homologous phase dependence of its connectivity state.

In **Chapter 3**, I describe an experiment which tests predictions of this theta phase-dependent connectivity model using invasive hippocampal recordings. We recorded local field potentials from the hippocampus in patients undergoing intracranial electrophysiological recording via implanted depth electrodes as part of their clinical care. We applied direct electrical stimulation to hippocampal network sites in lateral temporal cortex with putative projections to entorhinal cortex and hippocampus (Insausti et al., 1987; Catani & Thiebaut de Schotten, 2008; Zhong & Rockland, 2004), and measured the hippocampal response to lateral temporal stimulation using well-characterized early and late evoked-potential components (Matsumoto et al. 2004, Novitskaya et al. 2020). We hypothesized that if hippocampal receptivity to network input varies with the theta oscillation, then the hippocampal response to stimulation would differ according to hippocampal theta phase at the time of stimulation delivery.

In humans, unlike in animal models, direct recordings of hippocampus can only be collected opportunistically as part of a patient's clinical care for neurological disease or injury (i.e. via stereotactic electroencephalography, or sEEG). This method has a number of limitations. Electrodes are typically implanted in brain areas specifically affected by disease (often targeting the suspected seizure onset zone in patients with epilepsy); electrode placement is highly variable, according to the patient's pathology and clinical needs; and the constraints of working in a clinical setting can preclude long or complicated behavioral studies (see Parvizi & Kastner, 2018). Nonetheless, invasive recordings provide invaluable insight into ensemble activity. In particular, sEEG's high temporal resolution allows for unique investigation into the oscillatory dynamics of deep brain structures like the hippocampus.

In rodents, fissural theta trough versus peak are the phases commonly related to maximal versus minimal receptivity to external input (e.g., Hasselmo, 2005). However, previous studies in rodents have reported disparate phase angles relating to maximal entorhinal-hippocampal transmission, likely due to differences across studies in the targeted hippocampal layer. Because the theta oscillation arises from interlaminar dipoles (Goutagny et al., 2009; Kamondi et al., 1998), its observed phase varies according to electrode depth. Studies in rodents have therefore reported maximal entorhinal input variously at the recorded hippocampal trough (from fissural recording, as in Brankačk et al., 1993), peak (from pyramidal layer recording, as in Douchamps et al., 2013), and falling phases (from recording in variable layers, as in Siegle & Wilson, 2014). Thus, we anticipated 180-degree separation in phases associated with maximal versus minimal receptivity in humans, without strong hypotheses for which phase angles would be associated with these states given the localization uncertainty in electrodes placed for clinical purposes in human subjects. We therefore tested this hypothesis by first analyzing continuous variation in

amplitude based on theta phase following stimulation. We used a novel method to account for the phase-dependence of amplitude values that occurs irrespective of stimulation. To test selectivity, we analyzed theta phase dependence for non-hippocampal control locations in the amygdala and orbitofrontal cortex.

3.2 Materials and Methods

Electrode localization

sEEG electrodes were localized using MRIcron (v1.0.20190902; Rorden & Brett, 2000) and the Statistical Parametric Mapping package (SPM12; Penny et al., 2011). Pre-implant T1-weighted structural MRI and post-implant computed tomography (CT) were acquired as part of clinical care. For each subject, we performed tissue-type segmentation on the MRI (with default SPM12 tissue probability maps and warping parameters; see Ashburner & Friston, 2005; Mechelli et al., 2005) then normalized the MRI to MNI space (ICBM Average Brain template MNI152; Mazziotta et al., 1995). We applied this same transformation to the CT, which had been co-registered to the MRI by normalized mutual information. We then localized electrodes within MNI space by visual inspection of the CT. The anatomical location of each electrode was confirmed by atlas-guided inspection of the MRI (Allen Human Brain Atlas; Ding et al., 2016). We were unable to obtain imaging data for one subject and therefore relied on the electrode localization provided by the clinical team (comprising surrounding tissue type and anatomical structure for each electrode).

sEEG recording and stimulation

sEEG depth electrodes (~1-mm diameter, ~2-mm contact length, 5-10-mm contact spacing; AD-Tech, Oak Creek, WI) were implanted prior to study participation according to clinical need.

Recordings were acquired using a Neuralynx ATLAS system with a scalp electrode reference and ground. Data were recorded at a resolution of 0.15 μV (5000 μV input range) and a sampling rate of 20 kHz or 32 kHz. Digital bandpass filters (FIR) from 0.1 to 5000 Hz were applied at the time of recording. Data were re-referenced offline to the common average of ipsilateral depth electrodes (Zhang & Jacobs 2015, Van Der Meij et al., 2012) and downsampled to 1 kHz. Data were epoched about stimulation pulses and baseline corrected (epoch: -750 ms to 500 ms, baseline: -750 ms to -2 ms). To prune excessively noisy or artifactual data, epochs were excluded according to their signal range (excluded if > 800 μV) and kurtosis (excluded if > 2 SD over channelwise mean kurtosis; Mean epochs pruned per channel ± SD, hippocampus: $n = 208 \pm 329$ epochs; amygdala: $n = 275 \pm 333$ epochs; orbitofrontal cortex: $n = 250 \pm 347$ epochs. Mean epochs included in analyses per channel ± SD, hippocampus: $n = 1194 \pm 599$ epochs; amygdala: $n = 1341 \pm 348$ epochs; orbitofrontal cortex: $n = 1479 \pm 263$ epochs. Channels were excluded from analyses if < 200 epochs remained following pruning. $n = 3$ hippocampal channels, $n = 3$ amygdala channels, and $n = 5$ orbitofrontal channels were excluded from analyses on this basis.

Electrical stimuli were generated with a Grass Instruments S88 stimulator in conjunction with CCU1 constant current units and SIU5 stimulus isolators. Stimulation was delivered across two adjacent lateral temporal sEEG electrodes. The electrical stimulus comprised a constant-current, symmetric-biphasic square wave with 5 mA intensity and 0.6 ms total duration. Stimulation polarity was reversed across the two electrodes such that stimulation on the lateral electrode was anodic-leading and stimulation on the medial electrode was cathodic-leading. For simplicity we refer to each electrical stimulus as a “single pulse.”

Stimulating electrodes used for the experiment were selected during a preliminary stimulation session to identify electrodes with hippocampal functional connectivity (i.e., for which stimulation would evoke downstream hippocampal evoked potentials) and for which stimulation would not be clinically problematic. Potential stimulating electrode pairs were identified in lateral temporal cortex and adjacent white matter based on well-characterized structural and functional connectivity of these regions with ipsilateral entorhinal cortex and hippocampus (Insausti et al., 1987; Catani & Thiebaut de Schotten, 2008; Zhong & Rockland, 2004). Of these, we excluded electrodes where stimulation provoked seizure or afterdischarges during clinical testing. To evaluate functional connectivity with hippocampus, trains of stimulation were delivered to each potential electrode pair (0.5 Hz; 30 pulses per pair). Mean EPs for each hippocampal electrode were visualized in real-time and manually inspected. The lateral temporal electrode pair for which stimulation elicited the largest mean EP for hippocampal electrodes was selected for the experimental protocol. A single pair of stimulating electrodes was selected for each participant (n = 16 total stimulating electrodes).

Participants remained in bed throughout the preliminary stimulation session and experimental session. They were not instructed to perform any task and were free to rest or otherwise occupy themselves. Study protocols were approved by the Northwestern University Institutional Review Board. All subjects provided written informed consent prior to participation.

Theta phase estimation

We estimated hippocampal theta (3 – 8 Hz) phase at the time of stimulation onset for each trial. This was done separately for each electrode because theta phase shifts across space in the hippocampus (see **Chapter 1**). Electrodes for invasive recordings are placed according to clinical need, and their locations therefore vary across subjects in both laminar depth and

location on the long axis. As the phase shift is stable across layers and septotemporal distance (Lubenov & Siapas, 2009), phase at a given hippocampal macroelectrode is consistent relative to other hippocampal macroelectrodes (Zhang & Jacobs, 2015). To account for this offset, we estimated phase independently for each electrode. First, trial epochs were truncated at +50 ms (i.e., 50 ms following stimulation onset) to avoid contamination of the phase estimate by the stimulation EP. After applying a zero-phase bandpass-filter (3-8 Hz 2^{nd}-order Butterworth IIR), we estimated phase angle at the time of stimulation onset using the Hilbert transform.

We assessed the accuracy of this approach using stimulation-free pseudotrials. For each hippocampal electrode, we first performed zero-phase bandpass filtering (3-8 Hz, 2^{nd}-order Butterworth IIR) across a continuous stimulation-free period (from the same recording as used in the main analysis). We then applied the Hilbert transform to obtain ground-truth phase angles for each timepoint. We created stimulation-free trials by pseudorandomly selecting trial-length epochs during this stimulation-free period. We observed the ground-truth phase values at the timepoints corresponding to each trial's mock stimulation onset. Epochs from the first and last 5s of the recording sessions were excluded to reduce filter edge artifact contamination.

Next, we created an ostensibly phase-balanced model of stimulation for each channel by binning stimulation trials at 90˚ intervals (centered at 0˚, 90˚, 180˚, and 270˚) and computing the grand average across bins. We added this model stimulation to each stimulation-free trial, yielding pseudotrials. We estimated pseudotrial phase angle at t = 0 using the approach described for stimulation trials and compared the estimates to the ground truth phase angles.

Analysis of narrowband theta activity

To assess whether theta-frequency activity was present in hippocampus and control regions, we characterized narrowband activity across the power spectrum during a continuous stimulation-free period (from the same recording as used in the main analysis; all rest periods had duration > 90s). We estimated oscillatory power at 50 logarithmically-spaced frequency intervals from 1-50 Hz using the fast Fourier transform. To identify frequencies where reliable oscillations were present, we first estimated the background $1/f$ power spectrum using a robust linear fit to the log-log scaled power spectrum (Lega et al., 2012). We subtracted this background from the power spectrum and identified positive local maxima in the resultant curves, following four-frequency boxcar smoothing to eliminate noisy peaks (Lega et al., 2012). We performed this analysis for individual electrodes as well as for the mean power spectrum across all analyzed electrodes within each ROI. For each identified peak frequency, we assessed whether its power consistently exceeded the background $1/f$ spectrum by performing one-sample t-tests of the corrected spectrum power versus 0 across electrodes.

Quantification of hippocampal EPs

As a measure of the hippocampal response to stimulation, we quantified the trialwise amplitudes of early and late components in the stimulation EP. We first estimated component timecourses for each electrode. To avoid phase-dependent differences in component shape or timecourse from biasing this estimate (i.e., in the case of non-uniform stimulation phase distributions), we computed a phase-balanced EP for each electrode by binning stimulation trials according to theta phase at stimulation onset (at 90˚ intervals, centered at 0˚, 90˚, 180˚, and 270˚) and computing the mean across bins. We then observed the grand average phase-balanced trial across electrodes. We quantified component timecourses by searching for the first two negative minima following

stimulation artifact (on a search window of +20 ms to +500 ms after stimulation; see e.g., Kubota et al., 2013) on the grand average trial across electrodes. Component edges were estimated as the nearest inflection points within 150 ms of the local maximum. A minimum interval of 50 ms was required between peaks. For each trial, we computed the average signal amplitude across each component timecourse. This method was selected rather than peak estimation (as in e.g. Matsumoto et al. 2004) in order to produce a more noise-indifferent estimate for single trials.

Circular-linear analysis of theta phase and hippocampal response amplitude

We performed circular-linear analyses to determine whether the hippocampal response varied continuously with theta phase at stimulation onset. For each electrode, we found the circular-linear correlation coefficient between phase at stimulation onset and component amplitude (Berens, 2009). We z-scored these values via permutation testing (n = 500), wherein each electrode's trial phase values and component amplitudes were repeatedly randomly paired. The circular-linear correlations were evaluated using a one-sample t-test comparing the electrode z-scores against zero. To investigate the timecourse of the continuous phase-amplitude relationship, we performed a follow-up timepoint analysis. For each electrode, we computed the circular-linear correlation coefficient between phase at stimulation onset and EP amplitude at every timepoint. We identified peaks in the phase-amplitude relationship by searching for the first two maxima following stimulation artifact (on a search window of +20 to +500 ms after stimulation). This method was modified from our procedure to identify components in the EP amplitude timecourse (see **Quantification of hippocampal EPs**).

Comparison of hippocampal EPs following stimulation at binned phase angles

To test how specific phase angles were related to hippocampal responsiveness to stimulation, we analyzed trials according to theta phase at stimulation onset. We estimated local broadband theta

phase at stimulation onset for each trial and binned trials to 90˚ intervals, centered on peak, trough, rising and falling phase angles. By taking the means within each bin, we obtained average peak, trough, rising and falling stimulation trials for each electrode. We then compared component amplitudes across peak versus trough and rising versus falling trials using paired t-tests.

Comparison of stimulation trials to phase-matched stimulation-free trials

Direct comparison of component amplitudes according to phase at stimulation onset is complicated because oscillatory phase necessarily predicts future amplitude, regardless of any phase-dependent differences in the effects of stimulation on EPs. We therefore used stimulation-free trials to account for the ongoing theta oscillation. Stimulation-free trials were captured for each electrode at 100-ms intervals across stimulation-free periods at the beginning and end of the recordings. Stimulation-free trials were recorded and preprocessed using the same approach as stimulation trials (for trial pruning by kurtosis, kurtosis scores were compared only to other stimulation-free trials from the same channel). Phase was estimated for each trial at $t = 0$ using the same methods as for stimulation trials (i.e., truncating at +50 ms after stimulation onset, filtering, and applying the Hilbert transform). In order to more closely match the non-evoked activity present in the stimulation trials, we randomly resampled stimulation-free trials using the phase angle distributions of the stimulation trials as sampling weights.

Timepoint analysis of EP amplitude following stimulation at theta peak versus trough

As a follow-up to our analysis of peak versus trough effects on component amplitudes, we investigated whether phase dependence was temporally restricted to components. For each electrode, we computed the difference between average peak and trough trials at each timepoint.

To assess the contribution of the non-evoked signal over time, we repeated this procedure on stimulation-free trials. To measure phase dependence related to the evoked signal, we compared peak-trough amplitude differences across stimulation and stimulation-free trials.

Oscillatory synchronization between the stimulation site and hippocampus

Although we estimated hippocampal theta phase angle at the time of stimulation onset to avoid bias from the evoked response, this timepoint is not the most relevant to hippocampal receptivity to external input. As stimulation was applied to lateral temporal network afferents and conveyed via polysynaptic signaling, there was likely some latency between stimulation onset and the relevant transmission to hippocampus (i.e., the timepoint when entorhinal input receptivity would be relevant).

Oscillatory synchronization (i.e., phase coupling) is a known mechanism that supports interregional communication (see Fries, 2005; Fell & Axmacher, 2011). We therefore estimated this latency by observing theta phase locking and phase offset between the stimulation site and hippocampus. First, we estimated 3 – 8 Hz theta phase angle for each electrode across a continuous, stimulation-free period in the recording. For each timepoint, we then obtained the angular distance between each hippocampal electrode and its corresponding lateral temporal electrode that was used for stimulation. We thereby computed the phase-locking value (PLV; mean resultant vector length of lateral temporal-hippocampal angular distance on the unit circle) and mean phase offset (the circular mean of lateral temporal-hippocampal angular distances) for each hippocampal electrode.

We applied the Rayleigh test to the mean phase offsets to assess whether the phase lag distribution was uniform. We used permutation testing to determine whether the observed phase

locking was greater than expected by chance. To achieve this, we broke the continuous hippocampal and lateral temporal phase estimates into 500-ms epochs. We then obtained the mean PLV across all epochs. To z-score these PLVs, we used permutation testing (n = 500), wherein hippocampal and lateral temporal epochs were repeatedly randomly paired. We performed a one-sample t-test comparing z-scores against zero to assess phase locking.

3.3 Results

Participants and stimulation protocol

Data were collected from eight individuals with refractory epilepsy (two male; mean age ± SD: 37 ± 10 years; range 28-55 years; **Table 3.1**) undergoing invasive electrophysiological monitoring as part of their inpatient clinical care at the Northwestern Memorial Hospital Comprehensive Epilepsy Center. All participants had stereotactic EEG (sEEG) depth macroelectrodes (Ad-Tech, Oak Creek, WI) implanted in hippocampus, amygdala, lateral temporal cortex, and orbitofrontal cortex, in addition to other regions. All stimulating electrodes were localized to lateral temporal cortex and adjacent white matter (**Fig. 3.1a,b**).

In seven participants, the experimental stimulation protocol consisted of trains of single pulses delivered at either 0.5 Hz (~60 pulses per train) or approximately 1 Hz (with an interpulse interval range of 1-1.25 s, jittered pseudorandomly, ~1200 pulses per train; interpulse interval and range of jitter values were selected to enable data analysis for a secondary experiment). These train types were alternated with approximately two minutes of rest between trains. In one participant, stimulation was delivered at 0.5 Hz only. The number of stimulation pulses delivered ranged from 241 to 2566 (**Table 3.1**). Stimulation did not elicit seizure or clinically significant afterdischarges in any participant.

Table 3.1. Participant characteristics.

Sex	Age	Hemisphere of electrodes	# hippocampal recording electrodes analyzed	Pulses delivered	Stimulation protocol
F	28	Right	3	1721	0.5Hz and 1Hz
F	29	Left	3	1576	0.5Hz and 1Hz
F	30	Left	3	1170	0.5Hz and 1Hz
F	44	Left	4	241	0.5Hz
F	55	Left	1	2566	0.5Hz and 1Hz
F	47	Left	3	1036	0.5Hz and 1Hz
M	31	Left	4	1766	0.5Hz and 1Hz
M	29	Right	2	982	0.5Hz and 1Hz

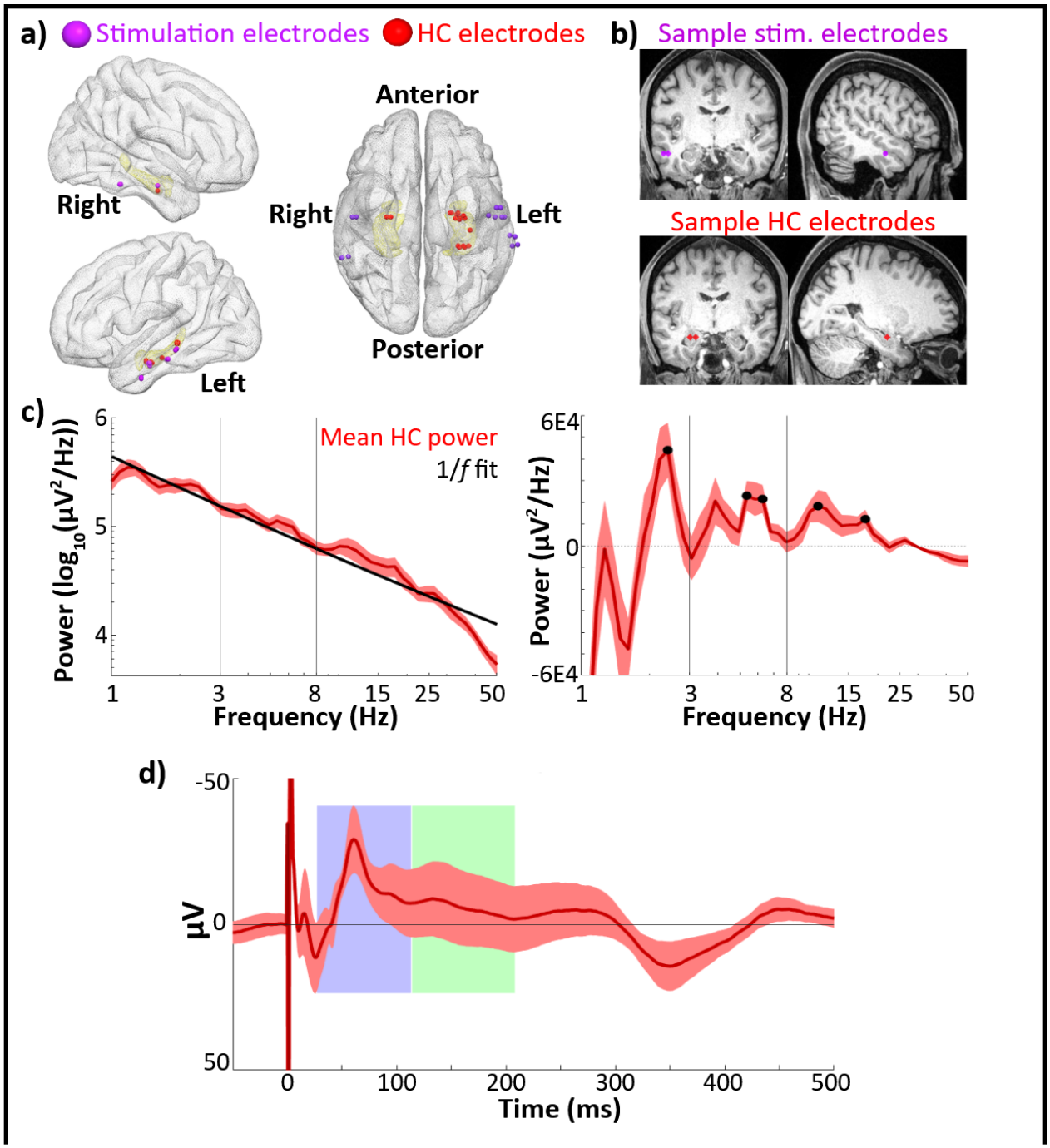
a)
Stimulation electrodes
HC electrodes
Right
Left
Anterior
Posterior
Right
Left
b)
Sample stim. electrodes
Sample HC electrodes
c)
Mean HC power
1/f fit
Power (log10(μV²/Hz))
Frequency (Hz)
Power (μV²/Hz)
Frequency (Hz)
d)
μV
Time (ms)

Figure 3.1. Hippocampal recordings and evoked response. A) Group-level electrode localization for lateral temporal stimulating electrodes (n = 14) and hippocampal recording electrodes (n = 18) plotted on an MNI template (Holmes et al., 1998). Amygdala and hippocampus are highlighted in yellow. Electrodes are enlarged ~500% for visualization purposes. Note: Imaging was unavailable in one subject (see **Materials and methods: Electrode localization**). Hippocampal recording electrodes did not align to the template brain hippocampus in one subject and are not shown in this image. B) Locations of lateral temporal stimulating electrodes (top) and recording electrodes in hippocampus (bottom) in one sample participant. C) Mean power spectral densities across all hippocampal recording electrodes (n = 23). Power was assessed during a recorded pre-stimulation rest period. Left: Mean power spectral density (red) and estimated 1/f fit (black). Right: Mean 1/*f*-corrected power spectral density across hippocampal recording electrodes. Significant peaks in oscillatory power marked in black. Error bars indicate ±1 SEM across electrodes. D) Phase-balanced grand average hippocampal EP (i.e., 0˚, 90˚, 180˚, and 270˚ phase bins contribute equally to the average) elicited by lateral temporal stimulation. Error bars indicate ±1 SEM across hippocampal recording electrodes. Identified early and late negative components are highlighted in blue and green. The Y-axis shows negative values in the upwards direction to emphasize the negative-going EP components of interest.

Hippocampal recordings showed narrowband oscillations within the 3-8Hz theta range

To ensure the presence of theta activity in hippocampal local field potentials (LFPs), we assessed the power spectral densities of recordings taken during a rest period before the stimulation experiment. We estimated oscillatory power during this pre-stimulation period rather than during the experimental session to avoid contaminating the estimate with the evoked response to stimulation. We located narrowband oscillations by fitting a 1/*f* background distribution to the power spectrum (**Fig. 3.1c**), subtracting this background, and estimating local peaks in the resultant curve (see **Materials and Methods: Analysis of narrowband theta activity**). All analyzed hippocampal recording electrodes (as well as all amygdala and OFC control region recording electrodes) showed at least one narrowband oscillation in the 3-8Hz range. Across hippocampal recording electrodes, multiple local peaks in oscillatory power were detected within

the 3-8Hz theta band (**Fig. 3.1c**). Peaks where power was significantly greater than the 1/f background spectrum across electrodes were detected within the 3-8 Hz theta range at 5.3 Hz and 6.3 Hz (t-test of corrected power versus 0, 5.3 Hz: $t(22) = 3.4$, $p = 0.003$; 6.3 Hz: $t(22) = 3.3$, $p = 0.003$). An additional peak was detected at 3.9 Hz; however, power at this lower frequency was only marginally above the 1/*f* background spectrum (3.9 Hz: $t(22) = 1.9$, $p = 0.07$). Peaks with significant power above background were also detected at 2.4 Hz, 11.0 Hz, and 17.7 Hz (**Fig. 3.1c**; all $p < 0.05$ on t-test of corrected power versus 0).

Hippocampal evoked potentials showed characteristic early and late negative components

Hippocampal EP components were estimated to occur from 27-113 ms (early) and 114-208 ms (late) post-stimulation (**Fig. 3.1d**; see **Materials and Methods: Quantification of hippocampal EPs**). The observed component latencies were consistent with values reported by previous studies of human hippocampal response to direct electrical stimulation of polysynaptic afferents (e.g., Kubota et al., 2013; Novitskaya et al., 2020).

Hippocampal EP amplitudes varied according to theta phase at stimulation onset

We performed circular-linear analyses to determine whether hippocampal receptivity to lateral temporal stimulation varied continuously (i.e., sinusoidally) with the phase of the theta oscillation. We first assessed whether amplitudes of the early and late EP components (**Fig. 3.1d**) varied with theta phase at stimulation onset (see **Materials and Methods: Theta phase estimation**). For each electrode, we computed circular-linear correlation between hippocampal phase at stimulation onset and component amplitude across stimulation trials. Permutation testing was used to assess whether periodicity in evoked response amplitude was above chance. Both early and late component amplitudes were significantly predicted by theta phase at

stimulation onset (**Fig. 3.2a**. Mean z-score ± SD, early: $z = 1.3 \pm 1.9$; late: z 1.2 ± 1.6. t-test of z-scores versus 0, early: $t(22) = 3.3$, $p = 0.003$, *Cohen's d* = 0.7; late: $t(22) = 3.7$, $p = 0.001$, *Cohen's d* = 0.8. Mean r ± SD, early: $r = 0.080 \pm 0.066$; late: $r = 0.076 \pm 0.051$).

To assess whether the phase-amplitude relationship was appropriately captured by the early and late components, we performed an exploratory analysis of the phase-amplitude relationship across all timepoints in the peri-stimulation period. Additionally, to investigate whether the observed effect was caused by phase-dependent changes in the evoked response (as opposed to phase-dependent amplitude of the non-evoked, theta oscillatory component of the signal), we assessed the timecourse of the phase-amplitude relationship for the non-evoked response by performing the same analysis for phase-matched, stimulation-free trials (see **Materials and methods: Comparison of stimulation trials to phase-matched stimulation-free trials**).

In both stimulation-free and stimulation trials, the phase-amplitude relationship was strongest before and up to stimulation onset (**Fig. 3.2b,c**). The asymmetric dropoff about t = 0 likely relates to the phase estimation method (i.e., amplitude before stimulation is more strongly predictive of phase because it contributes directly to the phase estimate; see **Fig. 3.6b**). In stimulation-free trials, the phase-amplitude relationship timecourse following t = 0 was generally smooth and monotonic (**Fig. 3.2b**). In contrast, stimulation trials exhibited local increases in circular-linear correlation (**Fig. 3.2c**). Qualitatively, the local increases appeared to coincide with the early and late EP components (as plotted in **Fig. 3.1d**). Using the same peak-finding method that identified peaks in the EP (see **Materials and Methods: Quantification of hippocampal EPs**), we found peaks in the phase-amplitude relationship at +50 ms and +135 ms following stimulation onset, which aligns closely with the early and late EP components (+62 ms and +134

ms, respectively; **Fig. 3.2c**). Stimulation trials also exhibited a sharp local decrease from approximately +0 to +5 ms following stimulation, likely due to phase-independent artifact during and immediately after the stimulation pulse (**Fig. 3.2c**). These findings indicate that hippocampal theta phase at stimulation onset predicts its responsiveness to lateral temporal stimulation, and that these effects are well captured by analyses of characteristic early and late components of the hippocampal EP.

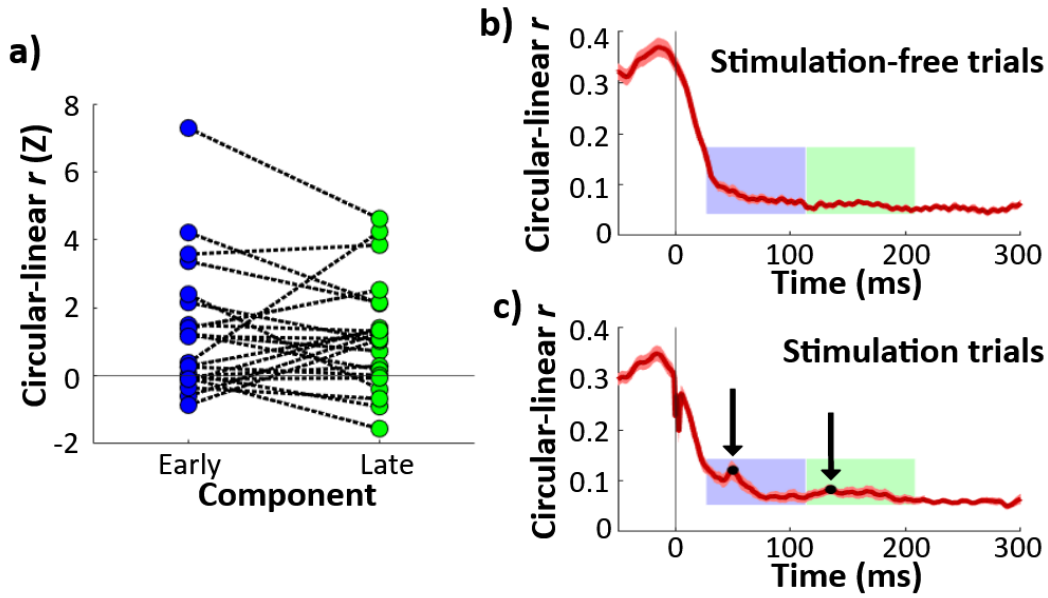

Figure 3.2. Continuous theta phase predicted response amplitude during early and late EP components. A) Z-scored circular-linear correlation r for the relationship between hippocampal theta phase at stimulation onset and EP component amplitude. Each line represents one electrode. Z-scores are shown for early (left) and late (right) components. Horizontal line shows chance-level circularity. Both early and late components showed significant theta-circularity (** $p < 0.01$). B) Circular-linear r plotted for each timepoint for stimulation-free trials, Error bars indicate ±1 SEM across hippocampal recording electrodes. Early and late component timecourses highlighted in blue and green for reference. C) As B, for stimulation trials. Local maxima denoted in black.

Hippocampal EP amplitudes varied for theta peak versus trough

Given the previous rodent findings of maximal differences in receptivity to input at specific hippocampal theta phase angles (e.g., trough versus peak; Brankačk et al., 1993; Hasselmo et al., 2002), we tested whether the phase-dependent responsivity of the hippocampus to stimulation identified in the analyses above varied for specific theta phase angles. We estimated theta phase at stimulation onset for each trial (see **Materials and Methods: Theta phase estimation**) and binned trials to 90˚ intervals, centered on peak, trough, rising and falling phases. By taking the means within each bin, we obtained average peak, trough, falling, and rising angle stimulation trials for each electrode (**Fig. 3.3a, c**).

As phase at a given timepoint predicts future amplitude by definition, when trials are sorted according to theta phase at stimulation, differences are expected in the post-stimulation signal simply owing to the ongoing theta oscillation. We therefore isolated the evoked response from this non-evoked oscillation in order to assess whether the evoked response itself varied according to stimulation phase. We estimated the non-evoked oscillation using phase-matched stimulation-free trials (see **Materials and Methods: Comparison of stimulation trials to phase-matched stimulation-free trials**). We binned stimulation-free trials to 90˚ intervals using the same approach as for the stimulation trials. By taking the mean of stimulation-free trials within each bin, we estimated the non-evoked component of the peak and trough EPs for each electrode (red lines in **Fig. 3.3a,c**). As expected, the non-evoked component was an oscillation with asymmetrical coherence drop-off around stimulation onset (see Fig. **3.6b**). Finally, to isolate the evoked response, we subtracted this non-evoked component from its corresponding EP. This procedure abolished pre-stimulus amplitude differences between peak versus trough and rising

versus falling trials across hippocampal recording electrodes, indicating good removal of the ongoing oscillatory component (Paired t-test on mean amplitudes -100 to 0 ms, peak versus trough: $t(22) = 0.47$, $p = 0.6$; rising versus falling: $t(22) = 1.4$, $p = 0.2$).

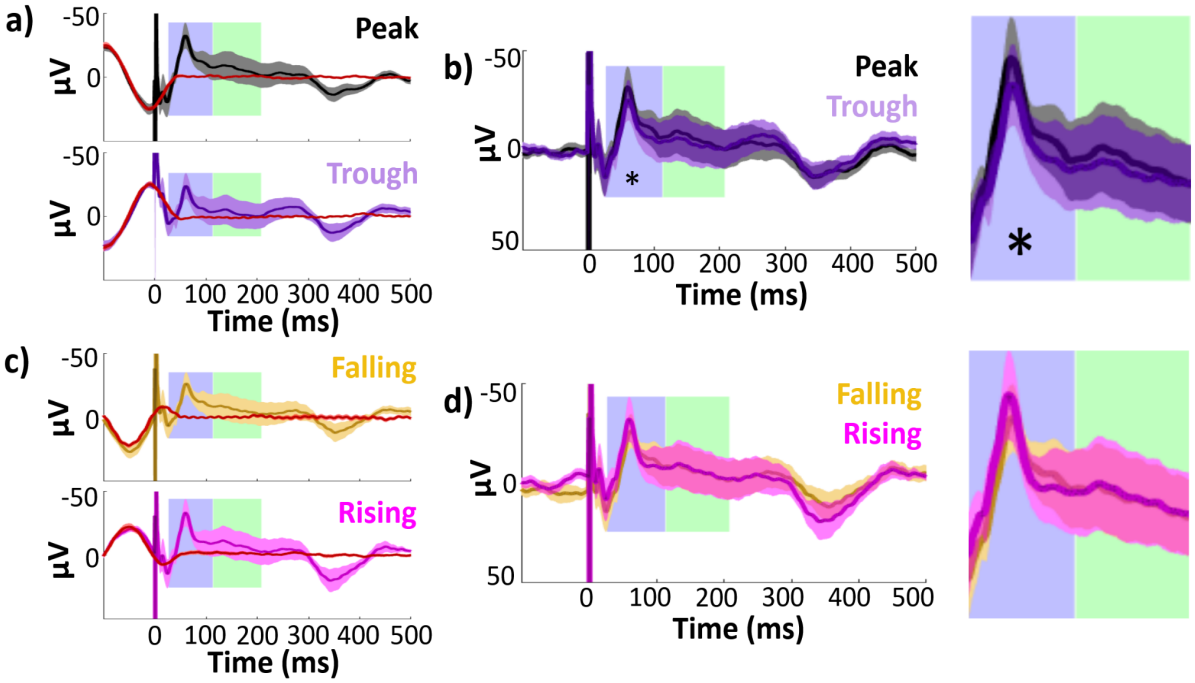

Figure 3.3. Hippocampal EPs and isolated responses binned according to theta phase at stimulation delivery. Early and late component timecourses highlighted in blue and green for reference. A) Mean hippocampal EPs elicited by lateral temporal stimulation at theta peak (black) and trough (purple), alongside phase-matched stimulation-free trials (red; see **Materials and Methods: Comparison of stimulation trials to phase-matched stimulation-free trials**). Error bars indicate ± 1 SEM across recording electrodes. Theta oscillation is visible around stimulation at t = 0. The isolated response was obtained by subtracting the mean phase-matched stimulation-free trial from the EP. B) Isolated hippocampal evoked responses to peak and trough stimulation. The non-evoked oscillatory component is abolished in the isolated response. Asterisk indicates isolated response components with significant amplitude differences across phase bins at 180˚ intervals (i.e., peak versus trough or rising versus falling trials; * $p \leq 0.05$). Left: Full timecourse. Right: Enlarged panels showing component timecourses. C, D) As in A) and B), for stimulation at theta falling (yellow) versus rising (magenta) phase angles.

The early and late EP components showed significant amplitude differences following peak versus trough stimulation (**Fig. 3.4a**. Paired t-test across hippocampal recording electrodes, early: $t(22) = -2.7$, $p = 0.01$, *Cohen's d* = -0.2; late: $t(22) = -2.6$, $p = 0.02$, *Cohen's d* = -0.08. Mean peak - trough amplitude difference ± SD, early: *diff* = -4.9 ± 8.5 μV, *diff* = -3.9 ± 7.2 μV). Isolation of the evoked response (**Fig. 3.3b**) reduced the differences between peak and trough stimulation in the late component (**Fig. 3.4b**. Paired t-test: $t(22) = -1.1$, $p = 0.3$, *Cohen's d* = -0.04). However, the peak versus trough effect in the early component persisted through the isolation procedure (**Fig. 3.4b**. Paired t-test: $t(22) = -2.1$, $p = 0.05$, *Cohen's d* = -0.2; mean amplitude difference ± SD, early: *diff* = -4.8 ± 11 μV; late: *diff* = -2.2 ± 10 μV).

No difference in EP amplitude was observed for rising versus falling stimulation conditions (**Fig. 3.3c**) for either early or late components (**Fig. 3.4c**. Paired t-test across hippocampal recording electrodes, early: $t(22) = 0.45$, $p = 0.7$, *Cohen's d* = 0.04; late: $t(22) = 0.55$, $p = 0.6$, *Cohen's d* = 0.03; mean falling - rising amplitude difference ± SD: early: *diff* = 1.1 ± 11.3 μV; late: *diff* = 1.6 ± 14.0 μV). As was the case in the overall EP, no differences were observed in the isolated response for falling versus rising stimulation (**Fig. 3.4d**. Paired t-test across hippocampal recording electrodes, early: $t(22) = 0.14$, $p = 0.9$, *Cohen's d* = 0.02; late: $t(22) = 0.41$, $p = 0.7$, *Cohen's d* = 0.02; mean falling - rising amplitude difference ± SD, early: *diff* = 0.52 ± 16.6 μV; late: *diff* = 1.4 ± 16.2 μV).

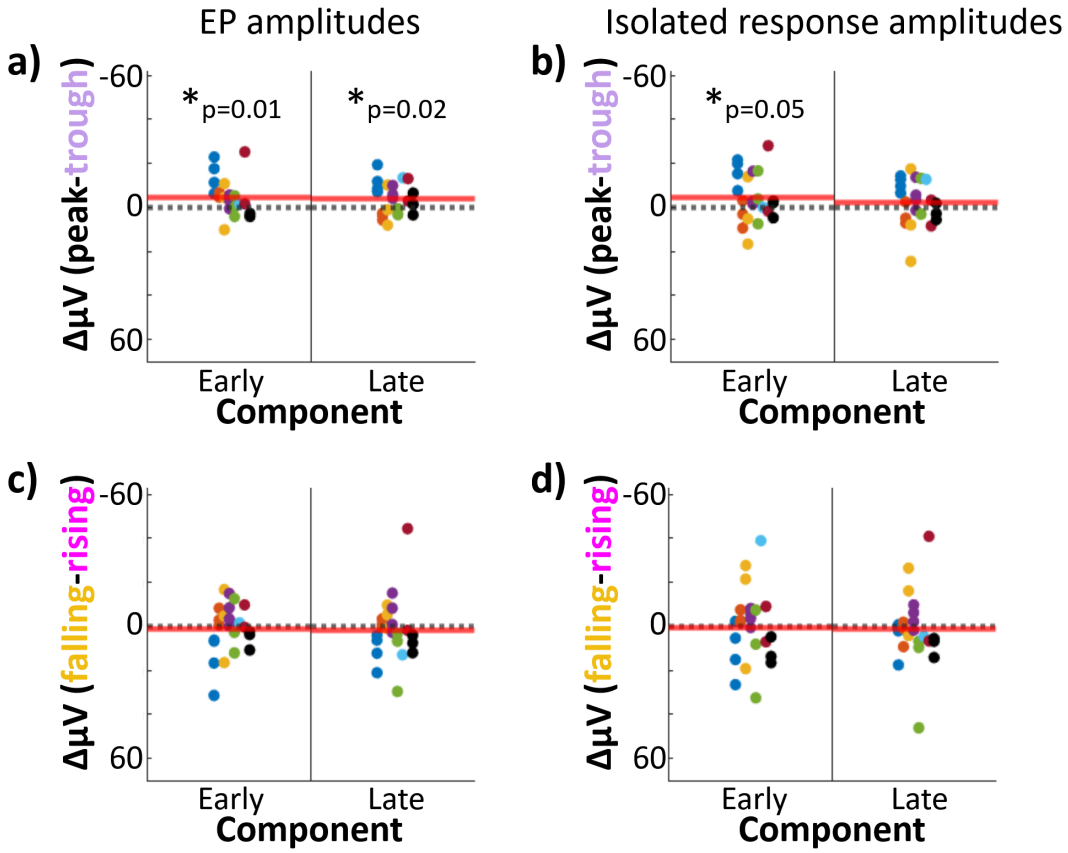

Figure 3.4. Stimulation at theta peak versus trough produced differences in early-component amplitude. Hippocampal component amplitudes by theta phase of stimulation. A, C) Difference between hippocampal EP component amplitudes elicited by lateral temporal stimulation delivered at peak versus trough (a) and falling versus rising (c) phases. Each dot represents one electrode; dot color indicates participant-of-origin. Red line indicates the mean difference across electrodes. Left: early component amplitude difference. Right: late component amplitude difference. B, D) As in A) and C), but for the isolated hippocampal response (i.e., EP minus phase-matched stimulation-free trials).

Control regions did not show early-component specific periodicity in the response to stimulation

To assess whether theta-dependence of EP amplitude was specific to hippocampus, we performed the same analyses on data from recording electrodes in amygdala (n = 9) and orbitofrontal cortex (n = 22). Data from control regions was acquired concurrently with the hippocampal data described above.

In both control regions, stimulation EPs had distinct early and late negative components (**Fig. 3.5a**, e. In amygdala, components were estimated to span 35-70 ms (early) and 94-256 ms (late). In OFC, components spanned 22-74 ms (early) and 74-490 ms (late).

We performed circular-linear analyses to investigate whether control regions exhibited a continuous relationship between phase and EP amplitude. As we did in our analysis of the hippocampal phase-amplitude relationship (**Fig. 3.2b,c)**, we assessed the circular-linear correlation between phase and amplitude for each control region electrode at each timepoint of the EP. To control for the contribution of the non-evoked oscillatory signal to this relationship, we assessed the phase-amplitude relationship for both stimulation trials and stimulation-free trials. As was the case in the hippocampal EP, we observed the strongest phase-amplitude relationship before and up to stimulation onset (**Fig. 3.5b,f**), with asymmetric dropoff about t = 0 likely due to the phase estimation method. In contrast to the hippocampal EP (see **Fig. 3.2c**), both control regions showed more diffuse deviations in the phase-amplitude relationship. In particular, neither control region showed the clear, temporally-specific increase in circular-linearity during the early component which was present in the hippocampal EP.

As in the analysis of the hippocampal response, we next binned EP trials according to phase at stimulation onset and compared component amplitudes across peak and trough trials. The amygdala EP showed significant amplitude differences across peak and trough trials in the late component (paired t-test: $t(8) = -4.1$, $p = 0.003$, *Cohen's d* = -0.2), with greater amplitude for peak trials (**Fig. 3.5c**. Mean difference ± SD: -5.5 ± 4.0 μV). There was no significant amplitude difference in the early component ($t(8) = 0.85$, $p = 0.4$, *Cohen's d* = 0.3). This effect persisted after we isolated the evoked response using phase-matched stimulation-free trials (late: $t(8) =$

-3.1, $p = 0.02$, *Cohen's d* = -0.2; mean difference ± SD: -5.3 ± 5.2 μV). Similarly, we observed amplitude differences for amygdala rising versus falling trials selective to the late component (**Fig. 3.5d**. Early: $t(8) = -0.29$, $p = 0.8$, *Cohen's d*= -0.06; late: $t(8) = 2.7$, $p = 0.03$, *Cohen's d* = 0.1), which persisted through isolation of the evoked response (early: $t(8) = 1.2$, $p = 0.3$, *Cohen's d*= 0.2; late: $t(8) = 4.7$, $p = 0.002$, *Cohen's d* = 0.2).

We hypothesized that the phase-dependence of the late component may have been driven by secondary transmission from the hippocampus. However, we did not find a consistent correlation between hippocampal EP and amygdala late component timing (see**Hippocampal EP timing did not predict amygdala late component latency**).

In contrast, for orbitofrontal EPs, we found no differences in either peak versus trough or rising versus falling trial amplitude in either early or late components (**Fig. 3.5g,h.** Peak versus trough, early: $t(21) = 0.51$, $p = 0.6$, *Cohen's d* = 0.04; late: $t(21) = -0.77$, $p = 0.5$, *Cohen's d* = -0.1. Rising versus falling, early: $t(21) = -0.59$, $p = 0.6$, *Cohen's d* = -0.04; late: $t(21) = -0.08$, $p = 0.9$, *Cohen's d* = -0.007). While our response-isolation procedure revealed a marginal effect of peak versus trough stimulation on the orbitofrontal early component amplitude ($t(21) = 2.1$, $p = 0.05$, *Cohen's d* = 0.07), this effect may have been driven by poor performance of the sham-matching procedure for the orbitofrontal EP (see **Fig. 3.5g,h**; we observe poor abolishment of the underlying theta oscillation for both trough and rising stimulation trials).

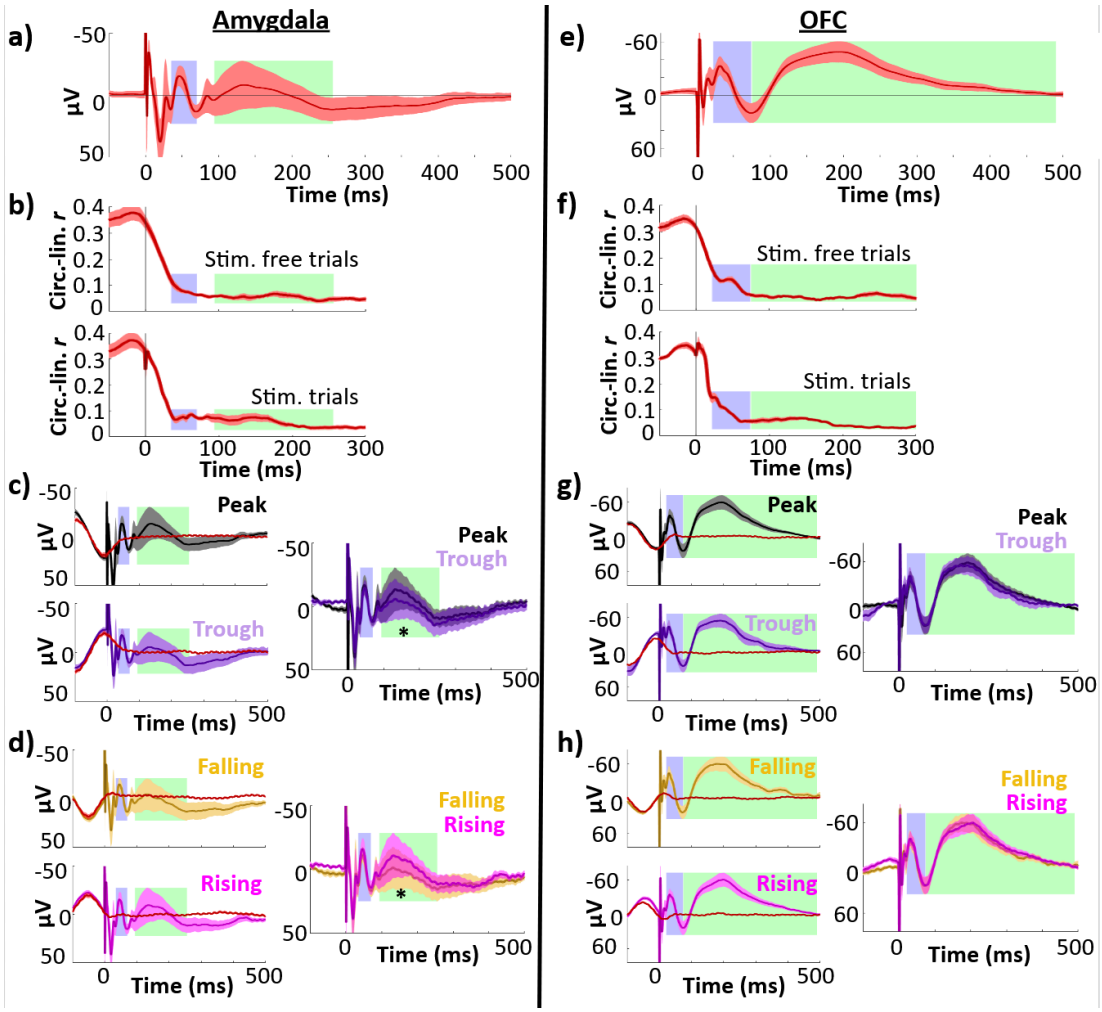

Figure 3.5. Control regions showed less temporal specificity in their phase-amplitude relationships and no difference in peak versus trough or falling versus rising early response amplitudes. Left column, amygdala (n = 9 electrodes); right column, OFC (n = 22 electrodes). Early (blue) and late (green) components are highlighted. Error bars indicate ±1 SEM across electrodes. A, E) Phase-balanced grand average EP. B, F) Phase-amplitude circular-linear r plotted for each timepoint in the peri-stimulation period for stimulation trials (top) and stimulation-free trials (bottom). C, G) Left: Mean EPs elicited by lateral temporal stimulation at local theta peak (black) and trough (purple), alongside phase-matched stimulation-free trials (red; see **Materials and Methods: Comparison of stimulation trials to phase-matched stimulation-free trials**). The isolated response was obtained by subtracting the mean phase-matched stimulation-free trial from the EP. Right: Isolated evoked responses to peak and trough stimulation. Asterisk indicates isolated response components with significant amplitude differences across phase bins at 180˚ intervals (i.e., peak versus trough or rising versus falling trials; * $p \leq 0.05$). D, H) As in C,G), for stimulation at local theta falling (yellow) versus rising (magenta) phase angles.

Analysis of variability across subjects

As the previous analyses were performed across individual electrodes, we assessed whether the circular-linear and binned effects of theta phase on response component amplitude were present across subjects. For each subject, we obtained the mean z-scored circular-linear r across hippocampal electrodes for early and late components (as described for individual hippocampal electrodes in **Materials and Methods: Circular-linear analysis of theta phase and hippocampal response amplitude**). Across subjects, we observed a positive phase-amplitude relationship in both early and late components (Mean z-score ± SD, early: $z = 1.0 \pm 1.3$; late: $z = 1.1 \pm 1.1$). This effect was marginal across subjects in the early component and reached significance in the late component (t-test of z-scores versus 0, early: $t(7) = 2.3$, $p = 0.06$, *Cohen's* $d = 0.8$; late: $t(7) = 2.8$, $p = 0.03$, *Cohen's* $d = 1.0$).

We used linear mixed-effects modeling (LME) to determine whether response component amplitudes differed for peak versus trough stimulation across subjects. We constructed an LME model for each response component with a fixed effect of phase and random effects on slope and intercept of both subject and electrode nested within subject [i.e., response amplitude ~ phase + (phase|subject/electrode)]. We then performed likelihood ratio tests to assess whether this model fit was improved by the inclusion of the fixed effect of phase. That is, after accounting for participant variance, we tested whether stimulation phase improved the prediction of response amplitude. Including the phase effect improved the model fit for the early component, with a marginal effect in the late component (one-sided likelihood ratio test for improvement, early: *LRStat* = 3.8, $p = 0.05$; late: *LRStat* = 3.3, $p = 0.06$). We then repeated this process using amplitude values from the isolated evoked response (i.e., following correction for non-evoked oscillatory activity, as in **Fig. 3.3**). The effect of phase was reduced in these models (early:

LRStat = 2.8, $p = 0.09$; late: *LRStat* = 0.9, $p = 0.3$), in accordance with the observed reduction in peak versus trough differences at the electrode level following correction for non-evoked oscillatory activity.

Phase angle estimates were consistent with ground-truth phase values in analysis of stimulation-free pseudotrials

The method we used to estimate hippocampal theta phase at the time of stimulation involved truncating the hippocampal recordings shortly after each stimulation pulse (see **Materials and methods: Theta phase estimatio**n). We assessed whether this approach yielded an accurate estimate of phase (i.e., one based on the ongoing oscillatory activity and without contamination by the evoked response or filter artifact) using "pseudotrials", epochs made from data collected during a continuous, stimulation-free period with an added model stimulation pulse and EP. We estimated the phase of these pseudotrials at mock stimulation onset (i.e., t = 0) using the same approach as for stimulation trials. As pseudotrials were created from continuous, stimulation-free data, we were also able to calculate "ground-truth" phase values (i.e., obtained in the absence of stimulation artifact or EP and without truncating the recording). We then measured the trialwise differences between ground-truth and estimated phase angles.

Across hippocampal recording electrodes, the mean difference between ground-truth and estimated phase was -11.2˚ (mean distance ± SD: -11.2. ± 4.6˚). This difference was highly concentrated (Rayleigh test: $z(22) = 22.9$, $p < 0.001$), indicating consistency of the phase angle estimate performance across electrodes (**Fig. 3.6a**). Although estimated phase angles were significantly more concentrated than ground-truth phase angles (two-tailed t-test on mean resultant vector lengths, $t(22) = 7.4$, $p < 0.001$, *Cohen's d* = 2.1), the distribution of mean

estimated phase angles was uniform (Hodges-Ajne test: $m(22) = 9$, $p = 0.9$). These findings demonstrate that the estimation approach introduced a small and consistent phase angle bias.

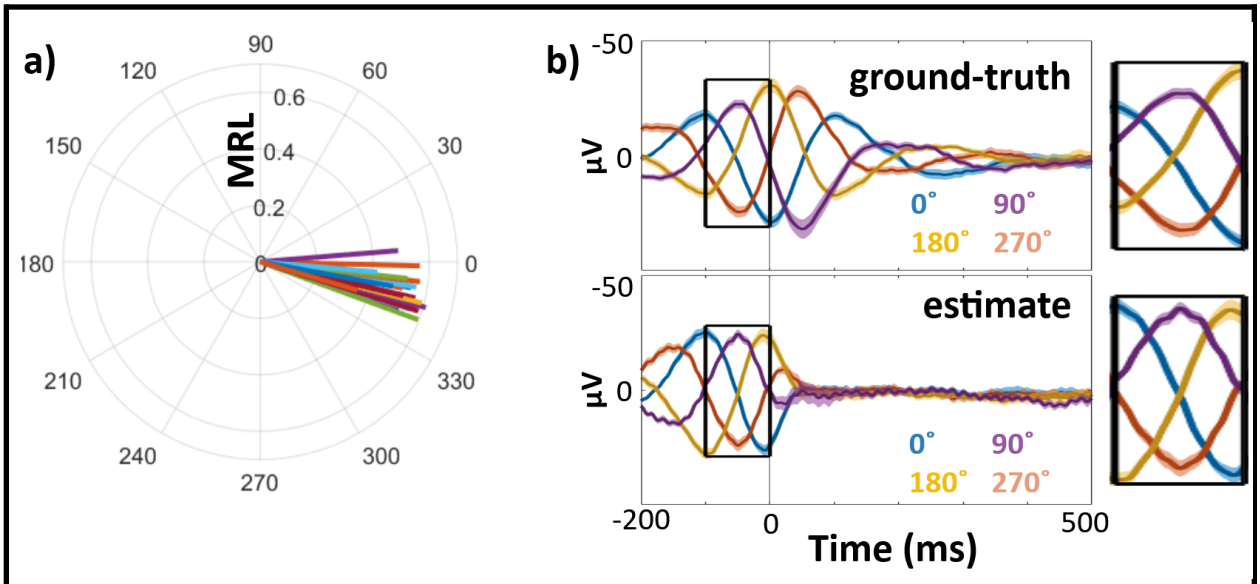

Figure 3.6. Phase estimation method yielded consistent, low-magnitude offset to ground-truth phase in pseudotrial analysis. Comparison of ground-truth and estimated phase angles from pseudotrials (stimulation-free resting data with added model stimulation artifact and EP). Validation was performed across all hippocampal channels included in the main EP analysis (n = 23). A) Mean phase angle and mean resultant length (MRL) of trialwise distance between ground-truth and estimated phases. Each line represents one hippocampal channel. B) Left: Mean stimulation-free validation trials binned according to ground-truth (top) and estimated (bottom) phase at mock stimulation onset. Line color indicates bin center (0˚, 90˚, 180˚, 270˚). Right: enlarged panels from -100 ms to 0 ms, showing similarity of theta phase at t=0 across ground-truth (top) and estimated (bottom) bins.

We also observed differences in the intertrial theta coherence across trials binned by ground-truth versus estimated phase (**Fig. 3.6b**). Because the phase estimation approach involves truncating the epoch at +50 ms following stimulation onset, signal after this point does not contribute to the phase estimate. Theta coherence therefore decreases asymmetrically about t = 0, with a more

rapid drop-off after t = 0 than before it. In contrast, trials binned according to ground-truth phase show symmetrical declines in coherence before and after t = 0.

To assess whether this bias impacted our analyses, we re-performed our binning analyses after accounting for each electrode's estimated bias (**Fig. 3.6b**). In other words, we adjusted the phase angle label for each trial according to the electrode-specific bias. After this correction, we observed the same pattern of phase-dependence as in the original analysis, with enhancement of the EP by stimulation at peak versus trough in both early and late components (early: $t(22) = -2.5$, $p = 0.02$, *Cohen's d* = -0.2; late: $t(22) = -2.7$, $p = 0.01$, *Cohen's d* = -0.09) and no effect of falling versus rising phase stimulation (early: $t(22) = -0.22$, $p = 0.8$, *Cohen's d* = -0.02; late: $t(22) = 0.15$, $p = 0.9$, *Cohen's d* = 0.007). Rebinning did not impact the results of the continuous, circular-linear analyses.

Order of stimulation pulses had no effect on phase distribution

One possible alternative explanation for the observed relationship between phase and EP amplitude was that over the course of the experimental session, stimulation induced changes in both the distribution of phase angles at stimulation onset and in the amplitude of the evoked response. We therefore performed control analyses to assess whether the theta phase distribution of stimulation pulses and their associated hippocampal evoked responses changed according to order in the experimental session.

For each hippocampal electrode, we divided stimulation trials into quartiles according to order of occurrence in the stimulation session. Within each quartile, we estimated the uniformity of stimulation phase distributions via Rao's spacing test statistic u (**Fig 3.7a**). Across electrodes, there was no change in the uniformity of stimulation phase distributions by order of occurrence

(one-way repeated measures ANOVA, effect of quartiles: $f(3) = 2.02$, $p = 0.1$; electrode:quartile interaction: $f(3) = 1.29$, $p = 0.07$. Mean Rao's $u \pm$ SD, quartile 1: $u = 148.0 \pm 14.5$; quartile 2: $u = 149.1 \pm 10.4$; quartile 3: $u = 148.6 \pm 12.8$; quartile 4: $u = 148.3 \pm 13.3$). Further, we observed no difference in mean phase angles across quartiles (**Fig. 3.7b**. Watson-Williams test: $f(3) = 0.02$, $p > 0.99$). We also assessed mean early and late component amplitude by quartile (component amplitudes calculated as in **Materials and Methods: Quantification of hippocampal EPs**). We observed an effect of quartile specifically on the late component amplitude (one-way repeated measures ANOVA, effect of quartiles: $f(3) = 4.3$, $p = 0.008$; electrode:quartile interaction: $f(3) = 3.1$, $p = 0.03$). No such effect was observed for the early component (one-way repeated measures ANOVA, effect of quartiles: $f(3) = 0.61$, $p = 0.6$; electrode:quartile interaction: $f(3) = 0.10$, $p > 0.9$). The absence of concomitant changes in stimulation phase distribution and evoked amplitude across quartiles supports that the observed phase-amplitude relationship was not driven by ordering in the experimental session.

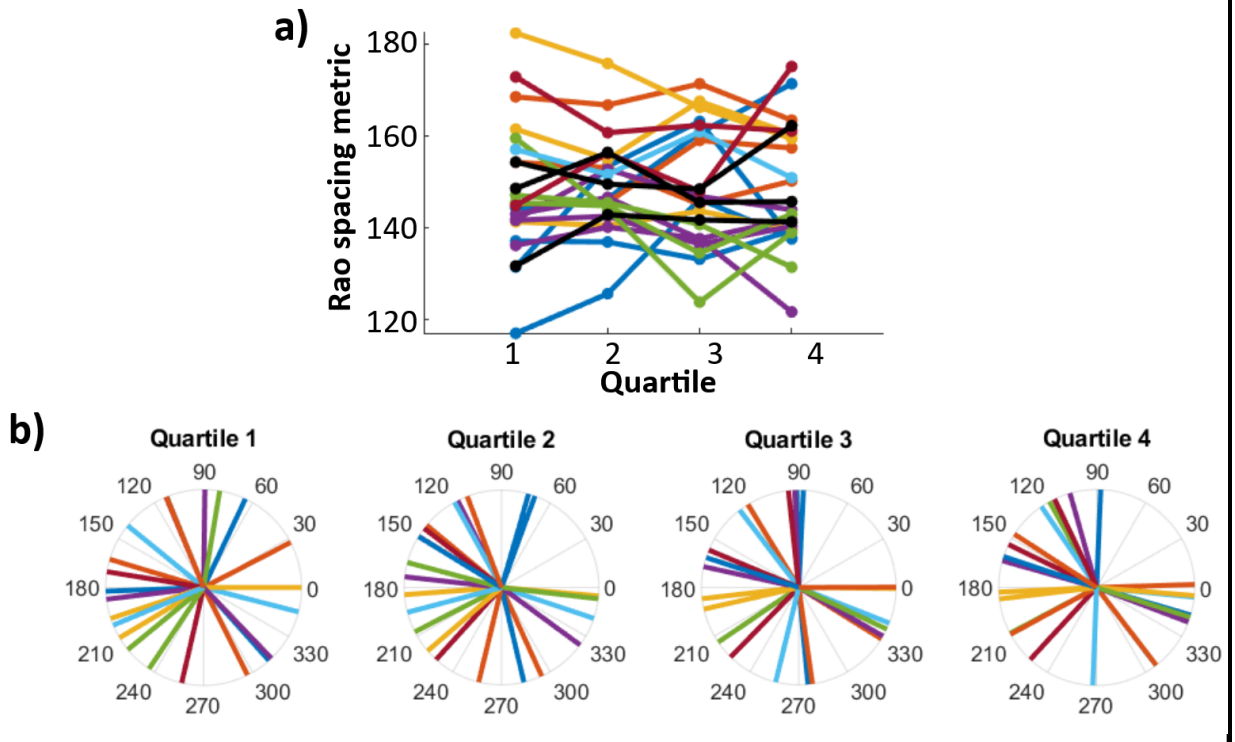

Figure 3.7. Theta phase distribution of stimulation pulses did not change according to order in the experimental session. Color indicates participant of origin. A) Rao's spacing test statistic u for stimulation phase angles in first, second, third, and fourth quartiles of the experimental session. Each dot is one hippocampal electrode (n = 23). B) Mean stimulation phase angle for each hippocampal electrode across quartiles. No significant differences are found in either distribution uniformity or directionality according to order in the experimental session.

Hippocampal peak versus trough EP amplitude differences were temporally localized to components

To complement the analyses of component amplitudes, we also performed an exploratory analysis of peak versus trough amplitude differences across all timepoints in the peri-stimulus trial period. As in the analyses above, we compared amplitudes across stimulation and stimulation-free trials in order to hone in on the stimulation-evoked response controlling for expected amplitude differences due to phase in the absence of stimulation. As expected, both stimulation and stimulation-free trials exhibited strong peak versus trough differences before t =

0 (**Fig. 3.8a, b**). In the stimulation-free trials, the peak-trough difference drops off asymmetrically about t = 0 (**Fig.3.8b**), likely related to the phase estimation method (which was used for both stimulation and stimulation-free trials and involved truncating each trial at +50ms; see **Fig. 3.8b**). Isolating the evoked response revealed that peak stimulation selectively enhanced signal negativity during the identified EP components, with consistent peak versus trough differences throughout the early component in particular (**Fig. 3.8c**). Notably, following stimulation, there were no peak versus trough differences until after approximately +40 ms, indicating that effects of phase on the subsequent amplitude of the EP components were not due to lingering differences in the ongoing oscillation irrespective of stimulation. These findings suggest that the effects of stimulation phase were temporally selective to the EP components.

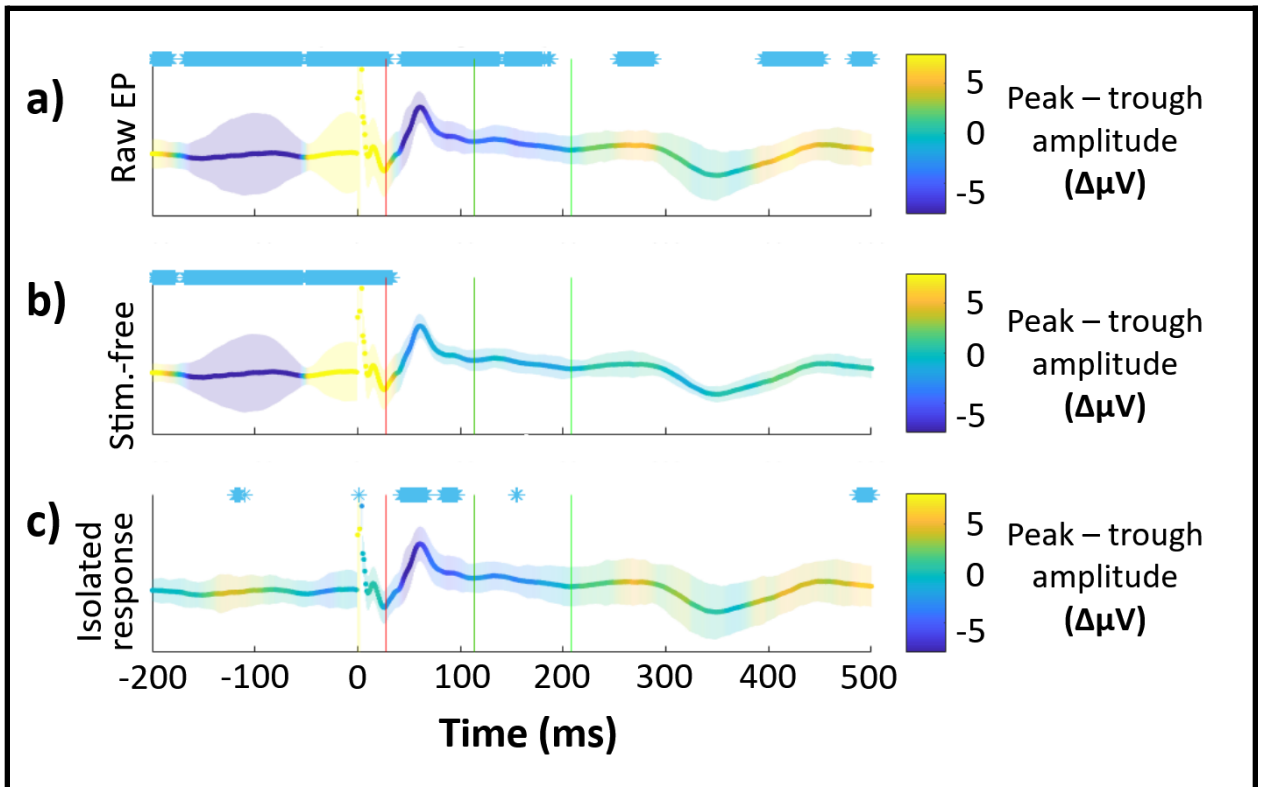

Figure 3.8. Effect of peak versus trough stimulation on hippocampal isolated response amplitude is temporally specific to components. The difference between peak and trough amplitude at each timepoint is colorized and plotted on top of the grand average hippocampal EP. Purple indicates greater negativity for peak stimulation trials, yellow indicates greater negativity for trough stimulation. Error bars indicate ±1 SEM of the peak – trough amplitude difference (a.u.). Timepoints where $p < 0.05$ (uncorrected, two-tailed) for non-zero amplitude difference between peak and trough are marked (*) for visualization. Component boundaries are marked with vertical lines (early: red, late: green). Plotted for: A) Raw EPs (i.e., stimulation trials). B) Stimulation-free trials only. C) Isolated evoked response (i.e., stimulation trials minus stimulation-free trials).

Offline theta bout incidence does not impact periodicity of the evoked response

In humans and non-human primates, hippocampal theta oscillations occur in intermittent, high-power bouts, typically lasting only a few theta cycles (Goyal et al., 2020). Bout incidence in the hippocampus and broader hippocampal network has been associated with spatial navigation (Kahana et al., 1999) and performance of non-spatial memory tasks (Raghavachari et al., 2001). Given the relevance of theta bouts to hippocampal function, we investigated whether the observed theta phase dependence of response amplitude was stronger in electrodes with greater bout incidence. As estimates of theta power during the stimulation protocol would be contaminated by the evoked response, we analyzed theta bout incidence during stimulation-free rest just prior to the experimental session. We used this measure as a proxy for the proportion of stimulation trials we expected to occur during periods of high theta power.

For each hippocampal electrode, we performed bout detection in the 3 – 8 Hz range during continuous periods of stimulation-free rest using the BOSC toolbox (see Whitten el al., 2011; Hughes et al., 2012). First, we computed power across the stimulation-free period using the Morlet wavelet transform ($w_0 = 6$; 50 frequency samples spaced logarithmically from 1 – 60 Hz). To isolate significant oscillations, we fit a $1/f$ background power spectrum for each electrode by

performing robust linear regression on the time-averaged power spectrum in log-log space. Then, for each sampled frequency, we identified timepoints where power exceeded the 95th percentile of the estimated χ^2 probability distribution of the background spectrum for a minimum duration of three cycles. We thereby obtained a theta bout-rate for each hippocampal electrode corresponding to the proportion of the recording where high-power oscillations were present in any of the 3 – 8 Hz frequency samples.

Across electrodes, detected bout incidence ranged from 27% to 73% of the recording (mean incidence ± SD = 48 ± 13%). We quantified response amplitude theta-periodicity for each electrode as the z-scored circular-linear correlation between hippocampal theta phase at stimulation onset and component amplitude . Bout rate was not associated with response theta periodicity in either the early (linear correlation: $r = 0.27$, $p = 0.2$) or late ($r = 0.0030$, $p = 0.99$) components. While we were methodologically unable to quantify the effect of bouts on individual trials, this finding suggests that resting bout incidence did not impact the phase-dependence of the hippocampal evoked response.

Accounting for estimated phase latency between the stimulation site and hippocampus does not produce consistent phase angles conferring maximal and minimal EP amplitude

There is necessarily a conduction delay between the lateral temporal stimulation site and its receipt in hippocampus. As functionally connected regions are frequently phase-synchronized (see Fell & Axmacher, 2011), we hypothesized that this delay would translate to a consistent theta phase lag between the stimulating electrodes and the hippocampus. This would produce a consistent angle offset between hippocampal theta phase at the time of stimulation (i.e., at $t = 0$, the timepoint which we used to characterize trial phase in the previous analyses) and the

stimulation's arrival at hippocampus.at the time of the relevant entorhinal-hippocampal transmission.

Permutation testing (see **Materials and Methods: Oscillatory synchronization between the stimulation site and hippocampus**) revealed significant phase locking between hippocampus and the stimulation site (Mean z-score ± SD: $z = 3.1 \pm 4.6$; t-test of z-scores against 0: $t(22) = 3.2$, $p = 0.004$, *Cohen's d* = 0.7. Mean PLV ± SD: 0.18 ± 0.1), indicating that individual hippocampal electrodes had consistent phase-lags to the stimulation site. However, across electrodes, the distribution of mean phase offsets was not significantly non-uniform (**Fig. 3.9a**. Rao's spacing test: $u(22) = 144.9$, $p = 0.5$). We noted a bimodal distribution of high-PLV phase latencies across electrodes, with clusters centered approximately 180° apart. Consequently, across electrodes with consistent phase-lags, stimulation delivered during the hippocampal peak may have arrived at to hippocampus at different phase angles across electrodes.

To assess whether the variability in transmission delay across electrodes impacted the observed relationship between theta phase and evoked response amplitude, we reanalyzed the relationship between component amplitude and specific theta phase angles (see **Figs. 3.3** and **3.4**) after accounting for the observed latency between the hippocampal electrode and the stimulation site. For example, for a hippocampal electrode with an observed phase lag of 180°, stimulation delivered at the hippocampal theta peak would arrive on average at the subsequent hippocampal theta trough. However, after rebinning trials according to latency, we found no difference across either peak versus trough (early: $t(22) = 1.7$, $p = 0.1$, *Cohen's d* = 0.2; late: $t(22) = 1.4$; $p = 0.2$, *Cohen's d* = 0.08) or rising versus falling (early: $t(22) = 1.1$, $p = 0.3$, *Cohen's d* = 0.1; late: $t(22)$

= 0.30, p = 0.8, *Cohen's d* = 0.01) component amplitudes. The rebinning procedure had no effect on the unbinned, circular-linear analyses.

We observed clustering of phase latencies near 0° and 180° (**Fig. 3.9a**), a possible indicator of volume conduction between the two sites. To investigate, we reanalyzed phase-locking between hippocampus and the stimulation site after adopting a bipolar referencing scheme wherein data were re-referenced to the adjacent, lateral contact on the depth electrode (rather than the average of ipsilateral depth electrodes, as in all previous analyses). After re-referencing, the significant phase-locking between hippocampus and the stimulation site persisted (**Fig. 3.9b**. Mean z-score ± SD: z = 2.3 ± 3.8; t-test of z-scores against 0: $t(22)$ = 2.9, p = 0.009, *Cohen's d* = 0.6. Mean PLV ± SD: 0.15 ± 0.1). The qualitative clustering of phase latencies near 0° and 180° were also present in the re-referenced analysis.

After rebinning trials according to the latency estimated under bipolar referencing conditions, we found a significant difference across rising versus falling late component amplitudes (early: $t(22)$ = -0.57, p = 0.6, *Cohen's d*= -0.06; late: $t(22)$ = -2.35, p = 0.03, *Cohen's d* = -0.1), which persisted following correction for the non-evoked oscillation (late: $t(22)$ = -2.50, p = 0.02, *Cohen's d* = -0.1. Abolition of the non-evoked oscillation was performed using the same procedure as in **Fig. 3.3**; see **Materials and Methods: Comparison of stimulation trials to phase-matched stimulation-free trials**). No differences were found across peak versus trough trials for either the raw EP (early: $t(22)$ = -0.18, p = 0.9, *Cohen's d* = -0.01; late: t = 0.04, p > 0.9, *Cohen's d* = 0.002) or the isolated response (early: $t(22)$ =-0.31, p = 0.8, *Cohen's d* = -0.04; late: t = -0.33, p = 0.7, *Cohen's d* = -0.02).

Qualitatively, phase offsets from within the same participant were highly concentrated, indicating low theta phase shift across hippocampal electrodes despite variable laminar depths and septotemporal placement within individual subjects. While previous studies have reported relatively small phase angle shifts across the human hippocampal long axis (Zhang & Jacobs, 2015) relative to the 180˚ pole-to-pole shift observed in rodents (Patel et al., 2012), this finding implies that the recorded oscillation was also resilient to changes in recording depth. This may be the result of recording from large interlaminar macroelectrodes (see **Discussion**).

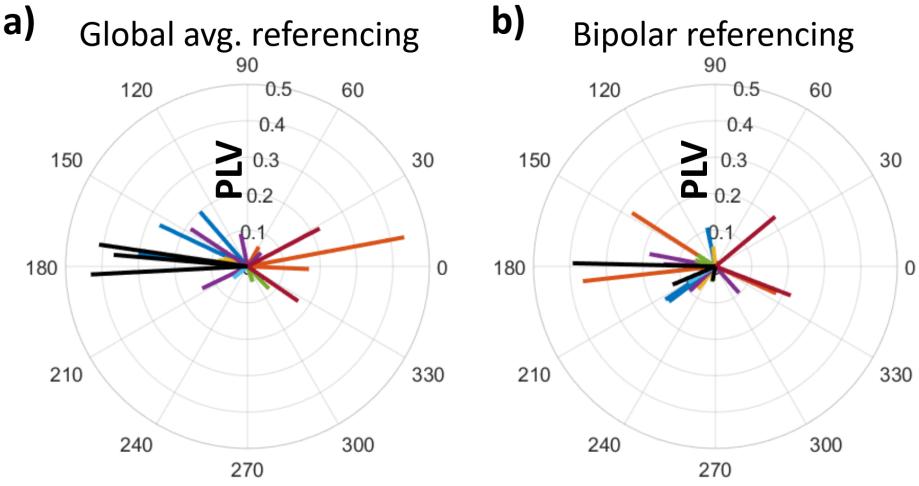

Figure 3.9. Distributions of phase offsets between lateral temporal and hippocampal theta were uniform across electrodes. A) Distribution of theta phase offsets between lateral temporal cortex and hippocampus under global average referencing scheme. Dashed line indicates circular-mean phase angle across electrodes. Each line represents one hippocampal electrode. Color indicates participant-of-origin for each electrode. Electrode line length indicates phase-locking value. B) As A), under bipolar referencing scheme wherein data from each electrode were referenced to the adjacent lateral contact on the same depth electrode.

Hippocampal EP timing did not predict amygdala late component latency

While phase-dependence of the hippocampal EP was observed most strongly during its early component (27-113 ms), phase-dependence of the amygdala EP was strongest during its late

component (94-256 ms). We hypothesized that the amygdala late effect may have been driven by secondary transmission from hippocampus. To investigate, we analyzed whether the amygdala late component preceded the hippocampal early component on a per-subject basis.

We analyzed data from all subjects with both amygdala and hippocampal electrodes (n = 3 subjects). For each subject, we computed the phase-balanced, grand average EP across electrodes for each of hippocampus and amygdala (as in **Materials and Methods: Theta phase estimation**). We then identified component timing on a per-subject basis, using the same procedure as described for the across-electrode dataset. For all subjects, the peak of the amygdala N2 was preceded by the peak of the hippocampal N1 for the grand average EPs (per subject timing of hippocampal N1, amygdala N2 peaks: [+34ms, +161ms], [+61ms, +130ms], [+133ms]).

Next, we assessed whether the timing of the amygdala response tracked the timing of the hippocampal early component across trials. For each subject, we computed the mean hippocampal and amygdala EPs across electrodes for each trial. We estimated trialwise component timing using the same procedure as described for the across-electrode dataset. We then assessed the correlation between the timing of the hippocampal N1 peak and the amygdala N2 peak. This analysis was restricted to trials which passed the exclusion criteria across all relevant amygdala and hippocampal channels (see **Materials and Methods: sEEG recording and stimulation**). No subjects showed a significant relationship between hippocampal and EP component timing (per subject component timing correlations, subject 1: r = -0.0005, $p > 0.9$; subject 2: r = 0.007, p = 0.9; subject 3: r = 0.04, p = 0.4).

3.4 Discussion

We investigated whether the human hippocampus varies in receptivity to external stimulation along with the local theta oscillation. Lateral temporal stimulation consistently evoked a hippocampal response with distinct early and late negative components. These component amplitudes were found to vary continuously with theta phase at stimulation onset. The continuous relationship between phase at stimulation onset and EP amplitude showed temporal specificity, with a notable increase during the early component. We additionally found that stimulation at theta peak versus theta trough yielded maximal differences in evoked response amplitude. This effect was most pronounced during the early negative component (27-113 ms after stimulation onset), where it persisted even after corrections for non-evoked oscillatory activity which emerged from the phase-sorting procedure. These findings suggest that human hippocampal connectivity to network afferents varies across the local theta oscillation.

As data in this study were collected opportunistically from participants undergoing clinically necessary invasive monitoring, hippocampal electrodes were implanted at variable laminar depths that could not be known due to the relative imprecision of CT/MRI. Nonetheless, we observed a consistent effect of phase angle on the recorded hippocampal response. The relatively small phase offset we observed between hippocampal sites from a given participant supports that the recorded oscillation was depth indifferent, perhaps owing to the large size and interlaminar placement of the macroelectrodes. Further studies would be necessary to determine subfield and layer-specific phase angles conferring maximum entorhinal input to the human hippocampus.

The observed effect of peak versus trough is likely specific to the synaptic distance and conduction delay between the stimulation site and hippocampus. While stimulating electrodes

were all located in lateral temporal cortex, their gyral locations varied according to clinical constraints. Accordingly, while phase offsets between lateral temporal cortex and hippocampus were non-uniform, there were pronounced differences in the offset angle between participants. It is possible that differences in transmission latencies contributed to the observed variance in peak-trough effects across participants. We hypothesize that stimulation targeting a different site in the hippocampal network would produce a similarly theta-periodic hippocampal response, albeit likely maximized at a different stimulation phase angle (i.e., not necessarily at the observed hippocampal theta peak). Further, it is possible that the relationship of theta phase to the evoked response amplitude varies with theta power, although we were methodologically unable to assess theta power on a per-trial basis. Our exploratory analyses of theta power during an offline period did not find any relationship between power and the phase-amplitude relationship (see **Results: Offline theta bout incidence does not impact periodicity of the evoked response**), although quantifying power during a period other than stimulation is not ideal. Future research could address this issue, potentially by cueing stimulation based on an online assessment of theta power.

One limitation is that this study was performed in individuals with refractory epilepsy. Temporal lobe epilepsy is associated with episodic memory impairments (Mayeux et al., 1980; Helmstaedter & Kockelmann, 2006) thought to be caused by structural abnormalities as well as interictal epileptiform activity in the hippocampus and hippocampal cortical network (Helmstaedter & Kockelmann, 2006; Gelinas et al., 2016). Nonetheless, iEEG recordings from individuals with temporal lobe epilepsy have previously been used to study mechanisms for hippocampal function (Lega et al., 2012; Long et al., 2014; Fell et al., 2011; Wixted et al., 2014). To enhance the study's generalizability, we rejected trials with recorded epileptiform activity and

ensured during data collection that the stimulation protocol did not elicit afterdischarges or spiking. It is still however unclear whether epilepsy-related changes to hippocampal structure and network connectivity influenced our findings. This limitation partially motivated the experiments described in **Chapter 4**, which investigate phase-dependence of hippocampal function in healthy participants.

Phase dependence of the response to stimulation has, however, been demonstrated in non-epilepsy model organisms. Previous studies have reported phase-dependent responses to external stimulation across diverse neocortical areas. Direct electrical stimulation of sensory cortices has been found to differentially induce long-term potentiation or depression depending on local field potential phase (e.g., with beta- and gamma-dependence in rodent visual cortex [Wespatat et al., 2004] and beta-dependence in primate sensorimotor cortex [Zanos et al., 2018]). In humans, local oscillatory phase has been found to relate to the amplitude of the cortical response evoked by transcranial magnetic stimulation (Kundu et al., 2014). These findings support that oscillatory phase relates generally to local excitability. Thus, one part of our analysis strategy was to assess whether any observed phase dependence was specific to (or specifically enhanced in) hippocampus. We investigated the phase dependence of stimulation response in two control regions: amygdala and orbitofrontal cortex. Like hippocampus, both regions have anatomical (Shi & Cassell, 1997; Iwai et al., 1987; Morecraft et al., 1992) and functional (Roy et al., 2009; Du et al., 2020) connectivity with the lateral temporal stimulation site. But while amygdala is physically adjacent to hippocampus and densely connected with hippocampus and entorhinal cortex (Saunders et al., 1988; Pikkarainen et al., 1999; see Chrobak et al., 2000) – and might therefore be expected to show hippocampus-like phase dependence of input receptivity -- orbitofrontal cortex is more distant both in space and connectivity. Indeed, we observed

significant theta phase dependence in the amygdala EP but no such effect in orbitofrontal cortex. As was the case in hippocampus, the amygdala showed greater response amplitude when stimulation was applied at theta peak relative to trough. The amygdala also showed greater response amplitude to stimulation at theta rising phase relative to falling phase. Unlike hippocampus, this effect was present exclusively in the late component. The presence of early components in the amygdala and orbitofrontal EPs supports connectivity between these control regions and the lateral temporal stimulation site. However, we note that the stimulation site was chosen on the basis of its functional connectivity with hippocampus as measured via the stimulation-evoked potential, and not based on connectivity with these other brain areas. Performing network-targeted stimulation for each control region could provide stronger evidence for the effect's selectivity to hippocampus.

This study used direct electrical stimulation as a proxy for endogenous network signaling. Follow-up studies are required to assess whether and how these changes in human hippocampal connectivity due to theta phase relate to memory processing. Nonetheless, by demonstrating phase dependence of input receptivity in the human hippocampus, this study suggests a homology with the phase dependence previously characterized in rodent models in relation to memory encoding and retrieval.

Chapter 4: Investigating memory performance as a function of stimulation-entrained theta

4.1 Introduction

In **Chapter 3**, I described a set of experimental findings which demonstrate that the human hippocampus undergoes theta-cyclic changes in its response to stimulation of its cortical afferents. These results provide foundational support for the phase-dependent optimization of encoding versus retrieval previously evidenced in rodents via behavioral testing (Siegle & Wilson, 2014; see **Chapter 1.3**). In **Chapter 4**, I describe two experiments I performed in an attempt to extend these findings from human hippocampal physiology to human hippocampal memory function. Unlike the study described in **Chapter 3**, these experiments were carried out in healthy young adults who were not undergoing clinical invasive monitoring, and therefore do not have the same limitations with regard to generalization of findings from temporal lobe epilepsy patients.

The experiments described in this chapter investigate whether causally manipulating theta phase using noninvasive stimulation produces cyclic fluctuations in performance on specialized tasks of associative memory encoding (Experiment 1) and retrieval (Experiment 2). The logic of these experiments is that if theta-patterned rTMS is effective for entraining the hippocampal theta oscillation, then the effectiveness of memory encoding and retrieval is expected to vary with the phase of rTMS-entrained theta. Immediately following a train of theta-patterned rTMS, we presented brief (< 20 ms) associative visual memoranda aligned to the phase of the entraining stimulation. In Experiment 1, stimulation was delivered prior to presentation of a briefly-presented encoding stimulus; in Experiment 2, stimulation was delivered prior to

presentation of a briefly-presented retrieval cue. Based on the findings outlined in **Chapter 3**, we hypothesized that stimulation would induce periodic fluctuations in memory performance, with minimal and maximal performance occurring at a 180° interval. We further hypothesized that opposite phase angles would relate to maximal performance for encoding (Experiment 1) versus retrieval (Experiment 2).

As the human hippocampus cannot be stimulated directly with noninvasive methods, we stimulated functionally connected cortical locations in order to indirectly influence hippocampal activity, a strategy which was previously developed in our laboratory (Wang et. al, 2014). Stimulation of the hippocampal network has been shown to produce cumulative and enduring effects on hippocampal-dependent memory (Hebscher et al., 2021; Hermiller et. al, 2019; Tambini et al., 2018) as well as hippocampal network connectivity (Wang et al., 2014; replicated in Freedberg et al., 2019). Outside the hippocampal domain, network-targeted cortical TMS has been demonstrated to alter activity in otherwise stimulation-inaccessible structures including amygdala (Oathes et al., 2021), anterior cingulate cortex and caudate (Dowdle et al., 2018), and ventromedial prefrontal cortex (Hanlon et. al, 2016; see also Bergmann et al., 2021).

The experiments described in this chapter use a theta-burst rTMS protocol in an attempt to entrain the hippocampal theta oscillation. Theta-burst stimulation (TBS) – where high-frequency bursts of stimulation pulses are delivered at theta-periodic intervals – was initially developed in the context of direct electrical stimulation (Larson et al., 1986), where it was designed to closely match the characteristics of the hippocampal local field potential (Larson et al., 1986; Nguyen & Kandel, 1997; Staubli & Lynch, 1987). Direct electrical TBS has been used to induce synaptic plasticity in hippocampus (e.g., Buzsáki et al., 1987; Staubli & Lynch, 1987) as well as in

numerous neocortical areas (including barrel somatosensory cortex [Hardingham et al., 2003], auditory cortex [Hogsden et al., 2011]; and entorhinal cortex [Yun et al., 2002]; see Larson & Munkácsy, 2015). In a 2004 study by Huang and colleagues, theta-burst rTMS was demonstrated to induce long-lasting changes to excitability in primary motor cortex; since then, theta-burst rTMS protocols have been widely adopted to induce enduring changes to network excitability and connectivity (see Suppa et al., 2015; Demeter, 2016).

While most previous research on theta-burst rTMS has focused on the long-term or offline aftereffects of stimulation, a recent study from our laboratory investigated the immediate effects of theta-burst rTMS on hippocampus (Hermiller et al., 2020). Delivery of a single 2 s train of hippocampal network-targeted stimulation just before the onset of visual memoranda was found to enhance subsequent recollection memory, as well as fMRI correlates of hippocampal activity during encoding and retrieval. This effect was selectively driven by theta-burst rTMS (and not by stimulation delivered at a control frequency), suggesting that the immediate effects of theta-burst rTMS on memory may be driven by frequency-specific power enhancement in the hippocampus or broader hippocampal network (Fell et al., 2011). Single trains of theta-burst rTMS have also been demonstrated to enhance semantic memory encoding for up to 15 s following stimulation of dorsolateral prefrontal cortex (Demeter et al., 2016).

When delivered at a rhythm which is endogenously expressed at the stimulation site, rTMS has been previously demonstrated to produce local phase entrainment (Thut et al., 2011; Klimesch et al., 2003; Romei et al., 2016; Chung et al., 2018; see **Chapter 1**). However, no studies have reported attempted phase entrainment of deep, otherwise inaccessible structures via

network-targeted rTMS. The experiments described in this chapter therefore reflect a novel application of noninvasive stimulation to manipulate the phase of TMS-inaccessible brain areas.

4.2 Materials and methods

Following a baseline fMRI session, subjects underwent an experimental session of approximately 90 minutes during which they received theta-patterned rTMS while performing an associative memory task.

rTMS protocol

Stimulation was delivered on-line, i.e. interleaved with the behavioral task. rTMS was delivered using a MagPro X100 and Cool-B65 coil (MagVenture, Alpharetta, GA) with a frameless guidance system (Localite, Beuel DE).

Each rTMS trial comprised a 2 second train of 5 HZ theta burst stimulation (50 Hz biphasic triplets delivered at 200 ms intervals [Huang et al., 2005]), delivered to one of two stimulation sites (left-parietal in-network, or out-of-network vertex stimulation sites; see **Materials and Methods: Selection of stimulation targets**). 5Hz was selected as the patterning theta frequency based on previous work demonstrating a selective effect on hippocampal-dependent memory of 5Hz stimulation targeted to the hippocampal-cortical network (Hebscher et al., 2021; Hermiller et al. 2020; Tambini et al., 2018). Stimulation sites were alternated every fourth block of the experiment. The order of stimulation conditions was randomized and counterbalanced across subjects.

Stimulation intensity was calibrated according to the resting motor threshold for the right abductor pollicis brevis (i.e., with stimulation of the primary motor cortex ipsilateral to the in-network stimulation site; as in Hermiller et. al, 2020). Stimulation intensity in the

experimental protocol was set to 80% of resting motor threshold (see e.g. Huang & Rothwell, 2004). The same stimulation parameters were used for both in-network and out-of-network stimulation sites.

Selection of stimulation targets

MRI data for TMS guidance and selection of in-network stimulation targets were acquired prior to the main experimental session using a Siemens 3T Prima whole-body scanner with 64-channel head-neck coil. Structural MRI was acquired with a T1 scan sequence. The MRI sequence parameters and functional connectivity analyses were replicated from work and custom AFNI scripts (Cox, 1996) previously published by the laboratory (for a full description, see Wang et. al 2014). fMRI data were used to generate individualized connectivity maps to a seed voxel in the left hippocampus. The seed voxel was set for each participant as the voxel in the middle of the hippocampal body with strong connectivity to the contralateral hippocampus, nearest the MNI coordinate [-24, -18, -18]. We then identified TMS-accessible sites on the surface of the lateral parietal cortex with clusters of high functional connectivity to this seed. We searched for high-connectivity clusters within the angular and supramarginal gyri, searching preferentially for clusters nearest the MNI coordinate [-47, -68, 36].

Out-of-network stimulation targets were selected as the coordinate on the interhemispheric fissure nearest the anatomical vertex, i.e. the midpoint between nasion and inion along the sagittal midline, corresponding to the location of electrode *Cz* in a 10-20 system. The anatomical vertex was selected as a control location where stimulation was unlikely to directly affect the hippocampal-cortical network or impact memory function (Bonnici et al., 2018; Freedberg et al., 2019; Yazar et al., 2017; Hebscher et al., 2020, Hebscher et al., 2021).

Visual stimuli

Each visual stimulus comprised a photographic image of a unique face on a black background (Althoff & Cohen, 1999), surrounded by a red, green, or blue frame. Pseudorandom pairings of faces and R/G/B color were created for each participant. Stimuli were balanced for sex, frequency of R/G/B color pairings, and associated latency values (see **Materials and Methods: Experiment design overview**) within groupings of 4 blocks, i.e. balanced within the 4 consecutive blocks at a single stimulation site (see **Materials and Methods: rTMS protocol**).

Experiment design overview

Both experiments made use of block design. Within each of 24 blocks, subjects studied and were tested on nine unique face-color associations (i.e. a face surrounded by a red, green, or blue frame). Faces were not repeated across blocks. Each face was therefore viewed only twice, once in its encoding trial and once in its test trial.

In Experiment 1, rTMS was applied during study in order to manipulate network theta phase at the onset of the encoding memorandum. In Experiment 2, rTMS was applied at test in order to manipulate network theta phase at the onset of the retrieval cue. In both experiments, theta phase at the onset of the visual stimulus was manipulated by presenting the stimulus at different latencies relative to the end of the rTMS train.

Between the study and test phases, participants engaged in a short (30 s) distractor task, during which they were instructed to inspect a unique series of abstract geometric images (see Voss & Paller, 2009). Each distractor image was presented for 3 s. The distractor task was included in an effort to reduce semantic rehearsal of face-color associations between study and test phases.

Just prior to the main experiment session, participants underwent two full training blocks. The stimulation site was alternated between blocks to reduce training effect in the main data, as well as to familiarize participants with stimulation during the memory task (see **Materials and Methods: rTMS protocol**). Task performance data from the training blocks were excluded from all described analyses. Stimuli which appeared in the training set were excluded from the main experiment.

Visual stimuli were presented via display monitor with 60Hz refresh rate. Stimulus presentation and trial timing were controlled by custom NeuroBS Presentation scripts (Neurobehavioral Systems, Berkeley, CA).

Experiment 1 design (rTMS delivered during study)

Each study trial in Experiment 1 (**Fig. 4.1**) began with presentation of a central crosshair on the display monitor. This central crosshair remained on-screen until the visual stimulus was presented. Participants were instructed to maintain blink-free fixation to the crosshair while it was on-screen. This served the purposes of 1) ensuring that the participant did not miss the brief visual stimulus by blinking; 2) ensuring that the encoding stimulus was presented within foveal vision; and 3) reducing the likelihood of hippocampal theta phase reset due to saccade in the period between stimulation and visual stimulus onset (Jutras et al., 2013; Kragel et al., 2020).

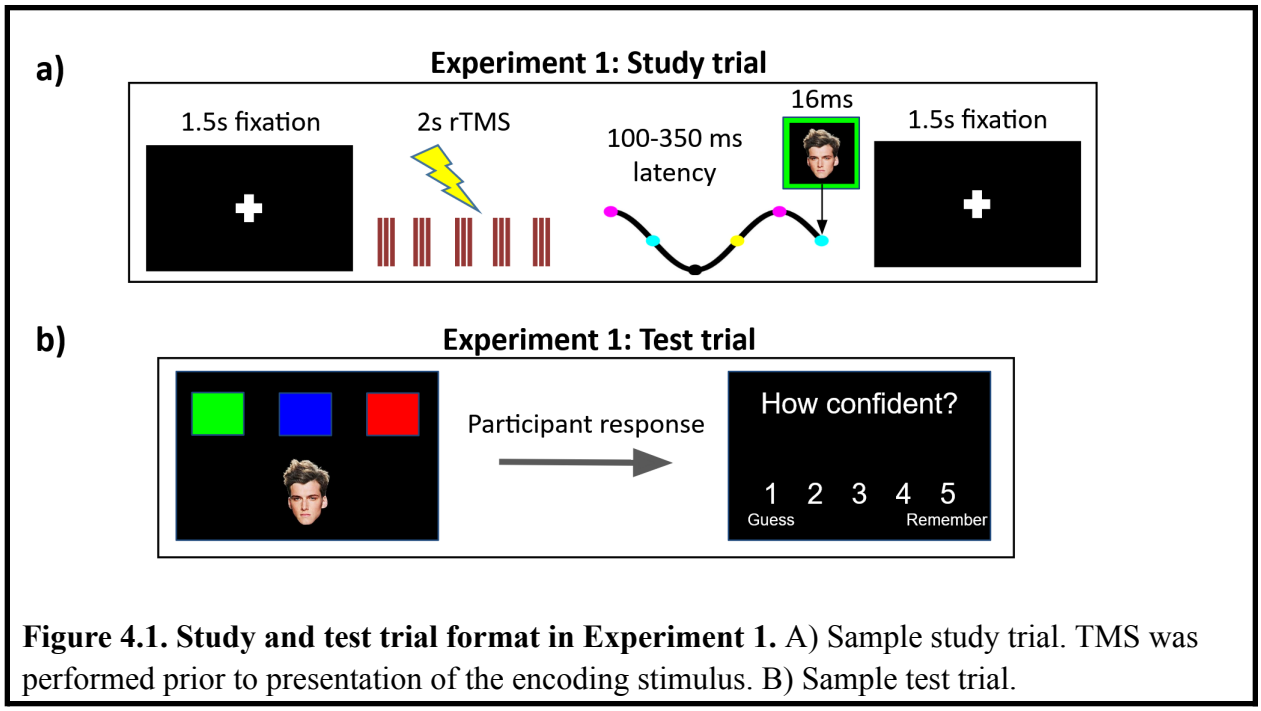

Figure 4.1. Study and test trial format in Experiment 1. A) Sample study trial. TMS was performed prior to presentation of the encoding stimulus. B) Sample test trial.

After 1.5s of blink-free fixation, participants were delivered 2 s of theta-patterned stimulation (see **Materials and Methods: rTMS protocol**). Stimulation was followed by some trial-specific latency. This latency took one of six values (100 ms, 150 ms, 200 ms, 250 ms, 300 ms, or 350 ms), corresponding to 90° intervals on the extrapolated 5 Hz entraining oscillation (**Fig. 4.2a**). The visual stimulus was then presented for one screen refresh period (< 17 ms) at the center of the screen, i.e. centered at the location of the fixation crosshair. Following visual stimulus presentation, the central fixation crosshair was displayed for a final 1.5 s. Between encoding trials, participants underwent 5 s of stimulation-free rest, during which they were instructed to blink and move their eyes freely.

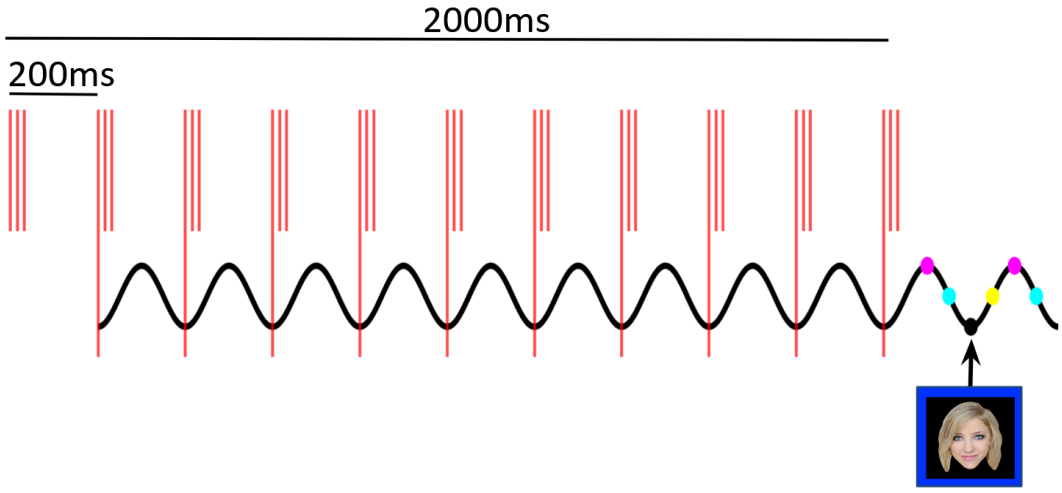

Figure 4.2. Schematic of visual stimulus alignment to the theta-patterned rTMS train. Theta-patterned stimulation (top; each line represents one biphasic stimulation pulse.) was applied in an effort to entrain 5 Hz theta activity in the hippocampal network. The visual stimulus is presented at some latency after the final stimulation burst. Pictured: an Experiment 1 study trial with 200 ms latency, corresponding to visual stimulus presentation at the trough of the 5 Hz entraining oscillation.

Following the brief distractor task (see **Materials and Methods: Experiment design overview**), participants were tested on the face-color associations learned during the most recent study phase (**Fig 4.2b**). Participants were presented a face stimulus and were asked to respond by right-handed keyboard input with the position of the matching R/G/B square (**Fig 4.2b**). R/G/B ordering at test was balanced within groupings of 4 blocks (as in **Materials and Methods: Visual stimuli**). Participants were free to visually explore the face stimulus, which remained onscreen until the participant responded. Face stimuli were presented in a randomized order with regard to their order during study. Participants were then asked to provide a confidence judgement. Confidence judgement ratings were queried with a 5-value Likert scale (1 = 'Guess', 5 = 'Remember').

Experiment 2 design (rTMS delivered during test)

Each study trial in Experiment 2 (**Fig. 4.3a**) comprised a 4 s presentation of the visual stimulus, during which participants were permitted to freely explore the memorandum. Study trials were presented to an intertrial interval of 2 s.

Following the distractor task, participants were tested on the face-color associations learned in the most recent study phase (**Fig. 4.3b**). After 1.5s of blink-free fixation, participants received 2 s of theta-patterned stimulation followed by a trial-specific latency. The retrieval cue – comprising only the face stimulus, without its associated R/G/B frame – was then presented for one screen refresh period at the center of the screen. Following visual stimulus presentation, the central fixation crosshair was displayed for an additional 1.5 s. Participants were then asked to select the R/G/B square associated with that face stimulus. Unlike in Experiment 1, the face stimulus was not on-screen during this query. Finally, participants then provided a confidence judgement for their response. Between encoding trials, participants underwent up to 5 s of stimulation-free rest. This rest period was set according to the participant's response latencies such that there was a minimum of 10 s between stimulation trains, matching the intertrain interval applied in Experiment 1.

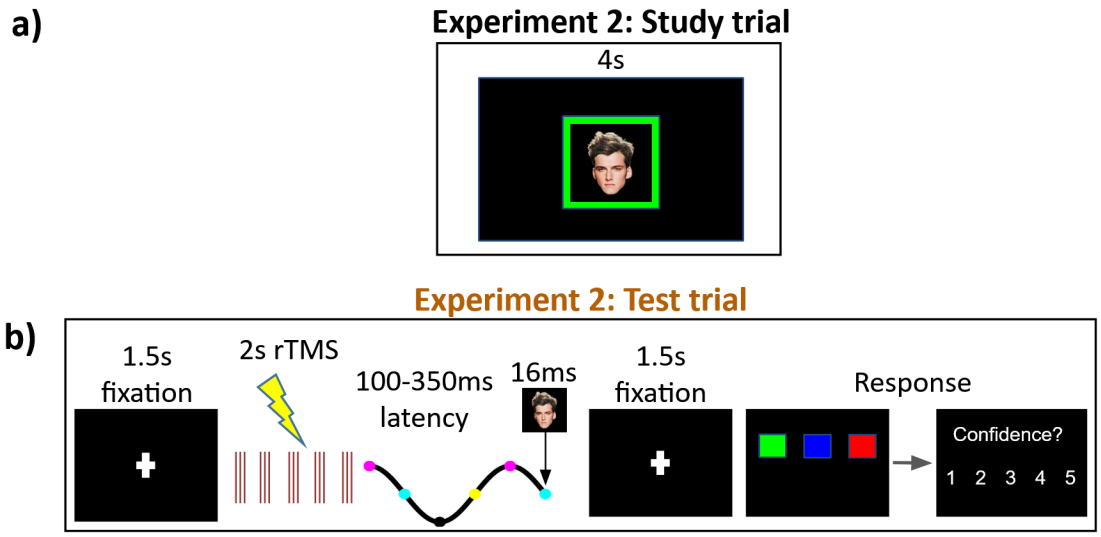

Figure 4.3. Study and test trial format in Experiment 2. A) Sample study trial. B) Sample test trial. rTMS was delivered prior to presentation of the retrieval cue.

Validation of visual stimulus timing

Timing data comprised: 1) visual stimulus timing via TTL outputs from the stimulus display computer which were issued simultaneously with the visual stimulus draw command to the display monitor, and 2) TMS pulse timing via stimulation artifact on a photosensor repurposed for this function (Brain Vision LLC, Morrisville NC) which was adhered to the display monitor (**Fig. 4.4**). Stimulus draw event markers and repurposed photosensor time series data were collected via EEG amplifier (Brain Vision LLC, Morrisville NC) and recorded using BrainVision PyCorder. Data were digitized to a sampling rate of 2000 Hz. Experiment timing and hardware setup were otherwise the same as described for the main experiment. To ensure the stimulus was onscreen during the desired frame, the NeuroBS draw command was issued half the display screen refresh period (or approximately 8 ms) in advance of the desired draw frame. For example, to present the visual stimulus at a latency of 150 ms, the intended draw command latency was 142 ms after the final theta burst tetanus.

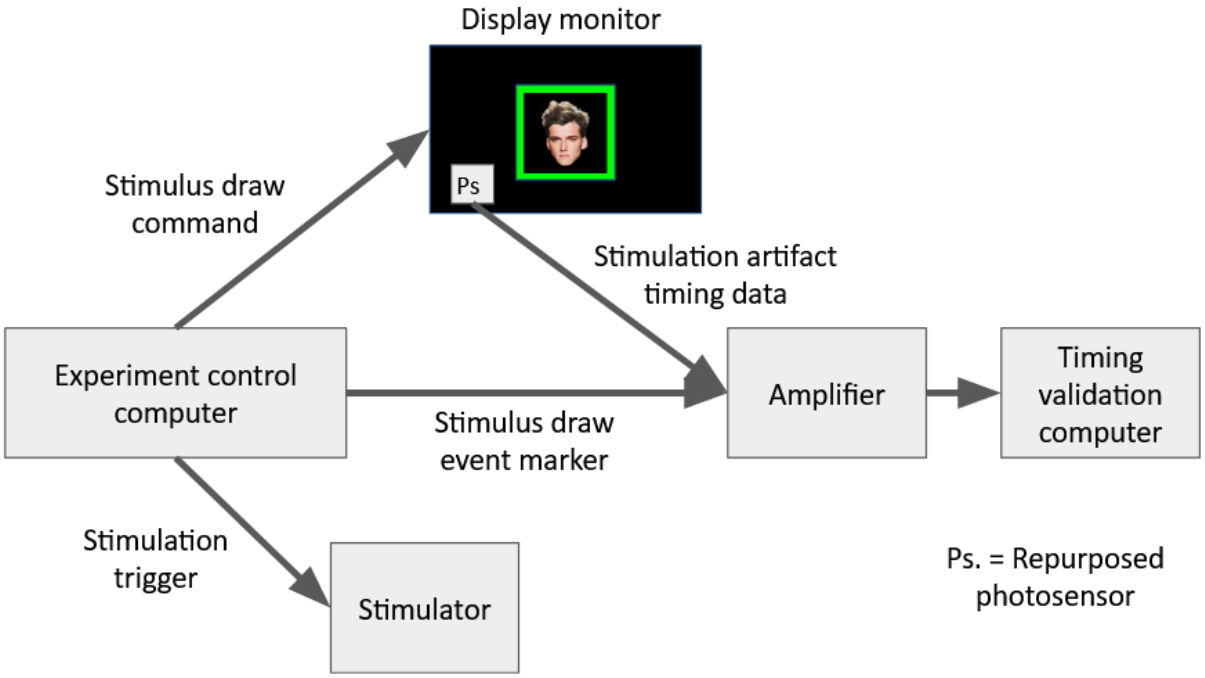

Figure 4.4. Setup for validation of visual stimulus timing relative to TMS. Custom NeuroBS Presentation scripts on the experimental computer were used to trigger the theta-patterned stimulation protocol via TTL output to the stimulator. The visual stimulus was cued for display at some latency after the stimulation trigger (e.g., 2150 ms). The actual timing of the visual stimulus was recorded via TTL output simultaneous with the draw command. Actual timing of the stimulation was recorded as by analysis of stimulation artifact on a photosensor adhered to the display monitor.

4.3 Results

Participants and in-network stimulation sites

Data were collected from 15 participants per experiment for a total of 30 participants. All participants passed standard MRI and TMS safety screenings (Rossi et al., 2009). Study protocols were approved by the Northwestern University Institutional Review Board. Subjects provided written informed consent prior to participation.

In-network stimulation targets were identified for each participant based on resting state fMRI connectivity analyses (see **Materials and Methods: Selection of stimulation targets**). We noted differences in stimulation site selection across Experiments 1 and 2. In-network target selection was restricted as-intended to the inferior parietal lobule across all participants in Experiment 2; however, stimulation was targeted anterior of the supramarginal gyrus in several participants in Experiment 1 (**Fig. 4.5;** see **Discussion**).

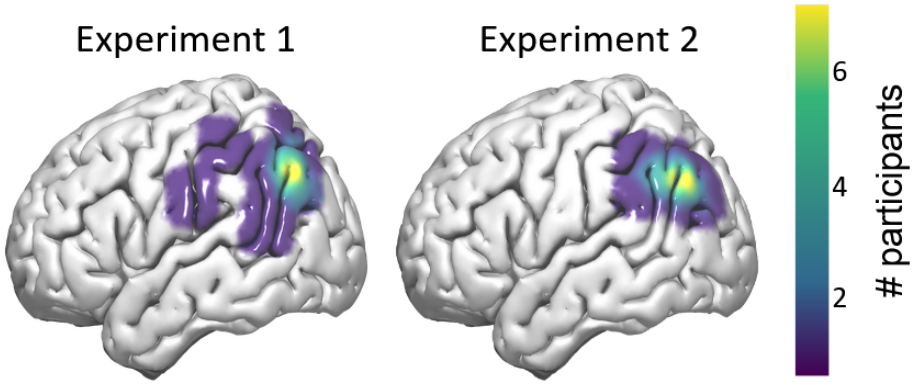

Figure 4.5. Left parietal (in-network) stimulation locations across the participant cohort. Group-level in-network stimulation locations plotted for Experiment 1 (left, n = 15 participants) and Experiment 2 (right, n = 15 participants) on an MNI template (Holmes et al., 1998). Color indicates the number of participants with overlapping stimulation sites to a 10mm radius. In-network stimulation locations were selected via analysis of functional connectivity with a hippocampal seed (see **Materials and methods: rTMS protocol**).

Visual stimuli were presented at desired latency from entraining stimulation

To verify that visual stimuli were presented at the desired lags relative to each rTMS train, we collected timing validation data (see **Materials and Methods: Validation of visual stimulus timing)** in a subset of n = 8 participants from Experiment 1.

Each biphasic stimulation pulse in the rTMS train evoked a highly stereotyped, monophasic stimulation artifact on the repurposed photosensor. The entraining stimulation protocol produced

a theta-patterned train of artifact (**Fig. 4.6a**), including gamma-frequency triplet bursts (**Fig. 4.6b;** see **Materials and Methods: rTMS protocol**). We identified the timepoint corresponding to the peak of the first pulse artifact (see **Fig. 4.6a**) as the onset of each stimulation train. We then compared the actual latency between stimulation onset and the visual stimulus draw command (see **Fig. 4.4**) to the intended latency for each trial. We term the time difference between observed and intended latency the trial's discrepancy.

Validation data were observed for a total of 1726 trials. The mean absolute discrepancy was < 1 ms (SD: 0.8 ms; **Fig. 4.6c**). In all but one observed trial, the absolute discrepancy was less than 3 ms, indicating that visual stimuli were presented within 6° of the intended phase in the 5Hz entraining oscillation. In a single observed trial, discrepancy was approximately 31 ms.

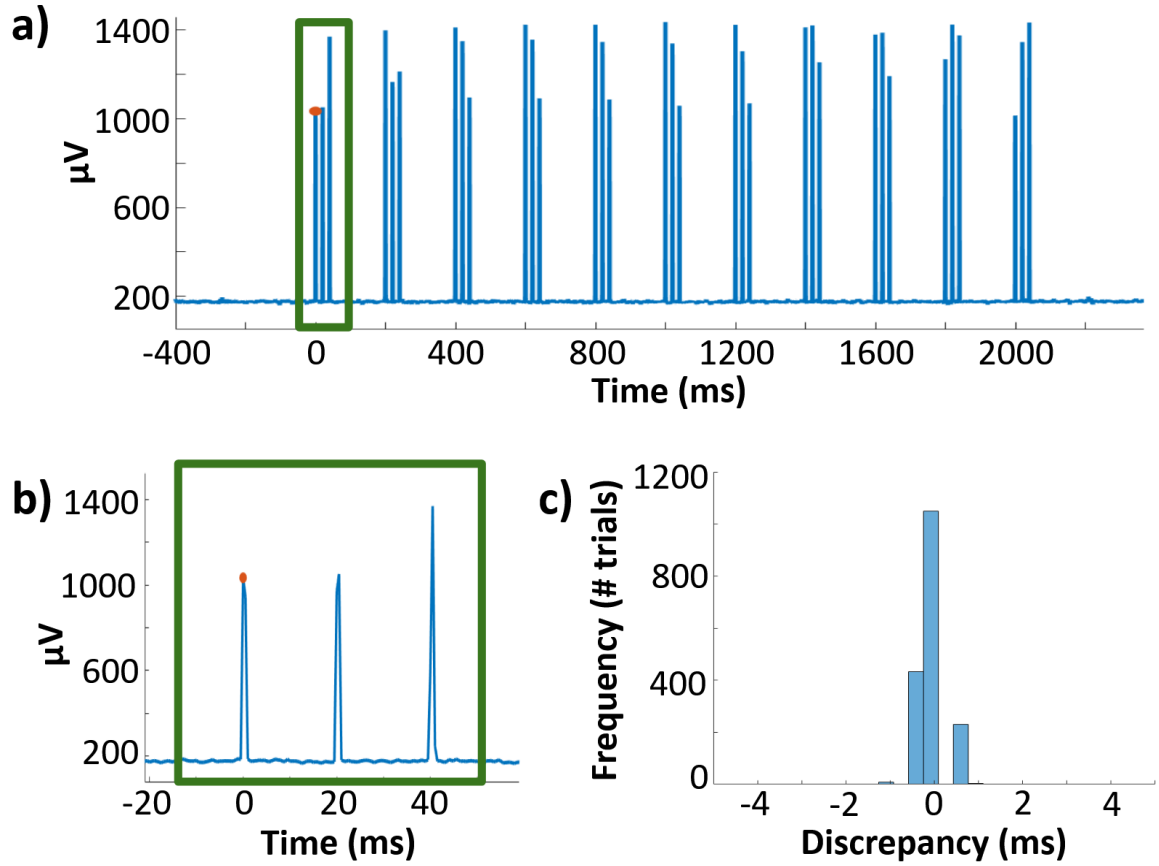

Figure 4.6. Visual stimuli were presented within 6° of desired phase on the entraining oscillation. A) Stimulation artifact on the repurposed photosensor during a sample stimulation train. Over the duration of the 2 s stimulation train, 11 gamma-frequency triplet bursts were delivered. Red marker indicates the estimated onset of the stimulation train, at the peak of the first pulse's artifact. B) Enlarged panel from A), showing the stimulation artifact during a single gamma-frequency triplet burst. C) Histogram of discrepancy (difference between actual and desired visual stimulus onset time) across n = 1726 validation trials . Negative values indicate that the visual stimulus was presented earlier than the desired phase angle. For visualization purposes, one outlying trial with a discrepancy of 31 ms is not pictured.

Stimulation did not impact overall memory performance or recall hit rate when delivered at either encoding or retrieval

Across stimulation and phase conditions, overall memory accuracy was significantly above chance in both Experiment 1 and Experiment 2 (mean hit rate ± SD, experiment 1: 0.49 ± 0.1; experiment 2: 0.62 ± 0.1. t-test of overall hit rates against chance, experiment 1: $t(14) = 6.1$, $p <$

0.001, *Cohen's d* = 2; experiment 2: $t(14) = 10.1$, $p < 0.001$, *Cohen's d* = 3). No effect of stimulation site was observed on overall memory accuracy for either experiment (**Fig. 4.7a**. Paired t-test of hit rates across following in-network versus out-of-network stimulation, experiment 1: $t(14) = -0.86$, $p = 0.4$, *Cohen's d* = -0.2; experiment 2: $t(14) = 1.0$, $p = 0.3$, *Cohen's d* = 0.2).

In the recent study from our laboratory supporting immediate effects of theta-burst rTMS on hippocampal activity (Hermiller et al., 2020; see **Introduction**), the primary behavioral effect of hippocampal-network targeted stimulation was to specifically enhance the proportion of hits which were recalled versus merely familiar. We therefore assessed whether stimulation produced similar effects in these experiments, despite differences in memoranda and task design compared to the 2020 study (see **Discussion**). We calculated the proportion of correct responses that were associated with a confidence judgement of 6 ('Remember') or lower. All participants used the full range of confidence judgements. However, we observed no enhancement of recall hit rate by in-network versus out-of-network stimulation (**Fig. 4.7b**) in either Experiment 1 (mean hit rate ± SD, in-network stimulation: 0.17 ± 0.1; out-of-network stimulation: 0.16 ± 0.2. Paired t-test of recall hit rates by stimulation site: $t(14) = 0.16$, $p = 0.9$, *Cohen's d* =0.03) or Experiment 2 (mean hit rate ± SD, in-network stimulation: 0.27 ± 0.2; out-of-network stimulation: 0.26 ± 0.2. Paired t-test of recall hit rates by stimulation site: $t(14) = 0.56$, $p = 0.6$, *Cohen's d* =0.07).

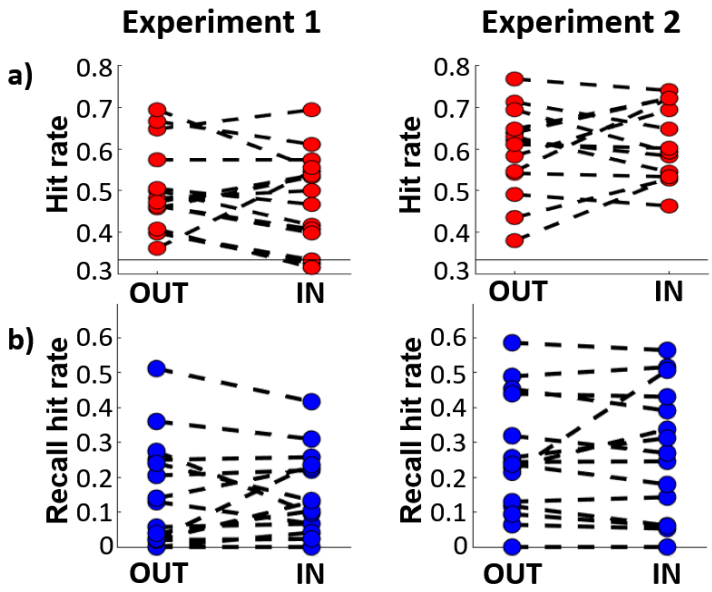

Figure 4.7. No effect of stimulation site on overall memory accuracy or proportion of recall hits. Dashed lines connect data from each participant for out-of-network (OUT) versus in-network (IN) trials. A) Overall memory accuracy by stimulation condition in Experiment 1 (left) and Experiment 2 (right). Horizontal line indicates chance performance. B) Recall hit rate (i.e., proportion of hits where the memorandum was remembered) by stimulation condition in Experiment 1 (left) and Experiment 2 (right).

Effect of phase on memory accuracy was observed when stimulation was delivered at encoding, but not retrieval

We next investigated the effect of stimulation phase on memory accuracy. Based on the *a priori* hypothesis that stimulation targeted to the hippocampal network would induce minimal and maximal performance at opposite phases on the entraining oscillation (see **Chapter 3**), we compared performance across trials with jitters at 180° intervals (i.e., peak versus trough and falling versus rising phases). To control for potential indirect effects of stimulation including sensory entrainment, we specifically tested whether these effects were present following in-network versus out-of-network stimulation. We restricted our initial analyses to only trials in the first theta cycle after stimulation, which we hypothesized would produce the strongest effect

of entrained phase on memory (due to entrainment decaying over time; Demeter et al., 2016; Solomon et al., 2021).

In Experiment 1, we observed an effect of in-network stimulation phase on memory performance specifically for rising versus falling trials (**Fig. 4.8b**. ΔHit rate ± SD, rising: 0.01 ± 0.1; falling: -0.11 ± 0.1. Paired t-test of Δhit rates: $t(14) = 3.0$, $p = 0.009$, *Cohen's d* = 1). In contrast, no effect was observed for peak versus trough trials (ΔHit rate ± SD, peak: 0.0 ± 0.2 ; trough: 0.0 ± 0.2. Paired t-test of Δhit rates: $t(14) = 0.14$, $p = 0.9$, *Cohen's d* = 0.04). Ad-hoc analyses of memory accuracy for each stimulation condition (**Fig. 4.8a**) suggested that the rising versus falling effect was primarily driven by the out-of-network stimulation condition. We observed a significant difference across rising and falling trials following out-of-network stimulation (**Fig. 4.8a.** Mean hit rate ± SD, rising: 0.47 ± 0.1; falling: 0.56 ± 0.1. Paired t-test of rising versus falling hit rate: $t(14) = -2.9$, $p = 0.01$, *Cohen's d* = -0.8) but not in-network stimulation (**Fig. 4.8a**. Mean hit rate ± SD, rising: 0.49 ± 0.2; falling: 0.45 ± 0.2. Paired t-test: $t(14) = 1.0$, $p = 0.3$, *Cohen's d* = 0.2).

In Experiment 2, we observed no effect of in-network stimulation on memory performance for either rising versus falling (**Fig. 4.8d**. ΔHit rate ± SD, rising: 0.03 ± 0.1; falling: -0.0 ± 0.2. Paired t-test of Δhit rates: $t(14) = 1.0$, $p = 0.3$, *Cohen's d* = 0.2) or peak versus trough trials (ΔHit rate ± SD, peak: 0.1 ± 0.1; trough: 0.0 ± 0.1. Paired t-test of Δhit rates: $t(14) = -1.3$, $p = 0.2$, *Cohen's d* = -0.5.

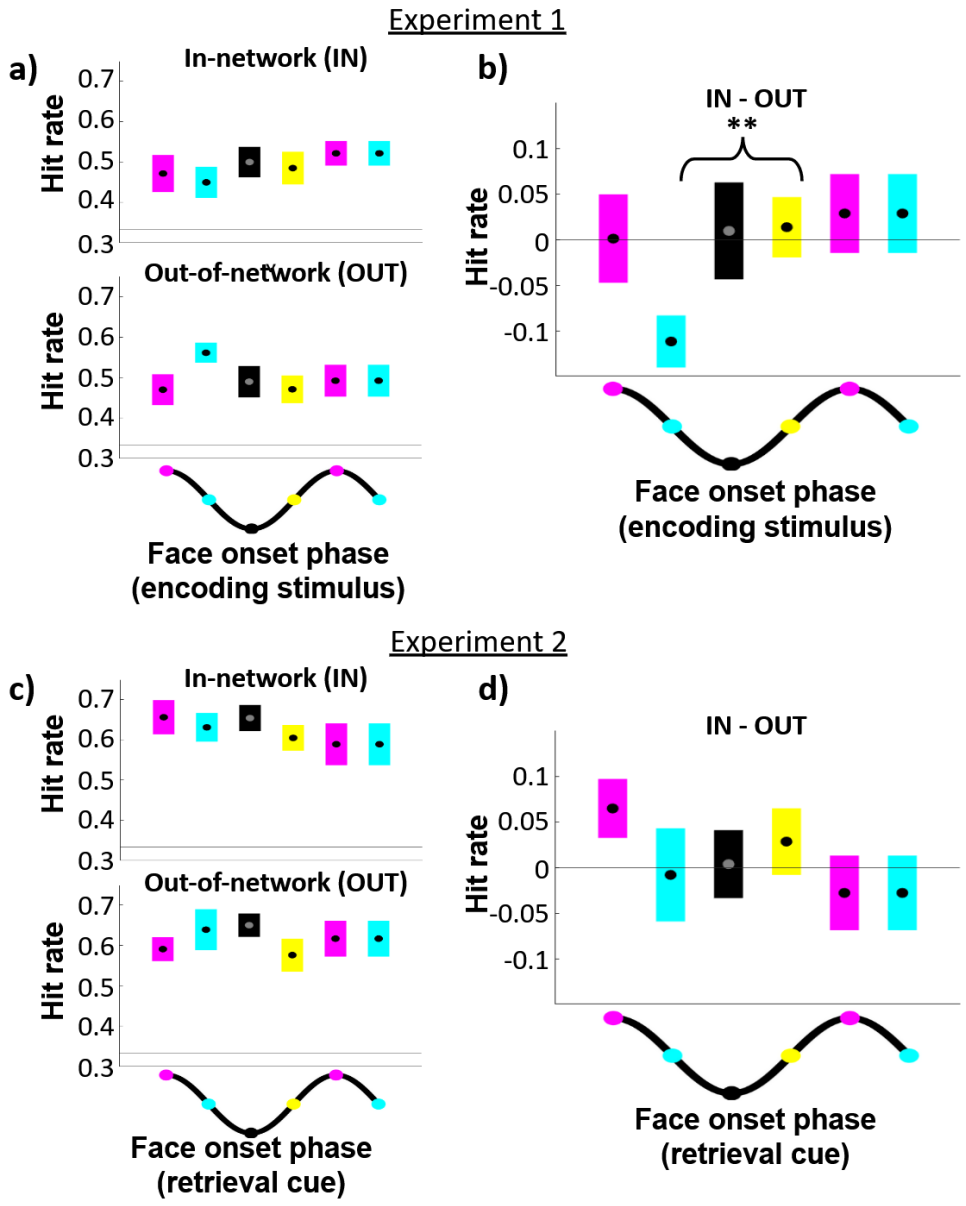

Figure 4.8. Hippocampal network-targeted entraining stimulation produces phase-dependent memory effect during encoding. Dots indicate mean hit rate across participants (n = 15 per experiment). Error patches indicate ± 1 SEM across participants. Patch color indicates extrapolated theta phase (see x-axis legend). **A)** Memory task performance in Experiment 1, sorted according to extrapolated phase of the entraining theta-patterned stimulation. Top: Following in-network stimulation. Bottom: Following out-of-network stimulation. Horizontal line indicates chance performance. **B)** Difference in hit rate across in-network and out-of-network stimulation. Horizontal line indicates no difference across stimulation conditions. Asterisk indicates phase conditions with significant hit rate differences across 180˚ intervals (** $p < 0.01$). **C, D)** As in panels A) and B), for Experiment 2.

Stimulation protocol did not produce cumulative effects on memory performance

The entraining rTMS protocol used in Experiments 1 and 2 resembles iTBS (see **Introduction)** in terms of train length and intertrain interval. However, whereas facilitatory iTBS protocols typically deliver 20 trains of 2 s TBS, our entraining stimulation was delivered in blocks of 9 trains, with a variable interval between blocks (driven by variable participant response latencies as well as breaks between blocks). Modifying the number of trains delivered, intertrain interval, and rest period duration between sessions for theta-burst protocols has previously been demonstrated to diminish or reverse the original effect direction (Gamboa et al., 2010; Gamboa et. al, 2011; Benali et al., 2011).

It was therefore unclear whether the entraining rTMS protocol may have led to cumulative effects on network excitability, with consequent effects on task performance. To investigate, we assessed task performance according to position in the experimental session. For each participant, trials were divided into tertiles according to position in the stimulation session. Tertiles comprised 4 blocks each of in-network and out-of-network stimulation trials. Accuracy was then computed within each tertile. We observed no effect of experimental session order on memory performance in either Experiment 1 or Experiment 2 (**Fig 4.9a,d.** One-way repeated measures ANOVA (effect of tertiles), experiment 1: $f(2) = 0.12$, $p = 0.9$; experiment 2: $f(2) = 0.07$, $p = 0.9$. Participant:tertile interaction, experiment 1: $f(2) = 0.24$, $p = 0.8$; experiment 2: $f(2) = 0.14$, $p = 0.9$).

No effects were revealed by restricting the analysis to either in-network stimulation trials (**Fig 4.9b,e.** Effect of tertiles, experiment 1: $f(2) = 0.76$, $p = 0.5$; experiment 2: $f(2) = 0.03$, $p > 0.9$. Participant:tertile interaction, experiment 1: $f(2) = 0.69$, $p = 0.5$; experiment 2: $f(2) = 0.004$, $p > 0.99$) or out-of-network stimulation trials (**Fig. 4.9c,f.** Effect of tertiles, experiment 1: $f(2) =$

0.05, $p > 0.9$; experiment 2: $f(2) = 0.04$, $p > 0.9$. Participant:tertile interaction: experiment 1: $f(2) = 0.08$, $p = 0.9$; experiment 2: $f(2) = 0.18$, $p = 0.8$). These findings support that the entraining rTMS protocol did not produce cumulative effects on task performance.

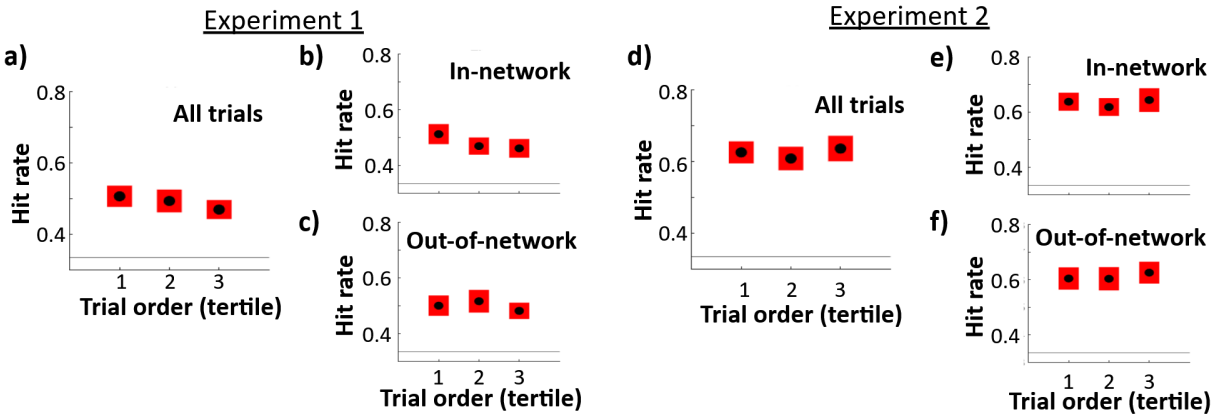

Figure 4.9. No effect of position in the experimental session on memory performance. Memory task performance presented as a function of position tertile in the experimental session. Dots indicate mean hit rate across participants ($n = 15$ per experiment). Error patches are drawn at ± 1 SEM. **A-C**) Task performance by tertile in Experiment 1: **A)** For all trials. **B)** Restricted to in-network stimulation trials. **C)** Restricted to out-of-network stimulation trials. **D-F)** As A-C), for Experiment 2. No effect of tertile on memory performance was observed in either experiment.

Participant response latency predicts memory accuracy when stimulation was delivered at retrieval, but not encoding

To assess how differences in task design may have contributed to differences in the effects of stimulation-induced theta phase on memory accuracy across experiments, we analyzed differences in participant response latencies and the relationships between trialwise response latency and accuracy. Response latencies were measured in each trial from the presentation of the R/G/B associates until the participant's keypress. Participant response latencies were significantly greater in Experiment 1 than Experiment 2 (mean response latency across participants ± SD, experiment 1: $\mu = 3404 \pm 1141$ ms; experiment 2: $\mu = 1584 \pm 442$ ms; paired

t-test: $t(14) = 4.8,\ p < 0.001$). No differences were observed between response times following in-network versus out-of-network stimulation in either experiment (paired t-test of mean latencies following in-network versus out-of-network stimulation, experiment 1: $t(14) = -0.36,\ p = 0.7$; experiment 2: $t(14) = -0.12,\ p > 0.9$).

To analyze the relationships between response latency and accuracy, we divided trials into quartiles according to response latency for each participant. Within each quartile, we then computed each participant's hit rate (**Fig. 4.10a,d**). We observed a marked negative relationship between response latency and accuracy which was specific to Experiment 2 (**Fig. 4.10d.** $r = -0.54$, $p < 0.001$). This relationship was present for both in-network stimulation trials (**Fig. 4.10e.** Linear correlation: $r = -0.47$, $p < 0.001$) and out-of-network stimulation trials (**Fig. 4.10f.** $r = -0.52$, $p < 0.001$). No such significant linear relationships between response latency and accuracy were observed for Experiment 1 (**Fig. 4.10a-c**. All trials: $r = –0.22$, $p = 0.08$; in-network trials: $r = -0.14$, $p = 0.3$; out-of-network trials: $r = -0.20$, $p = 0.1$).

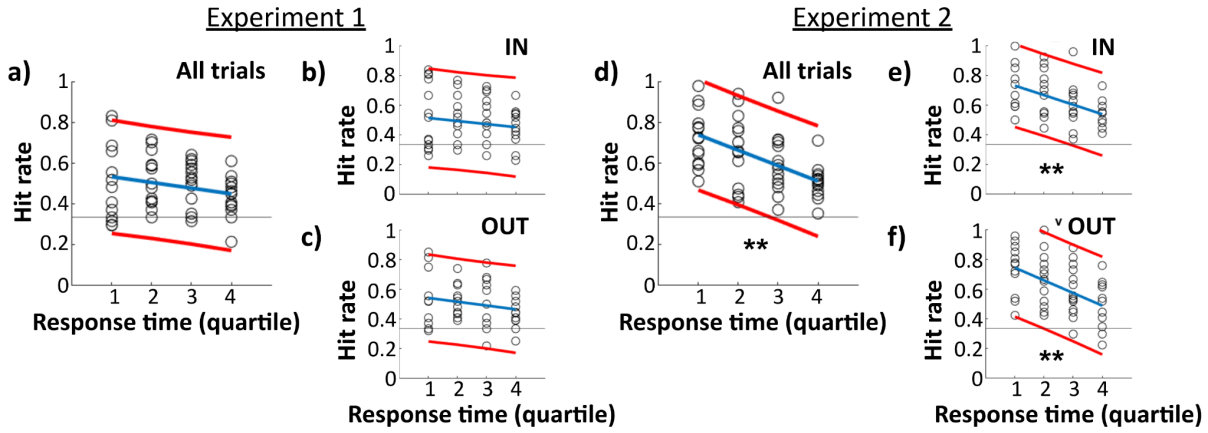

Figure 4.10. Differences in the relationship between response time and performance across Experiments 1 and 2. Each circle represents mean memory performance in that quartile for one participant (n = 15 per experiment). Linear regression (blue) plotted alongside 95% prediction intervals (red). Asterisk indicates a significant linear relationship between performance and response time (**$p < 0.001$). Horizontal line indicates chance memory performance. **A)** Memory task performance across all trials in Experiment 1. **B-C)** Memory task performance in Experiment 1 following in-network (**B**) or out-of-network (**C**) stimulation, sorted according to response time. **D-F)** As in panels A-C), for Experiment 2.

4.4 Discussion

The experiments described in this chapter investigated whether hippocampal memory function varies with the phase of theta-patterned rTMS targeted to functionally connected cortical sites. We hypothesized that if network-targeted stimulation successfully entrained hippocampal theta phase, then memory encoding and retrieval performance would vary continuously with the phase of the entrained oscillation. Based on the findings outlined in **Chapter 3**, we hypothesized that opposite phases in the entrained oscillation would relate to optimal encoding versus retrieval performance.

After controlling for indirect effects of stimulation, we observed an effect of phase exclusively when stimulation was delivered at encoding, with significant differences in subsequent memory

accuracy for memoranda encoded at the ostensible falling versus rising theta phases. However, no effect of phase was observed when stimulation was delivered at retrieval. Further, *ad hoc* testing revealed that the effect observed at encoding was primarily driven by differences in performance induced by the control stimulation, rather than the network-targeted entrainment.

Several factors may have contributed to these unexpected results. We note that disparities in the locations of in-network stimulation sites may have reduced the efficacy of our network-targeted oscillatory entrainment. In particular, we observe that in a subset of participants in Experiment 1, the ostensible in-network stimulation was delivered to the postcentral gyrus (**Fig. 4.5**), anterior of the anatomical targets where stimulation has been previously demonstrated to impact hippocampal function (Cash et al., 2022). We speculate that the more disparate site selection in Experiment 1 was driven by experimenter error. However, site selection error is unlikely to account for the lack of phase effect at retrieval, as stimulation was appropriately restricted to the inferior parietal lobule for all participants in Experiment 2.

These experiments reflected a novel attempt to use noninvasive stimulation to manipulate the oscillatory phase of deep structures. However, it is unclear whether network-targeted stimulation successfully entrained the hippocampal theta phase in either experiment. In previous investigations of phase entrainment at the cortical target, stimulation has been found to enhance oscillatory power at the stimulated frequency (see **Chapter 1.2**). We therefore expected that successful phase entrainment of hippocampal theta would coincide with enhancement of hippocampal theta power. As hippocampal theta power in the prestimulus period is associated with improved subsequent memory (Fell et al., 2011), we anticipated that in-network stimulation would enhance overall (i.e., phase-indifferent) memory accuracy. However, in-network

stimulation did not impact overall accuracy relative to out-of-network control stimulation in either experiment.

A previous study from our laboratory observed enhancement of recall hits – but not of overall memory accuracy – by single trains of network-targeted, theta-burst rTMS delivered before memorandum presentation (Hermiller et al., 2020). In contrast, we observed no effects of stimulation site on recall hit rate. It is unclear to what extent differences in the memory task across that study and the experiments described in this chapter (including visual stimulus duration; control stimulation locations; memorandum type; and confidence judgement reporting) contributed to this difference, in addition to the off-target stimulation noted above. Nevertheless, these findings suggest that single trains of theta-burst, network-targeted stimulation failed to consistently entrain the phase of the hippocampal theta oscillation.

Without evidence for successful phase entrainment by network-targeted stimulation, it is difficult to draw conclusions about the role of theta phase in human hippocampal memory. These experiments demonstrate the need for alternative approaches, including alternative causal manipulations of hippocampal theta phase, to investigate the impact of theta phase-dependent connectivity changes (**Chapter 3**) on memory performance.

Chapter 5: Discussion

5.1 Conclusions

Hippocampal-dependent memory is thought to be supported by distinct connectivity states, with strong input to the hippocampus benefitting encoding and weak input benefitting retrieval. Previous research in rodent models suggests that the hippocampal theta oscillation orchestrates the transition between these states, with opposite phase angles predicting minimal versus maximal input; however, it is unclear whether a homologous phase-dependence exists in humans. In this dissertation, I presented two lines of research investigating this question: first, by assessing whether human hippocampal connectivity varies with theta phase; and second, by assessing whether human hippocampal-dependent memory varies with theta phase.

In the study described in **Chapter 3**, we used intracranial stimulation to probe hippocampal connectivity with network afferents over the course of the theta oscillation. We found a significant continuous relationship between hippocampal theta phase at stimulation onset and the amplitude of the evoked hippocampal response. Maximal differences in evoked response amplitude were obtained when stimulation was delivered across a consistent 180° interval on the local theta oscillation. These findings demonstrate that the human hippocampus undergoes theta-locked changes in network connectivity, supporting a homology with the phase-dependence of memory performance previously observed in animal models.

In the studies described in **Chapter 4**, we investigated the relationship between human hippocampal theta phase and memory performance. We attempted to phase-entrain the hippocampus via rTMS targeted to functionally connected cortical locations; however, we were unable to verify the efficacy of this method. In particular, there was no effect of

hippocampal-network targeted stimulation versus out-of-network stimulation on overall memory accuracy or recollection accuracy, suggesting a failure to enhance hippocampal theta power. Although we observed an effect of phase on memory encoding, with significant accuracy differences across the ostensible rising versus falling phases, it is unlikely that this effect was caused specifically by hippocampal phase entrainment. Understanding the role of phase-dependent connectivity changes in memory therefore remains a crucial avenue for research into human hippocampal function.

5.2 Future directions

Local theta phase and hippocampal network connectivity

In **Chapter 1**, I described how the theta oscillation varies throughout the hippocampus, undergoing phase shifts both across hippocampal layers and down the long axis. Previous studies of hippocampal phase-dependent connectivity have suggested that hippocampal connectivity relates to phase as recorded at some particular hippocampal depth – commonly, that entorhinal input is maximized at theta trough, as measured near the CA1 fissure (e.g., Hasselmo, 2002). Studies which target different hippocampal layers (and positions on the long axis) have reported different specific phase angles relating to minimal and maximal connectivity; but as theta phase shift is consistent between layers (Lubenov & Siapas, 2009), these findings have been interpreted as merely layer-shifted versions of the nominal, fissural model (e.g., Siegle & Wilson, 2014; Hyman et al., 2003; Douchamps et al., 2013).

In **Chapter 3**, we observed changes in hippocampal connectivity related to the phase of the local theta oscillation (that is, the theta oscillation as recorded from an interlaminar macroelectrode). Hippocampal electrodes varied across and within subjects in both laminar depth and position on

the long axis. Despite this variable placement – and concomitant variable theta phase across electrodes – we observed consistent changes in local connectivity according to specific local theta phase angles. I hypothesize that changes in hippocampal connectivity related to the theta oscillation may 1) coincide with local, rather than unitary theta phase; and 2) occur locally, rather than globally across the hippocampus. In other words, hippocampal network connectivity changes may occur slicewise down the septotemporal axis (according to e.g. fissural theta phase within that coronal slice), rather than globally across the hippocampus according to phase at some particular location.

Previous work has demonstrated functional specialization along the long axis, with septal versus temporal hippocampus variously associated for example with non-spatial versus spatial memory, emotionally-valenced versus non-valenced learning, and large- versus small-scale spatial representations (see Poppenk et al., 2013; Strange et al., 2014). Connectivity changes according to local theta phase may be one mechanism contributing to this segregation of function. Septal versus temporal hippocampus segments receive projections from distinct portions of entorhinal cortex, with a smooth mapping of entorhinal to hippocampal space (Canto et al., 2008; see Strange et al., 2014). The proposed model of slicewise connectivity change may therefore relate to a smooth connectivity gradient across the entorhinal cortex, where input from dorsolateral versus ventromedial entorhinal cortex (using gradient directions in rodent) is enhanced at a given timepoint.

This model may help explain the consistent relationship between fissural theta phase and connectivity observed in animal studies, despite differences in long-axis recording locations. In addition to the findings described in **Chapter 3** related to local theta phase, the 2014 study by

Siegle & Wilson demonstrated that disruptive optogenetic stimulation produced dissociable effects on encoding versus retrieval according to local theta phase. While this finding is not consistent with the extant model of global hippocampal connectivity changes – which predicts different phase angles associated with encoding versus retrieval, according to the local phase offset to some reference location – it may be explained by the proposed slicewise phase-dependence. Research assessing this model might characterize the phase angles associated with some putatively segregated hippocampal function. If connectivity changes occur globally across the hippocampus, then the same timepoint is likely to be associated with e.g. spatial and nonspatial encoding. In contrast, if connectivity changes occur locally, then different timepoints are likely to be associated with spatial versus nonspatial encoding, according to the magnitude of long axis phase shift (such that septal and temporal fissural theta are respectively at trough).

Hippocampal-dependent memory and theta phase

Why did we attempt to entrain hippocampal theta noninvasively in our investigation of theta phase and memory? Noninvasive entrainment of the theta oscillation primarily appealed as an opportunity to investigate phase-dependent memory in the healthy hippocampus. Invasive recordings are obtained opportunistically in patients undergoing clinical monitoring and treatment for neurologic disease or injury. Participants in the study described in **Chapter 3** were undergoing monitoring for suspected temporal lobe epilepsy, which is associated with episodic memory impairment (Mayeux et al., 1980; Helmstaedter & Kockelmann, 2006) as well as changes to hippocampal structure and function (Helmstaedter & Kockelmann, 2006; Gelinas et al., 2016). It is unclear whether disease-related changes to the hippocampus might impact the relationship between hippocampal network connectivity and memory function. In addition, the logistical constraints of working with patients undergoing invasive monitoring – including a

small subject pool, limited duration of the experiment session, and variable placement of recording and stimulating electrodes – may restrict the length and design complexity of studies using invasive rather than noninvasive methods.

Despite these limitations, future research may use invasive methods to characterize the relationship between endogenous theta phase and memory. In the study described in **Chapter 3**, stimulation pulses were delivered without regard for theta phase; I performed *post hoc* sorting according to phase at stimulation onset to analyze the effect of phase on hippocampal network connectivity. Analogously, future work could investigate memory performance according to theta phase at stimulus presentation (or, perhaps more relevantly, according to the timing of the hippocampal evoked response).

Invasive stimulation may also prove an important tool to carry out causal manipulations of theta phase during task performance. Recent work by Solomon and colleagues demonstrated that direct electrical theta burst stimulation of the human medial temporal lobe rapidly evokes theta oscillations in widespread brain regions. Oscillations were preferentially induced at the frequency of stimulation, and decayed within only a few theta cycles of the end of stimulation (Solomon et al., 2021), supporting that the effect was related to phase-entrainment of the endogenous theta rhythm. Numerous studies in animal models have demonstrated the effectiveness of direct electrical stimulation of hippocampal afferents to induce hippocampal theta oscillations (with theta-patterned stimulation, as in McNaughton et al., 2006; Shirvalkar et al., 2010) as well as to modify hippocampal theta phase (by inducing phase-reset with single-pulse stimulation; Williams & Givens, 2003). Further research would be necessary to

determine whether and how to optimally apply direct electrical stimulation to consistently modify hippocampal theta phase.

References

Addante, R. J., Watrous, A. J., Yonelinas, A. P., Ekstrom, A. D., & Ranganath, C. (2011). Prestimulus theta activity predicts correct source memory retrieval. *Proceedings of the National Academy of Sciences*, *108*(26), 10702–10707. https://doi.org/10.1073/pnas.1014528108

Althoff, R. R., & Cohen, N. J. (1999). Eye-movement-based memory effect: A reprocessing effect in face perception. *Journal of Experimental Psychology: Learning, Memory, and Cognition*, *25*, 997–1010. https://doi.org/10.1037/0278-7393.25.4.997

Arnolds, D. E. a. T., Lopes Da Silva, F. H., Aitink, J. W., Kamp, A., & Boeijinga, P. (1980). The spectral properties of hippocampal EEG related to behaviour in man. *Electroencephalography and Clinical Neurophysiology*, 324–328.

Arnulfo, G., Hirvonen, J., Nobili, L., Palva, S., & Palva, J. M. (2015). Phase and amplitude correlations in resting-state activity in human stereotactical EEG recordings. *NeuroImage*, *112*, 114–127. https://doi.org/10.1016/j.neuroimage.2015.02.031

Ashburner, J., & Friston, K. J. (2005). Unified segmentation. *NeuroImage*, *26*(3), 839–851. https://doi.org/10.1016/j.neuroimage.2005.02.018

Baisden, R. H., Woodruff, M. L., & Hoover, D. B. (1984). Cholinergic and non-cholinergic septo-hippocampal projections: A double-label horseradish peroxidase-acetylcholinesterase study in the rabbit. *Brain Research*, *290*(1), 146–151. https://doi.org/10.1016/0006-8993(84)90745-5

Benali, A., Trippe, J., Weiler, E., Mix, A., Petrasch-Parwez, E., Girzalsky, W., Eysel, U. T., Erdmann, R., & Funke, K. (2011). Theta-Burst Transcranial Magnetic Stimulation Alters Cortical Inhibition. *Journal of Neuroscience*, *31*(4), 1193–1203. https://doi.org/10.1523/JNEUROSCI.1379-10.2011

Berens, P. (2009). CircStat: A MATLAB Toolbox for Circular Statistics. *Journal of Statistical Software*, *31*, 1–21. https://doi.org/10.18637/jss.v031.i10

Bergmann, T. O., Varatheeswaran, R., Hanlon, C. A., Madsen, K. H., Thielscher, A., & Siebner, H. R. (2021). Concurrent TMS-fMRI for causal network perturbation and proof of target engagement. *NeuroImage*, *237*, 118093. https://doi.org/10.1016/j.neuroimage.2021.118093

Berry, S. D., & Thompson, R. F. (1978). Prediction of Learning Rate from the Hippocampal Electroencephalogram. *Science*, *200*(4347), 1298–1300. https://doi.org/10.1126/science.663612

Bonnici, H. M., Cheke, L. G., Green, D. A. E., FitzGerald, T. H. M. B., & Simons, J. S. (2018). Specifying a Causal Role for Angular Gyrus in Autobiographical Memory.

Journal of Neuroscience, *38*(49), 10438–10443. https://doi.org/10.1523/JNEUROSCI.1239-18.2018

Borhegyi, Z., Varga, V., Szilágyi, N., Fabo, D., & Freund, T. F. (2004). Phase Segregation of Medial Septal GABAergic Neurons during Hippocampal Theta Activity. *Journal of Neuroscience*, *24*(39), 8470–8479. https://doi.org/10.1523/JNEUROSCI.1413-04.2004

Bragin, A., Jando, G., Nadasdy, Z., Hetke, J., Wise, K., & Buzsaki, G. (1995). Gamma (40-100 Hz) oscillation in the hippocampus of the behaving rat. *Journal of Neuroscience*, *15*(1), 47–60. https://doi.org/10.1523/JNEUROSCI.15-01-00047.1995

Brankačk, J., Stewart, M., & E. Fox, S. (1993). Current source density analysis of the hippocampal theta rhythm: Associated sustained potentials and candidate synaptic generators. *Brain Research*, *615*(2), 310–327. https://doi.org/10.1016/0006-8993(93)90043-M

Buzsáki, G., Haas, H. L., & Anderson, E. G. (1987). Long-term potentiation induced by physiologically relevant stimulus patterns. *Brain Research*, *435*(1), 331–333. https://doi.org/10.1016/0006-8993(87)91618-0

Buzsáki, G., Lai-Wo S., L., & Vanderwolf, C. H. (1983). Cellular bases of hippocampal EEG in the behaving rat. *Brain Research Reviews*, *6*(2), 139–171. https://doi.org/10.1016/0165-0173(83)90037-1

Buzsáki, G., & Moser, E. I. (2013). Memory, navigation and theta rhythm in the hippocampal-entorhinal system. *Nature Neuroscience*, *16*(2), Article 2. https://doi.org/10.1038/nn.3304

Canto, C. B., Wouterlood, F. G., & Witter, M. P. (2008). What Does the Anatomical Organization of the Entorhinal Cortex Tell Us? *Neural Plasticity*, *2008*, e381243. https://doi.org/10.1155/2008/381243

Cash, R. F. H., Hendrikse, J., Fernando, K. B., Thompson, S., Suo, C., Fornito, A., Yücel, M., Rogasch, N. C., Zalesky, A., & Coxon, J. P. (2022). Personalized brain stimulation of memory networks. *Brain Stimulation*, *15*(5), 1300–1304. https://doi.org/10.1016/j.brs.2022.09.004

Catani, M., & Thiebaut de Schotten, M. (2008). A diffusion tensor imaging tractography atlas for virtual in vivo dissections. *Cortex*, *44*(8), 1105–1132. https://doi.org/10.1016/j.cortex.2008.05.004

Chrobak, J. J., Lörincz, A., & Buzsáki, G. (2000). Physiological patterns in the hippocampo-entorhinal cortex system. *Hippocampus*, *10*(4), 457–465. https://doi.org/10.1002/1098-1063(2000)10:4<457::AID-HIPO12>3.0.CO;2-Z

Chung, S. W., Rogasch, N. C., Hoy, K. E., Sullivan, C. M., Cash, R. F. H., & Fitzgerald, P. B. (2018). Impact of different intensities of intermittent theta burst stimulation on the cortical properties during TMS-EEG and working memory performance. *Human Brain Mapping*, *39*(2), 783–802. https://doi.org/10.1002/hbm.23882

Cox, R. W. (1996). AFNI: Software for Analysis and Visualization of Functional Magnetic Resonance Neuroimages. *Computers and Biomedical Research*, *29*(3), 162–173. https://doi.org/10.1006/cbmr.1996.0014

Davachi, L. (2006). Item, context and relational episodic encoding in humans. *Current Opinion in Neurobiology*, *16*(6), 693–700. https://doi.org/10.1016/j.conb.2006.10.012

Demeter, E. (2016). Enhancing Cognition with Theta Burst Stimulation. *Current Behavioral Neuroscience Reports*, *3*(2), 87–94. https://doi.org/10.1007/s40473-016-0072-7

Demeter, E., Mirdamadi, J. L., Meehan, S. K., & Taylor, S. F. (2016). Short theta burst stimulation to left frontal cortex prior to encoding enhances subsequent recognition memory. *Cognitive, Affective, & Behavioral Neuroscience*, *16*(4), 724–735. https://doi.org/10.3758/s13415-016-0426-3

Ding, S.-L., Royall, J. J., Sunkin, S. M., Ng, L., Facer, B. A. C., Lesnar, P., Guillozet-Bongaarts, A., McMurray, B., Szafer, A., Dolbeare, T. A., Stevens, A., Tirrell, L., Benner, T., Caldejon, S., Dalley, R. A., Dee, N., Lau, C., Nyhus, J., Reding, M., … Lein, E. S. (2016). Comprehensive cellular-resolution atlas of the adult human brain. *Journal of Comparative Neurology*, *524*(16), 3127–3481. https://doi.org/10.1002/cne.24080

Douchamps, V., Jeewajee, A., Blundell, P., Burgess, N., & Lever, C. (2013). Evidence for Encoding versus Retrieval Scheduling in the Hippocampus by Theta Phase and Acetylcholine. *Journal of Neuroscience*, *33*(20), 8689–8704. https://doi.org/10.1523/JNEUROSCI.4483-12.2013

Dowdle, L. T., Brown, T. R., George, M. S., & Hanlon, C. A. (2018). Single pulse TMS to the DLPFC, compared to a matched sham control, induces a direct, causal increase in caudate, cingulate, and thalamic BOLD signal. *Brain Stimulation: Basic, Translational, and Clinical Research in Neuromodulation*, *11*(4), 789–796. https://doi.org/10.1016/j.brs.2018.02.014

Du, J., Rolls, E. T., Cheng, W., Li, Y., Gong, W., Qiu, J., & Feng, J. (2020). Functional connectivity of the orbitofrontal cortex, anterior cingulate cortex, and inferior frontal gyrus in humans. *Cortex*, *123*, 185–199. https://doi.org/10.1016/j.cortex.2019.10.012

Duncan, K., Tompary, A., & Davachi, L. (2014). Associative Encoding and Retrieval Are Predicted by Functional Connectivity in Distinct Hippocampal Area CA1 Pathways. *Journal of Neuroscience*, *34*(34), 11188–11198. https://doi.org/10.1523/JNEUROSCI.0521-14.2014

Eichenbaum, H. (2000). A cortical–hippocampal system for declarative memory. *Nature Reviews Neuroscience*, *1*(1), Article 1. https://doi.org/10.1038/35036213

Eichenbaum, H. (2004). Hippocampus: Cognitive Processes and Neural Representations that Underlie Declarative Memory. *Neuron*, *44*(1), 109–120. https://doi.org/10.1016/j.neuron.2004.08.028

Ekstrom, A. D., Caplan, J. B., Ho, E., Shattuck, K., Fried, I., & Kahana, M. J. (2005). Human hippocampal theta activity during virtual navigation. *Hippocampus*, *15*(7), 881–889. https://doi.org/10.1002/hipo.20109

Fell, J., & Axmacher, N. (2011). The role of phase synchronization in memory processes. *Nature Reviews Neuroscience*, *12*(2), Article 2. https://doi.org/10.1038/nrn2979

Fell, J., Ludowig, E., Staresina, B. P., Wagner, T., Kranz, T., Elger, C. E., & Axmacher, N. (2011). Medial Temporal Theta/Alpha Power Enhancement Precedes Successful Memory Encoding: Evidence Based on Intracranial EEG. *Journal of Neuroscience*, *31*(14), 5392–5397. https://doi.org/10.1523/JNEUROSCI.3668-10.2011

Fernández, G., Brewer, J. B., Zhao, Z., Glover, G. H., & Gabrieli, J. D. E. (1999). Level of sustained entorhinal activity at study correlates with subsequent cued-recall performance: A functional magnetic resonance imaging study with high acquisition rate. *Hippocampus*, *9*(1), 35–44. https://doi.org/10.1002/(SICI)1098-1063(1999)9:1<35::AID-HIPO4>3.0.CO;2-Z

Freedberg, M., Reeves, J. A., Toader, A. C., Hermiller, M. S., Voss, J. L., & Wassermann, E. M. (2019). Persistent Enhancement of Hippocampal Network Connectivity by Parietal rTMS Is Reproducible. *ENeuro*, *6*(5), ENEURO.0129-19.2019. https://doi.org/10.1523/ENEURO.0129-19.2019

Fries, P. (2005). A mechanism for cognitive dynamics: Neuronal communication through neuronal coherence. *Trends in Cognitive Sciences*, *9*(10), 474–480. https://doi.org/10.1016/j.tics.2005.08.011

Gamboa, O. L., Antal, A., Laczo, B., Moliadze, V., Nitsche, M. A., & Paulus, W. (2011). Impact of repetitive theta burst stimulation on motor cortex excitability. *Brain Stimulation*, *4*(3), 145–151. https://doi.org/10.1016/j.brs.2010.09.008

Gamboa, O. L., Antal, A., Moliadze, V., & Paulus, W. (2010). Simply longer is not better: Reversal of theta burst after-effect with prolonged stimulation. *Experimental Brain Research*, *204*(2), 181–187. https://doi.org/10.1007/s00221-010-2293-4

Gelbard-Sagiv, H., Mukamel, R., Harel, M., Malach, R., & Fried, I. (2008). Internally Generated Reactivation of Single Neurons in Human Hippocampus During Free Recall. *Science*, *322*(5898), 96–101. https://doi.org/10.1126/science.1164685

Gelinas, J. N., Khodagholy, D., Thesen, T., Devinsky, O., & Buzsáki, G. (2016). Interictal epileptiform discharges induce hippocampal–cortical coupling in temporal lobe epilepsy. *Nature Medicine*, *22*(6), Article 6. https://doi.org/10.1038/nm.4084

Goutagny, R., Jackson, J., & Williams, S. (2009). Self-generated theta oscillations in the hippocampus. *Nature Neuroscience*, *12*(12), Article 12. https://doi.org/10.1038/nn.2440

Goyal, A., Miller, J., Qasim, S. E., Watrous, A. J., Zhang, H., Stein, J. M., Inman, C. S., Gross, R. E., Willie, J. T., Lega, B., Lin, J.-J., Sharan, A., Wu, C., Sperling, M. R., Sheth, S. A., McKhann, G. M., Smith, E. H., Schevon, C., & Jacobs, J. (2020).

Functionally distinct high and low theta oscillations in the human hippocampus. *Nature Communications*, *11*(1), Article 1. https://doi.org/10.1038/s41467-020-15670-6

Greenberg, J. A., Burke, J. F., Haque, R., Kahana, M. J., & Zaghloul, K. A. (2015). Decreases in theta and increases in high frequency activity underlie associative memory encoding. *NeuroImage*, *114*, 257–263. https://doi.org/10.1016/j.neuroimage.2015.03.077

Hanlon, C. A., Dowdle, L. T., Moss, H., Canterberry, M., & George, M. S. (2016). Mobilization of Medial and Lateral Frontal-Striatal Circuits in Cocaine Users and Controls: An Interleaved TMS/BOLD Functional Connectivity Study. *Neuropsychopharmacology*, *41*(13), Article 13. https://doi.org/10.1038/npp.2016.114

Hanslmayr, S., Spitzer, B., & Bäuml, K.-H. (2009). Brain Oscillations Dissociate between Semantic and Nonsemantic Encoding of Episodic Memories. *Cerebral Cortex*, *19*(7), 1631–1640. https://doi.org/10.1093/cercor/bhn197

Hardingham, N., Glazewski, S., Pakhotin, P., Mizuno, K., Chapman, P. F., Giese, K. P., & Fox, K. (2003). Neocortical Long-Term Potentiation and Experience-Dependent Synaptic Plasticity Require α-Calcium/Calmodulin-Dependent Protein Kinase II Autophosphorylation. *Journal of Neuroscience*, *23*(11), 4428–4436. https://doi.org/10.1523/JNEUROSCI.23-11-04428.2003

Hasselmo, M. E. (2005). What is the function of hippocampal theta rhythm?—Linking behavioral data to phasic properties of field potential and unit recording data. *Hippocampus*, *15*(7), 936–949. https://doi.org/10.1002/hipo.20116

Hebscher, M., Ibrahim, C., & Gilboa, A. (2020). Precuneus stimulation alters the neural dynamics of autobiographical memory retrieval. *NeuroImage*, *210*, 116575. https://doi.org/10.1016/j.neuroimage.2020.116575

Hebscher, M., Kragel, J. E., Kahnt, T., & Voss, J. L. (2021). Enhanced reinstatement of naturalistic event memories due to hippocampal-network-targeted stimulation. *Current Biology*, *31*(7), 1428-1437.e5. https://doi.org/10.1016/j.cub.2021.01.027

Helmstaedter, C., & Kockelmann, E. (2006). Cognitive Outcomes in Patients with Chronic Temporal Lobe Epilepsy. *Epilepsia*, *47*(s2), 96–98. https://doi.org/10.1111/j.1528-1167.2006.00702.x

Hermiller, M. S., Chen, Y. F., Parrish, T. B., & Voss, J. L. (2020). Evidence for Immediate Enhancement of Hippocampal Memory Encoding by Network-Targeted Theta-Burst Stimulation during Concurrent fMRI. *Journal of Neuroscience*, *40*(37), 7155–7168. https://doi.org/10.1523/JNEUROSCI.0486-20.2020

Hermiller, M. S., Karp, E., Nilakantan, A. S., & Voss, J. L. (2019). Episodic memory improvements due to noninvasive stimulation targeting the cortical–hippocampal network: A replication and extension experiment. *Brain and Behavior*, *9*(12), e01393. https://doi.org/10.1002/brb3.1393

Herweg, N. A., Solomon, E. A., & Kahana, M. J. (2020). Theta Oscillations in Human Memory. *Trends in Cognitive Sciences*, *24*(3), 208–227. https://doi.org/10.1016/j.tics.2019.12.006

Hogsden, J. L., Rosen, L. G., & Dringenberg, H. C. (2011). Pharmacological and deprivation-induced reinstatement of juvenile-like long-term potentiation in the primary auditory cortex of adult rats. *Neuroscience*, *186*, 208–219. https://doi.org/10.1016/j.neuroscience.2011.04.002

Holmes, C. J., Hoge, R., Collins, L., Woods, R., Toga, A. W., & Evans, A. C. (1998). Enhancement of MR Images Using Registration for Signal Averaging. *Journal of Computer Assisted Tomography*, *22*(2), 324–333.

Hölscher, C., Anwyl, R., & Rowan, M. J. (1997). Stimulation on the Positive Phase of Hippocampal Theta Rhythm Induces Long-Term Potentiation That Can Be Depotentiated by Stimulation on the Negative Phase in Area CA1 In Vivo. *Journal of Neuroscience*, *17*(16), 6470–6477. https://doi.org/10.1523/JNEUROSCI.17-16-06470.1997

Huang, Y.-Z., Edwards, M. J., Rounis, E., Bhatia, K. P., & Rothwell, J. C. (2005). Theta Burst Stimulation of the Human Motor Cortex. *Neuron*, *45*(2), 201–206. https://doi.org/10.1016/j.neuron.2004.12.033

Huang, Y.-Z., & Rothwell, J. C. (2004). The effect of short-duration bursts of high-frequency, low-intensity transcranial magnetic stimulation on the human motor cortex. *Clinical Neurophysiology*, *115*(5), 1069–1075. https://doi.org/10.1016/j.clinph.2003.12.026

Hughes, A. M., Whitten, T. A., Caplan, J. B., & Dickson, C. T. (2012). BOSC: A better oscillation detection method, extracts both sustained and transient rhythms from rat hippocampal recordings. *Hippocampus*, *22*(6), 1417–1428. https://doi.org/10.1002/hipo.20979

Huh, C. Y. L., Goutagny, R., & Williams, S. (2010). Glutamatergic Neurons of the Mouse Medial Septum and Diagonal Band of Broca Synaptically Drive Hippocampal Pyramidal Cells: Relevance for Hippocampal Theta Rhythm. *Journal of Neuroscience*, *30*(47), 15951–15961. https://doi.org/10.1523/JNEUROSCI.3663-10.2010

Hyman, J. M., Wyble, B. P., Goyal, V., Rossi, C. A., & Hasselmo, M. E. (2003). Stimulation in Hippocampal Region CA1 in Behaving Rats Yields Long-Term Potentiation when Delivered to the Peak of Theta and Long-Term Depression when Delivered to the Trough. *Journal of Neuroscience*, *23*(37), 11725–11731. https://doi.org/10.1523/JNEUROSCI.23-37-11725.2003

Insausti, R., Amaral, D. G., & Cowan, W. M. (1987). The entorhinal cortex of the monkey: II. Cortical afferents. *Journal of Comparative Neurology*, *264*(3), 356–395. https://doi.org/10.1002/cne.902640306

Iwai, E., Yukie, M., Suyama, H., & Shirakawa, S. (1987). Amygdalar connections with middle and inferior temporal gyri of the monkey. *Neuroscience Letters*, *83*(1), 25–29. https://doi.org/10.1016/0304-3940(87)90210-2

Jacobs, J. (2014). Hippocampal theta oscillations are slower in humans than in rodents: Implications for models of spatial navigation and memory. *Philosophical Transactions of the Royal Society B: Biological Sciences*, *369*(1635), 20130304. https://doi.org/10.1098/rstb.2013.0304

Jacobs, J., Hwang, G., Curran, T., & Kahana, M. J. (2006). EEG oscillations and recognition memory: Theta correlates of memory retrieval and decision making. *NeuroImage*, *32*(2), 978–987. https://doi.org/10.1016/j.neuroimage.2006.02.018

Joshi, A., Kale, S., Chandel, S., & Pal, D. (2015). Likert Scale: Explored and Explained. *British Journal of Applied Science & Technology*, *7*(4), 396–403. https://doi.org/10.9734/BJAST/2015/14975

Jung, R., & Kornmüller, A. E. (1938). A method of recording localized electrical potentials in subcortical regions of the brain. *Archiv Für Psychiatrie Und Nervenkrankheiten*, *109*, 1–30. https://doi.org/10.1007/BF02157817

Jutras, M. J., Fries, P., & Buffalo, E. A. (2013). Oscillatory activity in the monkey hippocampus during visual exploration and memory formation. *Proceedings of the National Academy of Sciences*, *110*(32), 13144–13149. https://doi.org/10.1073/pnas.1302351110

Kahana, M. J., Seelig, D., & Madsen, J. R. (2001). Theta returns. *Current Opinion in Neurobiology*, *11*(6), 739–744. https://doi.org/10.1016/S0959-4388(01)00278-1

Kahana, M. J., Sekuler, R., Caplan, J. B., Kirschen, M., & Madsen, J. R. (1999). Human theta oscillations exhibit task dependence during virtual maze navigation. *Nature*, *399*(6738), Article 6738. https://doi.org/10.1038/21645

Kamondi, A., Acsády, L., Wang, X.-J., & Buzsáki, G. (1998). Theta oscillations in somata and dendrites of hippocampal pyramidal cells in vivo: Activity-dependent phase-precession of action potentials. *Hippocampus*, *8*(3), 244–261. https://doi.org/10.1002/(SICI)1098-1063(1998)8:3<244::AID-HIPO7>3.0.CO;2-J

Klimesch, W., Doppelmayr, M., Russegger, H., & Pachinger, T. (1996). Theta band power in the human scalp EEG and the encoding of new information: *NeuroReport*, *7*(7), 1235–1240. https://doi.org/10.1097/00001756-199605170-00002

Klimesch, W., Sauseng, P., & Gerloff, C. (2003). Enhancing cognitive performance with repetitive transcranial magnetic stimulation at human individual alpha frequency. *European Journal of Neuroscience*, *17*(5), 1129–1133. https://doi.org/10.1046/j.1460-9568.2003.02517.x

Knox, D., & Keller, S. M. (2016). Cholinergic neuronal lesions in the medial septum and vertical limb of the diagonal bands of Broca induce contextual fear memory

generalization and impair acquisition of fear extinction. *Hippocampus*, *26*(6), 718–726. https://doi.org/10.1002/hipo.22553

Kragel, J. E., VanHaerents, S., Templer, J. W., Schuele, S., Rosenow, J. M., Nilakantan, A. S., & Bridge, D. J. (n.d.). Hippocampal theta coordinates memory processing during visual exploration. *ELife*, *9*, e52108. https://doi.org/10.7554/eLife.52108

Kubota, Y., Enatsu, R., Gonzalez-Martinez, J., Bulacio, J., Mosher, J., Burgess, R. C., & Nair, D. R. (2013). In vivo human hippocampal cingulate connectivity: A corticocortical evoked potentials (CCEPs) study. *Clinical Neurophysiology*, *124*(8), 1547–1556. https://doi.org/10.1016/j.clinph.2013.01.024

Kundu, B., Johnson, J. S., & Postle, B. R. (2014). Prestimulation phase predicts the TMS-evoked response. *Journal of Neurophysiology*, *112*(8), 1885–1893. https://doi.org/10.1152/jn.00390.2013

Larson, J., & Munkácsy, E. (2015). Theta-burst LTP. *Brain Research*, *1621*, 38–50. https://doi.org/10.1016/j.brainres.2014.10.034

Larson, J., Wong, D., & Lynch, G. (1986). Patterned stimulation at the theta frequency is optimal for the induction of hippocampal long-term potentiation. *Brain Research*, *368*(2), 347–350. https://doi.org/10.1016/0006-8993(86)90579-2

Lee, M. G., Chrobak, J. J., Sik, A., Wiley, R. G., & Buzsáki, G. (1994). Hippocampal theta activity following selective lesion of the septal cholinergic systeM. *Neuroscience*, *62*(4), 1033–1047. https://doi.org/10.1016/0306-4522(94)90341-7

Lega, B. C., Jacobs, J., & Kahana, M. (2012). Human hippocampal theta oscillations and the formation of episodic memories. *Hippocampus*, *22*(4), 748–761. https://doi.org/10.1002/hipo.20937

Long, N. M., Burke, J. F., & Kahana, M. J. (2014). Subsequent memory effect in intracranial and scalp EEG. *NeuroImage*, *84*, 488–494. https://doi.org/10.1016/j.neuroimage.2013.08.052

Lubenov, E. V., & Siapas, A. G. (2009). Hippocampal theta oscillations are travelling waves. *Nature*, *459*(7246), Article 7246. https://doi.org/10.1038/nature08010

Maass, A., Schütze, H., Speck, O., Yonelinas, A., Tempelmann, C., Heinze, H.-J., Berron, D., Cardenas-Blanco, A., Brodersen, K. H., Enno Stephan, K., & Düzel, E. (2014). Laminar activity in the hippocampus and entorhinal cortex related to novelty and episodic encoding. *Nature Communications*, *5*(1), Article 1. https://doi.org/10.1038/ncomms6547

Markowska, A. L., Olton, D. S., & Givens, B. (1995). Cholinergic manipulations in the medial septal area: Age-related effects on working memory and hippocampal electrophysiology. *Journal of Neuroscience*, *15*(3), 2063–2073. https://doi.org/10.1523/JNEUROSCI.15-03-02063.1995

Matsumoto, R., Nair, D. R., LaPresto, E., Najm, I., Bingaman, W., Shibasaki, H., & Lüders, H. O. (2004). Functional connectivity in the human language system: A cortico-cortical evoked potential study. *Brain*, *127*(10), 2316–2330. https://doi.org/10.1093/brain/awh246

Mayeux, R., Brandt, J., Rosen, J., & Benson, D. F. (1980). Interictal memory and language impairment in temporal lobe epilepsy. *Neurology*, *30*(2), 120–120. https://doi.org/10.1212/WNL.30.2.120

Mazziotta, J. C., Toga, A. W., Evans, A., Fox, P., & Lancaster, J. (1995). A probabilistic atlas of the human brain: theory and rationale for its development. *Neuroimage*, *2*(2), 89-101

McNaughton, N., Ruan, M., & Woodnorth, M.-A. (2006). Restoring theta-like rhythmicity in rats restores initial learning in the Morris water maze. *Hippocampus*, *16*(12), 1102–1110. https://doi.org/10.1002/hipo.20235

Mechelli, A., Price, C. J., Friston, K. J., & Ashburner, J. (2005). Voxel-Based Morphometry of the Human Brain: Methods and Applications. *Current Medical Imaging Reviews*, *1*(2), 105–113. https://doi.org/10.2174/1573405054038726

Meij, R. van der, Kahana, M., & Maris, E. (2012). Phase–Amplitude Coupling in Human Electrocorticography Is Spatially Distributed and Phase Diverse. *Journal of Neuroscience*, *32*(1), 111–123. https://doi.org/10.1523/JNEUROSCI.4816-11.2012

Mitchell, S. J., Rawlins, J. N., Steward, O., & Olton, D. S. (1982). Medial septal area lesions disrupt theta rhythm and cholinergic staining in medial entorhinal cortex and produce impaired radial arm maze behavior in rats. *Journal of Neuroscience*, *2*(3), 292–302. https://doi.org/10.1523/JNEUROSCI.02-03-00292.1982

Montgomery, S. M., & Buzsáki, G. (2007). Gamma oscillations dynamically couple hippocampal CA3 and CA1 regions during memory task performance. *Proceedings of the National Academy of Sciences*, *104*(36), 14495–14500. https://doi.org/10.1073/pnas.0701826104

Morecraft, R. J., Geula, C., & Mesulam, M.-M. (1992). Cytoarchitecture and neural afferents of orbitofrontal cortex in the brain of the monkey. *Journal of Comparative Neurology*, *323*(3), 341–358. https://doi.org/10.1002/cne.903230304

Nguyen, P. V., & Kandel, E. R. (1997). Brief theta-burst stimulation induces a transcription-dependent late phase of LTP requiring cAMP in area CA1 of the mouse hippocampus. *Learning & Memory*, *4*(2), 230–243. https://doi.org/10.1101/lm.4.2.230

Novitskaya, Y., Dümpelmann, M., Vlachos, A., Reinacher, P. C., & Schulze-Bonhage, A. (2020). In vivo-assessment of the human temporal network: Evidence for asymmetrical effective connectivity. *NeuroImage*, *214*, 116769. https://doi.org/10.1016/j.neuroimage.2020.116769

Oathes, D. J., Zimmerman, J. P., Duprat, R., Japp, S. S., Scully, M., Rosenberg, B. M., Flounders, M. W., Long, H., Deluisi, J. A., Elliott, M., Shandler, G., Shinohara, R. T., & Linn, K. A. (2021). Resting fMRI-guided TMS results in subcortical and brain network modulation indexed by interleaved TMS/fMRI. *Experimental Brain Research*, *239*(4), 1165–1178. https://doi.org/10.1007/s00221-021-06036-5

Parvizi, J., & Kastner, S. (2018). Promises and limitations of human intracranial electroencephalography. *Nature Neuroscience*, *21*(4), Article 4. https://doi.org/10.1038/s41593-018-0108-2

Patel, J., Fujisawa, S., Berényi, A., Royer, S., & Buzsáki, G. (2012). Traveling Theta Waves along the Entire Septotemporal Axis of the Hippocampus. *Neuron*, *75*(3), 410–417. https://doi.org/10.1016/j.neuron.2012.07.015

Penny, W. D., Friston, K. J., Ashburner, J. T., Kiebel, S. J., & Nichols, T. E. (2011). *Statistical Parametric Mapping: The Analysis of Functional Brain Images*. Elsevier.

Pikkarainen, M., Rönkkö, S., Savander, V., Insausti, R., & Pitkänen, A. (1999). Projections from the lateral, basal, and accessory basal nuclei of the amygdala to the hippocampal formation in rat. *Journal of Comparative Neurology*, *403*(2), 229–260. https://doi.org/10.1002/(SICI)1096-9861(19990111)403:2<229::AID-CNE7>3.0.CO;2-P

Poppenk, J., Evensmoen, H. R., Moscovitch, M., & Nadel, L. (2013). Long-axis specialization of the human hippocampus. *Trends in Cognitive Sciences*, *17*(5), 230–240. https://doi.org/10.1016/j.tics.2013.03.005

Raghavachari, S., Kahana, M. J., Rizzuto, D. S., Caplan, J. B., Kirschen, M. P., Bourgeois, B., Madsen, J. R., & Lisman, J. E. (2001). Gating of Human Theta Oscillations by a Working Memory Task. *Journal of Neuroscience*, *21*(9), 3175–3183. https://doi.org/10.1523/JNEUROSCI.21-09-03175.2001

Roberts, B. M., Clarke, A., Addante, R. J., & Ranganath, C. (2018). Entrainment enhances theta oscillations and improves episodic memory. *Cognitive Neuroscience*, *9*(3–4), 181–193. https://doi.org/10.1080/17588928.2018.1521386

Romei, V., Bauer, M., Brooks, J. L., Economides, M., Penny, W., Thut, G., Driver, J., & Bestmann, S. (2016). Causal evidence that intrinsic beta-frequency is relevant for enhanced signal propagation in the motor system as shown through rhythmic TMS. *NeuroImage*, *126*, 120–130. https://doi.org/10.1016/j.neuroimage.2015.11.020

Rorden, C., & Brett, M. (2000). Stereotaxic display of brain lesions. *Behavioural Neurology*, *12*(4), 191–200.

Rossi, S., Hallett, M., Rossini, P. M., & Pascual-Leone, A. (2009). Safety, ethical considerations, and application guidelines for the use of transcranial magnetic stimulation in clinical practice and research. *Clinical Neurophysiology*, *120*(12), 2008–2039. https://doi.org/10.1016/j.clinph.2009.08.016

Roy, A. K., Shehzad, Z., Margulies, D. S., Kelly, A. M. C., Uddin, L. Q., Gotimer, K., Biswal, B. B., Castellanos, F. X., & Milham, M. P. (2009). Functional connectivity of the human amygdala using resting state fMRI. *NeuroImage*, *45*(2), 614–626. https://doi.org/10.1016/j.neuroimage.2008.11.030

Saunders, R. C., Rosene, D. L., & Van Hoesen, G. W. (1988). Comparison of the efferents of the amygdala and the hippocampal formation in the rhesus monkey: II. Reciprocal and non-reciprocal connections. *Journal of Comparative Neurology*, *271*(2), 185–207. https://doi.org/10.1002/cne.902710203

Seager, M. A., Johnson, L. D., Chabot, E. S., Asaka, Y., & Berry, S. D. (2002). Oscillatory brain states and learning: Impact of hippocampal theta-contingent training. *Proceedings of the National Academy of Sciences*, *99*(3), 1616–1620. https://doi.org/10.1073/pnas.032662099

Senut, M. C., Menetrey, D., & Lamour, Y. (1989). Cholinergic and peptidergic projections from the medial septum and the nucleus of the diagonal band of broca to dorsal hippocampus, cingulate cortex and olfactory bulb: A combined wheatgerm agglutinin-apohorseradish peroxidase-gold immunohistochemical study. *Neuroscience*, *30*(2), 385–403. https://doi.org/10.1016/0306-4522(89)90260-1

Shapiro, M. L., & Eichenbaum, H. (1999). Hippocampus as a memory map: Synaptic plasticity and memory encoding by hippocampal neurons. *Hippocampus*, *9*(4), 365–384. https://doi.org/10.1002/(SICI)1098-1063(1999)9:4<365::AID-HIPO4>3.0.CO;2-T

Shi, C.-J., & Cassell, M. d. (1997). Cortical, thalamic, and amygdaloid projections of rat temporal cortex. *Journal of Comparative Neurology*, *382*(2), 153–175. https://doi.org/10.1002/(SICI)1096-9861(19970602)382:2<153::AID-CNE2>3.0.CO;2-2

Shirvalkar, P. R., Rapp, P. R., & Shapiro, M. L. (2010). Bidirectional changes to hippocampal theta–gamma comodulation predict memory for recent spatial episodes. *Proceedings of the National Academy of Sciences*, *107*(15), 7054–7059. https://doi.org/10.1073/pnas.0911184107

Solomon, E. A., Sperling, M. R., Sharan, A. D., Wanda, P. A., Levy, D. F., Lyalenko, A., Pedisich, I., Rizzuto, D. S., & Kahana, M. J. (2021). Theta-burst stimulation entrains frequency-specific oscillatory responses. *Brain Stimulation*, *14*(5), 1271–1284. https://doi.org/10.1016/j.brs.2021.08.014

Staubli, U., & Lynch, G. (1987). Stable hippocampal long-term potentiation elicited by 'theta' pattern stimulation. *Brain Research*, *435*(1), 227–234. https://doi.org/10.1016/0006-8993(87)91605-2

Stewart, M., & Fox, S. E. (1989). Two populations of rhythmically bursting neurons in rat medial septum are revealed by atropine. *Journal of Neurophysiology*, *61*(5), 982–993. https://doi.org/10.1152/jn.1989.61.5.982

Stewart, M., & Fox, S. E. (1991). Hippocampal theta activity in monkeys. *Brain Research*, *538*(1), 59–63. https://doi.org/10.1016/0006-8993(91)90376-7

Strange, B. A., Witter, M. P., Lein, E. S., & Moser, E. I. (2014). Functional organization of the hippocampal longitudinal axis. *Nature Reviews Neuroscience*, *15*(10), Article 10. https://doi.org/10.1038/nrn3785

Summerfield, C., & Mangels, J. A. (2005). Coherent theta-band EEG activity predicts item-context binding during encoding. *NeuroImage*, *24*(3), 692–703. https://doi.org/10.1016/j.neuroimage.2004.09.012

Suppa, A., Huang, Y.-Z., Funke, K., Ridding, M. C., Cheeran, B., Di Lazzaro, V., Ziemann, U., & Rothwell, J. C. (2016). Ten Years of Theta Burst Stimulation in Humans: Established Knowledge, Unknowns and Prospects. *Brain Stimulation*, *9*(3), 323–335. https://doi.org/10.1016/j.brs.2016.01.006

Tambini, A., Nee, D. E., & D'Esposito, M. (2018). Hippocampal-targeted Theta-burst Stimulation Enhances Associative Memory Formation. *Journal of Cognitive Neuroscience*, *30*(10), 1452–1472. https://doi.org/10.1162/jocn_a_01300

Tanaka, K. Z., Pevzner, A., Hamidi, A. B., Nakazawa, Y., Graham, J., & Wiltgen, B. J. (2014). Cortical Representations Are Reinstated by the Hippocampus during Memory Retrieval. *Neuron*, *84*(2), 347–354. https://doi.org/10.1016/j.neuron.2014.09.037

Tayler, K. K., Tanaka, K. Z., Reijmers, L. G., & Wiltgen, B. J. (2013). Reactivation of Neural Ensembles during the Retrieval of Recent and Remote Memory. *Current Biology*, *23*(2), 99–106. https://doi.org/10.1016/j.cub.2012.11.019

Thut, G., Schyns, P., & Gross, J. (2011). Entrainment of Perceptually Relevant Brain Oscillations by Non-Invasive Rhythmic Stimulation of the Human Brain. *Frontiers in Psychology*, *2*. https://www.frontiersin.org/articles/10.3389/fpsyg.2011.00170

Toth, K., Borhegyi, Z., & Freund, T. F. (1993). Postsynaptic targets of GABAergic hippocampal neurons in the medial septum-diagonal band of broca complex. *Journal of Neuroscience*, *13*(9), 3712–3724. https://doi.org/10.1523/JNEUROSCI.13-09-03712.1993

Vanderwolf, C. H. (1969). Hippocampal electrical activity and voluntary movement in the rat. *Electroencephalography and Clinical Neurophysiology*, *26*(4), 407–418. https://doi.org/10.1016/0013-4694(69)90092-3

Vivekananda, U., Bush, D., Bisby, J. A., Baxendale, S., Rodionov, R., Diehl, B., Chowdhury, F. A., McEvoy, A. W., Miserocchi, A., Walker, M. C., & Burgess, N. (2021). Theta power and theta-gamma coupling support long-term spatial memory retrieval. *Hippocampus*, *31*(2), 213–220. https://doi.org/10.1002/hipo.23284

Voss, J. L., & Paller, K. A. (2009). An electrophysiological signature of unconscious recognition memory. *Nature Neuroscience*, *12*(3), Article 3. https://doi.org/10.1038/nn.2260

Waldhauser, G. T., Braun, V., & Hanslmayr, S. (2016). Episodic Memory Retrieval Functionally Relies on Very Rapid Reactivation of Sensory Information. *Journal of Neuroscience*, *36*(1), 251–260. https://doi.org/10.1523/JNEUROSCI.2101-15.2016

Wang, D., Clouter, A., Chen, Q., Shapiro, K. L., & Hanslmayr, S. (2018). Single-Trial Phase Entrainment of Theta Oscillations in Sensory Regions Predicts Human Associative Memory Performance. *The Journal of Neuroscience*, *38*(28), 6299–6309. https://doi.org/10.1523/JNEUROSCI.0349-18.2018

Wang, J. X., Rogers, L. M., Gross, E. Z., Ryals, A. J., Dokucu, M. E., Brandstatt, K. L., Hermiller, M. S., & Voss, J. L. (2014). Targeted enhancement of cortical-hippocampal brain networks and associative memory. *Science*, *345*(6200), 1054–1057. https://doi.org/10.1126/science.1252900

Watrous, A. J., Lee, D. J., Izadi, A., Gurkoff, G. G., Shahlaie, K., & Ekstrom, A. D. (2013). A comparative study of human and rat hippocampal low-frequency oscillations during spatial navigation. *Hippocampus*, *23*(8), 656–661. https://doi.org/10.1002/hipo.22124

Wespatat, V., Tennigkeit, F., & Singer, W. (2004). Phase Sensitivity of Synaptic Modifications in Oscillating Cells of Rat Visual Cortex. *Journal of Neuroscience*, *24*(41), 9067–9075. https://doi.org/10.1523/JNEUROSCI.2221-04.2004

Whitten, T. A., Hughes, A. M., Dickson, C. T., & Caplan, J. B. (2011). A better oscillation detection method robustly extracts EEG rhythms across brain state changes: The human alpha rhythm as a test case. *NeuroImage*, *54*(2), 860–874. https://doi.org/10.1016/j.neuroimage.2010.08.064

Williams, J. m., & Givens, B. (2003). Stimulation-induced reset of hippocampal theta in the freely performing rat. *Hippocampus*, *13*(1), 109–116. https://doi.org/10.1002/hipo.10082

Winson, J. (1978). Loss of Hippocampal Theta Rhythm Results in Spatial Memory Deficit in the Rat. *Science*, *201*(4351), 160–163. https://doi.org/10.1126/science.663646

Wixted, J. T., Squire, L. R., Jang, Y., Papesh, M. H., Goldinger, S. D., Kuhn, J. R., Smith, K. A., Treiman, D. M., & Steinmetz, P. N. (2014). Sparse and distributed coding of episodic memory in neurons of the human hippocampus. *Proceedings of the National Academy of Sciences*, *111*(26), 9621–9626. https://doi.org/10.1073/pnas.1408365111

Yazar, Y., Bergström, Z. M., & Simons, J. S. (2017). Reduced multimodal integration of memory features following continuous theta burst stimulation of angular gyrus. *Brain Stimulation*, *10*(3), 624–629. https://doi.org/10.1016/j.brs.2017.02.011

Yun, S. H., Mook-Jung, I., & Jung, M. W. (2002). Variation in Effective Stimulus Patterns for Induction of Long-Term Potentiation Across Different Layers of Rat Entorhinal Cortex. *Journal of Neuroscience*, *22*(5), RC214–RC214. https://doi.org/10.1523/JNEUROSCI.22-05-j0003.2002

Zanos, S., Rembado, I., Chen, D., & Fetz, E. E. (2018). Phase-Locked Stimulation during Cortical Beta Oscillations Produces Bidirectional Synaptic Plasticity in Awake Monkeys. *Current Biology*, *28*(16), 2515-2526.e4. https://doi.org/10.1016/j.cub.2018.07.009

Zhang, H., & Jacobs, J. (2015). Traveling Theta Waves in the Human Hippocampus. *Journal of Neuroscience*, *35*(36), 12477–12487. https://doi.org/10.1523/JNEUROSCI.5102-14.2015

Zhong, Y.-M., & Rockland, K. S. (2004). Connections between the anterior inferotemporal cortex (area TE) and CA1 of the hippocampus in monkey. *Experimental Brain Research*, *155*(3), 311–319. https://doi.org/10.1007/s00221-003-1728-6